Department of Biology
University of Fribourg (Switzerland)

UNIVERSITÉ DE FRIBOURG
UNIVERSITÄT FREIBURG

Homeostatic control and isolation of new targets of TORC1 in budding yeast

THESIS
Presented to the Faculty of Sciences of the University of Fribourg (Switzerland) in consideration for the award of the academic grade *Doctor rerum naturalium*

by

Serena Raucci

from

Potenza, Italy

Thesis N°: XXXX

UNIPRINT
2018

Accepted by the Faculty of Science of the University of Fribourg (Switzerland) upon the recommendation of:

Prof. Robbie Loewith, University of Geneva, Geneva, Switzerland
Prof. Jörn Dengjel, University of Fribourg, Fribourg, Switzerland

Fribourg, ……..

Thesis supervisor:

……
(Prof. Claudio De Virgilio)

Dean:

……
(Prof……..)

Ai miei genitori,
i miei esempi, la mia forza

List of abbreviations:

4EBP1: 4E-binding protein 1
AMPK: AMP-activated protein kinase
ATP: Adenosine triphosphate
EGOC: Exit from rapamycin-induced GrOwth arrest Complex
EGO-TC: Ego ternary complex
FKBP12: FK506 Binding Protein 12
FLCN: Foliculin
FRB: FKBP12-Rapamycin-Binding
GAP: GTPase activating protein
GATOR: GAP activity toward Rags
GDP: Guanosine diphosphate
GEF: Guanine nucleotide exchange factors
GC-MS: Gas-chromatography mass spectrometry
GO: Gene ontology
GTP: Guanosine triphosphate
GTPase: Guanosine triphosphatase
HOPS: HOmotypic fusion and vacuole Protein Sorting
IAA: Indole-3-acetic acid
Kog1: Kontroller Of Growth 1
LeuRS: Leucyl t-RNA synthetase
LUX: Like AUX1 permease
mTORC1: Mammalian TORC1
NAA: 1-naphthaleacetic acid
NCR: Nitrogen catabolite repression
ORF: Open Reading Frame
PAS: Phagophore assembly site
PE: Phosphatidylethanolamine
PI3K: Phosphatidyl Inositol 3' Kinase
PKA: Protein Kinase A
PP2A: Type 2A protein phosphatase
Rag: Ras-related GTP binding protein
SEAC: Seh1-associated complex
SEACAT: SEAC subcomplex activating TORC1 signaling
SEACIT: SEAC subcomplex inhibiting TORC1 signaling
S6K1: S6 kinase beta-1
Tco89: Tor Complex One subunit with 89 kDa
TFA: Trifluoroacetic acid
TFEB: Transcription factor EB
TOR: Target Of Rapamycin
TORC1: Target Of Rapamycin Complex I
TOROID: TORC1 Organized in Inhibited Domain
TSC: Tuberous Sclerosis Complex
v-ATPase: Vacuolar ATPase

Summary

Eukaryotic cells regulate their growth, survival and metabolism in response to favorable or non-favorable environmental conditions. The target of rapamycin complex 1 (TORC1), a conserved serine/threonine kinase complex, is the central cell growth controller in all eukaryotic organisms. Localized at the vacuolar membrane in yeast and, when active, at the lysosomal surface in mammals, it modulates multiple catabolic and anabolic processes by phosphorylating its targets in response to several stimuli such as amino acids and different kinds of stresses. The regulation of TORC1 by amino acids occurs via the heterodimeric yeast Rag GTPases Gtr1-Gtr2 (RagA/B-RagC/D in mammals) and their regulators that include GTP exchange factors (GEFs) and GTPase activating proteins (GAPs). We previously reported that in yeast, the Lst4-Lst7 complex functions as a GAP for Gtr2. This complex localizes at the vacuolar surface upon amino acid starvation and is released from the vacuole into the cytosol when cells are re-fed with nutrients (Péli-Gulli et al., 2015).

In the first chapter of this thesis, we present a model in which the dynamic localization of the Lst4-Lst7 complex at the vacuole is regulated by TORC1-dependent phosphorylation of Lst4. We demonstrate that TORC1 directly phosphorylates Lst4 on several residues (*in vivo* and *in vitro*) within the intra-DENN loop, an unstructured region in the DENN domain of Lst4. Interestingly, the intra-DENN loop is necessary and sufficient to anchor the Lst4-Lst7 complex at the vacuolar membrane. While the Lst4 phosphorylation status regulates the localization of Lst4-Lst7 complex, it does not affect its GAP activity towards Gtr2. Notably, the expression of an Lst4 allele that cannot be phosphorylated by TORC1 induces hyperactivation of TORC1, leading to growth defects when cells are grown on a poor nitrogen source. In sum, our data reveal a feedback mechanism that prevents TORC1 hyperactivation in the presence of amino acids thereby contributing to the regulation of the homeostasis of the TORC1 activity.

In the second chapter, we elaborate a new method for the identification of unknown TORC1 targets. We combine the TORC1 *in vitro* kinase assay with mass spectrometry analysis using yeast-purified proteins as substrates of TORC1. As a proof of principle, we focus on Atg proteins which allowed us to discover new

targets of TORC1. Among these, we identified Atg29, which is also phosphorylated by TORC1 in vitro when purified from bacteria.

In the third chapter, we analyze the effects of the plant hormone Indole-3-acetic acid (IAA) on yeast cell growth, providing evidence *in vivo* and *in vitro* that this compound is a direct inhibitor of TORC1. We also present a screening of the yeast knockout collection performed in the presence of IAA or rapamycin, in which we compare the mutants hypersensitive to IAA with those hypersensitive to rapamycin. Combined, our data suggest that the TORC1 pathway is involved in the response to IAA, though this compound also impinges on other pathways important for growth.

In the final chapter, we discuss about open questions and future perspectives that could follow the studies addressed in the previous chapters.

Résumé

Les cellules eucaryotes adaptent leur croissance, leur survie et leur métabolisme aux conditions environnementales. Target Of Rapamycin Complex 1 (TORC1), un complexe protéique conservé et doté d'une activité sérine/thréonine kinase, est un régulateur clé de la croissance cellulaire dans tous les organismes eucaryotes. Localisé à la membrane vacuolaire chez la levure et, lorsqu'il est activé, à la surface lysosomale chez les mammifères, TORC1 module de multiples processus cataboliques et anaboliques en phosphorylant ses cibles en réponse à plusieurs stimuli tels que les acides aminés et différents types de stress. La régulation de TORC1 par les acides aminés implique l'hétérodimère des Rag GTPases Gtr1-Gtr2 chez la levure (RagA / B-RagC / D chez les mammifères) et leurs régulateurs qui incluent les facteurs d'échange de GTP (GEFs) et les protéines qui activent la GTPase (GAPs). Chez la levure, nous avons précédemment décrit le complexe Lst4-Lst7 comme jouant le rôle de GAP pour Gtr2. Ce complexe se localise à la surface vacuolaire lors de la privation d'acides aminés et s'en détache pour s'accumuler dans le cytosol lorsque les cellules sont stimulées à nouveau par ces nutriments (Péli-Gulli et al., 2015).

Dans le premier chapitre de cette thèse, nous poursuivons la caractérisation de Lst4. Nous présentons un modèle dans lequel la localisation dynamique du complexe Lst4-Lst7 au niveau de la vacuole est influencée par le niveau de phosphorylation de Lst4 par TORC1. En effet, TORC1 phosphoryle directement Lst4 sur plusieurs résidus (*in vivo* et *in vitro*) dans une région non structurée du domaine DENN de Lst4 appelée boucle intra-DENN. Cette boucle intra-DENN s'avère nécessaire et suffisante pour ancrer le complexe Lst4-Lst7 à la membrane vacuolaire. Si le niveau de phosphorylation de Lst4 régule la localisation du complexe Lst4-Lst7, il n'influence pas son activité GAP pour Gtr2. D'autre part, l'expression d'un allèle Lst4 qui ne peut pas être phosphorylé par TORC1 conduit à une hyperactivation de TORC1, entraînant un défaut de croissance des cellules lorsqu'elles sont cultivées en présence d'une source d'azote de moindre qualité. En résumé, nos données révèlent un mécanisme de feedback qui empêche l'hyperactivation de TORC1 en présence d'acides aminés, contribuant ainsi à la régulation fine de l'activité de TORC1.

Dans le deuxième chapitre, nous élaborons une méthode pour identifier de nouvelles cibles de TORC1. Pour cela, nous combinons l'essai *in vitro* de l'activité kinase de TORC1 avec l'analyse de spectrométrie de masse en utilisant des protéines purifiées à partir de levure comme substrats de TORC1. Comme preuve de principe, nous nous concentrons sur les protéines Atg. Parmi celles-ci, Atg29 s'avère être une cible de TORC1 *in vitro*, lorsqu'elle est purifiée à partir de la levure. Sa phosphorylation pour TORC1 est confirmée en utilisant Atg29 produite par recombinaison chez la bactérie.

Dans le troisième chapitre, nous analysons l'effet de l'hormone végétale indole-3-acide acétique (IAA) sur la croissance des cellules de levure, fournissant des preuves *in vivo* et *in vitro* que ce composé est un inhibiteur direct de TORC1. Nous présentons deux screens menés en parallele sur la collection de levures knockout pour rechercher des mutants hypersensibles à l'IAA et/ou hypersensibles à la rapamycine. Leur comparaison révèle que la voie TORC1 est impliquée dans la réponse à l'IAA. Néanmoins, ce composé affecte également d'autres voies importantes pour la croissance.

Dans le dernier chapitre, nous discutons des questions restées ouvertes et des voies à suivre pour développer plus avant les projets entamés dans ce travail de thèse.

Introduction

1. TOR and TOR Complexes

The target of rapamycin (TOR) protein, a serine/threonine kinase, was discovered in the budding yeast *Saccharomyces cerevisiae* due to the isolation of mutants that were resistant to the macrolide rapamycin (Heitman et al., 1991). This kinase is part of the phosphatidylinositol 3-kinase-related kinases family and it is evolutionarily conserved (Schmelzle and Hall, 2000). It was also identified in mammals, but while in mammals there is only one *TOR* gene, in yeast two genes exist that encode for this kinase, *TOR1* and *TOR2* (Brown et al., 1994; Chiu et al., 1994; Eltschinger and Loewith, 2016; Sabatini et al., 1994; Sabers et al., 1995).

TOR forms two different complexes, characterized by distinct structures and functions, TOR Complex 1 (TORC1) and TOR Complex 2 (TORC2), but only TORC1 is sensitive to rapamycin (Loewith et al., 2002).

TORC1 is formed by several subunits, as well as TORC2, some of them shared among the two complexes and/or highly conserved among eukaryotes as summarised in Table 1 (Eltschinger and Loewith, 2016).

TOR Complex 1

S. cerevisiae	Mammalian Ortholog
Tor1 or Tor2	mTor
Lst8	mLst8
Kog1	Raptor
Tco89	?
?	Pras40
?	Deptor

TOR Complex 2

S. cerevisiae	Mammalian Ortholog
Tor2	mTor
Lst8	mLst8
Avo1	mSin1
Avo2	?
Avo3	Rictor
Bit2, Bit61	Protor-1, -2
?	Deptor

Table 1: TORC1 and TORC2 components in *S. cerevisiae* and their orthologs in mammals.

Concerning the functions of these complexes, TORC1 is mainly involved in cell growth, proliferation, and entrance in quiescence via the regulation of protein synthesis and turnover and the regulation of catabolic and metabolic pathways (Chantranupong et al., 2015; Loewith and Hall, 2011; Rohde and Cardenas, 2004; Weisman, 2016; Workman et al., 2014), while TORC2 is linked to the cell surface area and regulates sphingolipids and ceramide biosynthesis (Eltschinger and

Loewith, 2016). In this introduction, we focus on the description of the TORC1 pathway.

1.1 Components and characteristics of the TOR Complex 1

In yeast, TORC1 is a dimeric multiprotein complex, in which the kinase Tor1 and/or Tor2 is assembled with Kog1, Lst8 and Tco89 (Loewith et al., 2002; Reinke et al., 2004).

Tor1/2 (Target Of Rapamycin 1/2) are large proteins, almost 70% identical among each other, with various domains and motifs. At the N-terminus of the proteins there are HEAT motifs in tandem (Andrade and Bork, 1995), protein-protein interaction domains (Groves and Barford, 1999), and the FAT domain (Alarcon et al., 1999; Bosotti et al., 2000). At the C-terminus there are the catalytic domain (Loewith et al., 2002) together with the FRB (FKBP12-Rapamycin-Binding) domain that is involved in the inhibition of TORC1 by rapamycin, allowing the interaction between TORC1 and the complex formed by the proline isomerase FK506 binding protein FKBP12 (ortholog of Fpr1 in yeast) and the drug (Heitman et al., 1991). Finally, in the very C-terminus of the proteins, there is a FATC domain that probably stabilizes the kinase domain (Dames et al., 2005; Yang et al., 2013).

Kog1 (Kontroller Of Growth 1) is one of the conserved subunits (Raptor in mammals), and it is involved in the interaction between TORC1 and the Rag GTPases (Sancak et al., 2008). It is encoded by an essential gene, as well as another component, the small protein Lst8 (Lethal with Sec Thirteen 8). The latter was initially identified by a mutation that, together with the *sec13-1* mutation, involved in a sorting defect in the secretory pathway, causes a synthetic lethal phenotype (Loewith et al., 2002; Roberg et al., 1997).

Finally, Tco89 (Tor Complex One subunit with 89 kDa) is a nonessential subunit of TORC1; its deletion confers a hypersensitivity to rapamycin, and combined with the deletion of *TOR1*, is synthetically lethal (Reinke et al., 2004).

TORC1 localization differs among the organisms. While in yeast this complex was shown to localize to the vacuole, an organelle involved in nutrient supply and autophagy regulation (Khalfan and Klionsky, 2002; Sturgill et al., 2008), the localization of mTORC1 is controversial since it was found in several localizations in

mammalian cells: cytoplasm and nucleus (Kim and Chen, 2000; Zhang et al., 2002), Golgi and ER (Liu and Zheng, 2007), late endosomes and autophagosomes (Mavrakis et al., 2007), and the lysosome (the equivalent of the vacuole in mammals), to which it is recruited in response to the availability of amino acids, via small GTP-binding proteins called Rag GTPases (Bar-Peled et al., 2012; Kim et al., 2008; Sancak et al., 2008, 2010).

The TOR1 Complex exerts multiple roles in the cell, being the main regulator of growth through its signaling pathway involved in the stimulation of anabolic processes (such as protein, lipid, and nucleotide biosynthesis) and the inhibition of catabolic processes (such as autophagy) (González and Hall, 2017).

TORC1 activity is regulated by different stimuli and this is translated in the phosphorylation of its targets. Despite the importance of and variety of processes in which TORC1 is involved, so far only a limited number of direct targets of this kinase have been identified. In yeast, relevant identified TORC1 substrates are: the autophagy-related protein Atg13 (Kamada, 2010; Klionsky et al., 2003), the PP2A phosphatase associated protein Tap42 (Di Como and Arndt, 1996; Jiang and Broach, 1999; Li et al., 2017; Yan et al., 2006), and the Sch9 protein kinase (Urban et al., 2007), but also the GATA-type transcription factor Gln3 (Bertram et al., 2000), the Sfp1 transcription factor (Lempiäinen et al., 2009), and the Ypk3 protein kinase (Yerlikaya et al., 2016).

In mammals, two proteins are well known to be mTORC1 substrates: the eukaryotic translation initiation factor 4E-binding protein 1 (4EBP1) and the Ribosomal protein S6 kinase beta-1 (S6K1) (Hara et al., 1998; Wang et al., 1998).

Notably, many other substrates of mTORC1 have been discovered, such as the phosphatidic acid phosphatase Lipin1, involved in the *de novo* lipid synthesis regulation (Peterson et al., 2011), the Atg proteins ULK1, mAtg13, and ATG14 (Hosokawa et al., 2009; Yuan et al., 2013), and the transcription factor EB (TFEB) (Roczniak-Ferguson et al., 2012) for the autophagy inhibition and regulation. Recently, another protein was identified as a substrate of mTORC1, the acetyltransferase p300. The authors proposed that the phosphorylation of p300 contributes to the mTORC1 regulation of several processes, such as protein and lipid synthesis, and especially autophagy (Wan et al., 2017).

2. Regulation of TORC1

Like the role and the structure of the TOR Complex 1, also its regulation is highly conserved among eukaryotes and involves different proteins and pathways. Interestingly, confirming the importance of the regulation of this complex, it is known that in humans mTORC1 deregulation is strongly linked to several diseases and cancers (Laplante and Sabatini, 2012).

The regulation is entrusted to upstream and downstream regulators that work on TORC1 according to the positive or negative stimuli that the cell receives from the environment: nutrients availability or different kinds of stresses such as heat shock in the case of TORC1 in yeast (Takahara and Maeda, 2012; Weisman, 2016), growth factors, nutrients, hormones, energy levels and stress like hypoxia, DNA damage and inflammation for TORC1 in mammalian cells (McCormick et al., 2011).

2.1 Stimuli

In yeast, TORC1 is responsive to external stimuli, such as amino acids, nitrogen and carbon sources, and to intracellular cues such as autophagy and ribosome biogenesis, that suggest that this complex is regulated also through negative feedback loops via its downstream pathways (Eltschinger and Loewith, 2016).

2.1.1 Carbon sources

Budding yeast prefers glucose or fructose over other carbon sources (e.g. glycerol or ethanol) for growth (Broach, 2012). Different pathways mediate the carbon sources signals.

Glucose activates Protein Kinase A (PKA) signaling pathway, while its absence induces Snf1 (homolog of AMPK in mammals). PKA promotes the fermentative processes (*e.g.* glycolysis), and inhibits the respirative growth and the stress response (Broach, 2012; Zaman et al., 2009). Snf1 is a kinase required for glucose repression of the genes involved in the nonfermentable processes and for the expression of the genes necessary for the utilization of alternative carbon sources in absence of glucose (McCartney and Schmidt, 2001). In shortage of glucose, Snf1 is

phosphorylated and active, regulating the transcription of several genes through the phosphorylation of Sch9, the transcriptional activator of amino acid biosynthetic genes Gcn4, and the transcriptional repressor Mig1 (a repressor for the invertase gene) (Lu et al., 2011; Shirra et al., 2008; Young et al., 2003; Zaman et al., 2009). Notably, in yeast, TORC1 activity is inhibited upon glucose starvation through the formation of the Kog1 bodies that lead to the dissassembly of TORC1 in these conditions. This process is reversible by refeeding cells with glucose and occurs via Snf1 that phosphorylates or allows the phosphorylation of Kog1 at serines 491 and 494 (Hughes Hallett et al., 2015). Interestingly, Snf1 phosphorylation also increases upon nitrogen starvation and TORC1 inactivation, suggesting a role of TORC1 in the regulation of Snf1 activity (Orlova et al., 2010).

Recently, it was published that glucose starvation leads to a TORC1 redistribution along the vacuole in foci that correspond to cylindrical structures called TOROIDs (TORC1 Organized in Inhibited Domain), formed by several TORC1 dimers assembled together (Prouteau et al., 2017). This structures are necessary for TORC1 inactivation, in fact Prouteau and coworkers proposed that this oligomerization of the kinase complex leads to an allosteric obstruction of the active site (Prouteau et al., 2017). The inhibition of TORC1 upon glucose starvation via the formation of the TOROIDs was confirmed using a Tor1 allele ($Tor1^{D330::3XGFP}$) that fails to be organized in these structures. Using this allele, cells are not sensitive to glucose starvation anymore showing Sch9 phosphorylation, suggesting that the glucose signaling on TORC1 activity occurs via the formation of the TOROIDs (Prouteau et al., 2017). Possibly then, the other mentioned Kog1 bodies may in fact represent TOROIDS.

In mammals, the regulation of mTORC1 by glucose is represented by a response to energy levels. Upon glucose starvation, the AMP-activated protein kinase (AMPK) inhibits mTORC1 through the phosphorylation of TSC2 (Inoki et al., 2003a) or maybe phosphorylating Raptor (the yeast Kog1 ortholog) (Gwinn et al., 2008). The phosphorylation of TSC2 by AMPK activates the TSC1-TSC2 GAP activity towards Rheb, which uultimately inhibits mTORC1. This then causes downregulation of S6K and 4EBP1 that tells cells to survive upon cellular energy levels depletion. Indeed, glucose starvation induces massive apoptosis in cells knocked out for TSC2 (Inoki et al., 2003a). In low glucose conditions, AMPK also phosphorylates Raptor causing its

interaction with the 14-3-3 protein and the consequent mTORC1 activity inhibition (Gwinn et al., 2008). Interestingly, cells lacking AMPK can still respond to glucose depletion via the Rag GTPases, suggesting the existence of AMPK-independent mechanisms by which glucose regulates mTORC1 (Saxton and Sabatini, 2017).

2.1.2 Nitrogen sources

Nitrogen is fundamental for cell survival, as it is part of amino acids, nucleotides and other cellular components (Smets et al., 2010). Yeast cells can distinguish the quality of the N-sources and they can preferentially use the better quality nitrogen sources, such ammonia or amino acid glutamine (Cooper, 1982; Stracka et al., 2014).
TORC1 is clearly regulated by the quality of the nitrogen source (Shamji et al., 2000; Stracka et al., 2014), with ammonia or glutamine being specifically competent TORC1 activators. Nevertheless, how TORC1 senses the quality of N-source is still poorly understood.

2.1.2.1 Amino acids

Among all the signals that regulate TORC1, amino acids have a crucial role since alone they are sufficient to activate TORC1 in unicellular organisms, while in multicellular organisms they work synergistically with growth factors and hormonal inputs (González and Hall, 2017; Nicastro et al., 2017). A big step forward was done by the discovery of the involvement of the Rag family of GTPases in the regulation of TORC1 through amino acids (Sancak et al., 2008). How Rag GTPases sense amino acids in yeast, however, remains still unclear (Powis and De Virgilio, 2016). Notably, Stracka and coworkers reported that amino acids can also activate TORC1 independently of Rag GTPases (Stracka et al., 2014). Interestingly, only arginine, asparagine, glutamine and ammonium sulphate, which are considered good quality nitrogen sources, (Godard et al., 2007), are able to maintain TORC1 active in a Rag GTPases independent manner (Stracka et al., 2014).

Interestingly, treating cells with cycloheximide, an inhibitor of translation elongation, activates TORC1, probably because this increases the intracellular pool of free amino acids (Beugnet et al., 2003; Binda et al., 2009; Urban et al., 2007).

An important amino acid that activates TORC1 is leucine which, together with the other branched-chain amino acids, is the most frequently used amino acid in eukaryotes proteomes (Avruch et al., 2009; Echols et al., 2002). Two ways in which leucine regulates TORC1 were identified: one involves the leucyl-tRNA synthetase (LeuRS) in both yeast and mammals (see below) (Bonfils et al., 2012; Han et al., 2012) and the other the Sestrin proteins identified only in mammals (Chantranupong et al., 2014; Parmigiani et al., 2014; Peng et al., 2014; Saxton et al., 2016a; Wolfson et al., 2016). Sestrin2 and to a lesser extend Sestrin1 and 3, bind leucine and GATOR2 (a positive upstream regulator of mTORC1, see paragraph 2.2.2), contributing to the regulation of mTORC1 via leucine (Chantranupong et al., 2014; Wolfson et al., 2016). In the absence of leucine, Sestrin2 sequesters GATOR2, disrupting its interaction with GATOR1 (a negative upstream regulator of mTORC1, see paragraph 2.2.2) that can thus promote the inactivation of mTORC1. In these conditions, mTORC1 does not localize to the lysosome anymore (Kim et al., 2015; Parmigiani et al., 2014). Peng and colleagues pointed out that Sestrins can also have a more active role in the regulation of Rag GTPases involved in the mTORC1 pathway. They proposed that, upon starvation, Sestrins are GDP dissociation inhibitors (GDI) for RagA/B, interacting and inactivating these Rag GTPases and so inhibiting mTORC1 (Peng et al., 2014).

Finally, arginine is among the amino acids which strongly activate TORC1, although in yeast the mechanism of this regulation is unknown. In mammals two mechanisms were discovered. One is via the lysosomal amino acid transporter SLC38A9, the other involves the sensing of cytosolic arginine levels through the CASTOR1/2 proteins (Chantranupong et al., 2016). SLC38A9 senses the presence of arginine at the lysosomal membrane and interacts with the complex Ragulator and the Rag GTPases to activate mTORC1 (Rebsamen et al., 2015; Wang et al., 2015). If SLC38A9 is a lysosomal arginine sensor, CASTOR1/2 are sensors for the cytosolic arginine (Chantranupong et al., 2016). The mechanism of action of these two proteins is similar to Sestrins, CASTOR1/2 bind GATOR2, but in the presence of arginine, this

interaction is prevented, releasing GATOR2 that inhibits GATOR1, thus activating mTORC1 (Gai et al., 2016; Saxton et al., 2016b; Xia et al., 2016).

2.2 Upstream regulation

Over the years, many upstream regulators have been discovered that contribute to the modulation of TORC1 activity, according to the amino acid availability. Several of them are conserved between yeast and mammals; others, such as the Rheb-TSC branch, are present only in the mTORC1 network (Fig. 1) (Nicastro et al., 2017).

a) b)

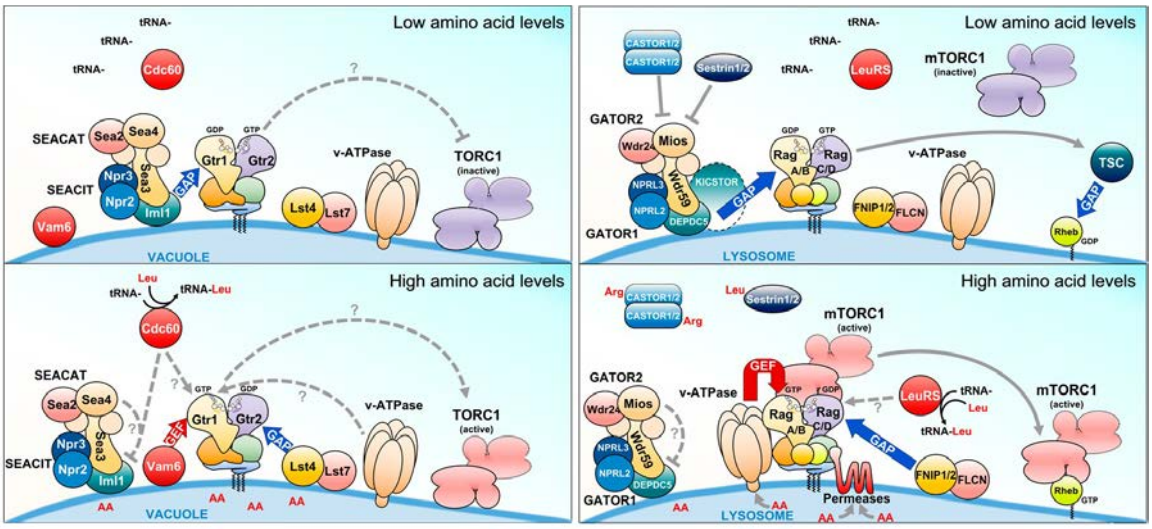

Figure 1. Upstream regulators of yTORC1 (a) and mTORC1 (b). Red and blue arrows determine the GTP exchange factors (GEF) and GTPase activating protein (GAP) activities, respectively. Taken from (Nicastro et al., 2017). More details in the next sections.

2.2.1 The Rag GTPases

The Ras-related GTP-binding proteins (Rag) GTPases are part of a bigger family of proteins, the GTP-binding proteins (GTPases). In general, GTPases are characterized by their capacity to bind and hydrolyze GTP. They exist in two forms: the active GTP-bound form and the inactive GDP-bound form and they are involved in the regulation of several processes such as signal transduction, differentiation and protein biosynthesis (Bourne et al., 1990; Gilman, 1987; Trahey and McCormick, 1987).

The Rag GTPases form a conserved family of small GTPases. Gtr1 and Gtr2 have been identified as the two Rag GTPases in *S. cerevisiae* (Nakashima et al., 1999), RagA, RagB, RagC, and RagD the four in mammals (Sekiguchi et al., 2001). RagA/B and RagC/D and their orthologs Gtr1 and Gtr2 in yeast, respectively, form a heterodimeric complex that in mammals is responsible, in the presence of amino acids, of the mTORC1 recruitment to the lysosome for its activation by Rheb (Sancak et al., 2008). In budding yeast, the mechanism is presumably different since TORC1 is already localized to the vacuole (Dubouloz et al., 2005; Powis et al., 2015).

The presence of amino acids supports the active conformation of the heterodimer: GTP-loaded Gtr1 or RagA/B and GDP-loaded Gtr2 or RagC/D. Vice versa, shortage of amino acids supports the inactive conformation of heterodimer: GDP-loaded Gtr1 or RagA/B and GTP-loaded Gtr2 or RagC/D, which inhibits TORC1 activity (Binda et al., 2009; Demetriades et al., 2014; Gao and Kaiser, 2006; Kim et al., 2008; Kira et al., 2014).

In the presence of amino acids, Gtr2 hydrolyzes GTP to GDP and undergoes a rotation of the G domain, the N-terminal GTPase domain responsible for guanine nucleotide-binding. Vice versa, considering the structure similarity between Gtr1 and Gtr2, it was speculated that when Gtr1 is GDP-loaded in absence of amino acids, it rotates its G domain (Fig. 2) (Gong et al., 2011; Jeong et al., 2012; Nicastro et al., 2017). This conformational change can explain why the heterodimer is active when Gtr1 is GTP-loaded and Gtr2 is GDP-loaded being able to interact more with TORC1 (in particular with Kog1 and Tco89 subunits). Similary, RagA/B^{GTP} and RagC/D^{GDP} interact preferentially with Raptor (the ortholog of Kog1) in the active conformation (Binda et al., 2009; Kira et al., 2014, 2016; Sancak et al., 2008; Sekiguchi et al., 2014; Tsun et al., 2013). Notably, the region affected by the rotation of the Gtr1 G domain corresponds in mammals to the one of RagA/B which interacts with Raptor (Gong et al., 2011), thus it can be speculated that when Gtr1 (or RagA/B) hydrolyses GTP, the rotation of its G domain masks the binding site for TORC1 .

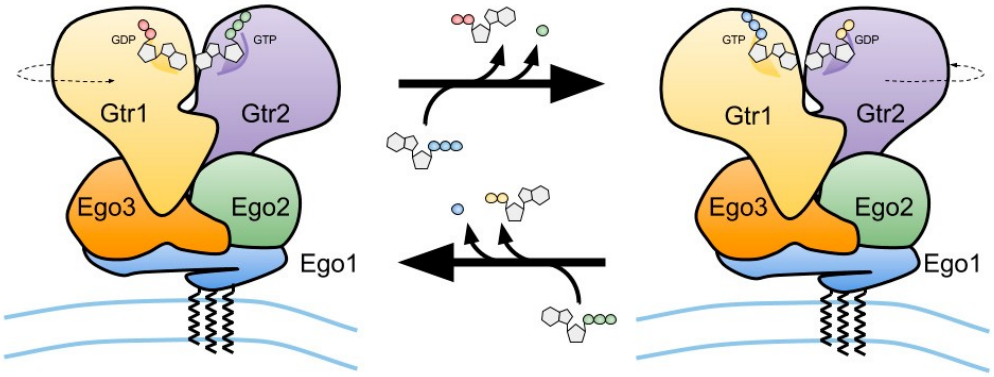

Figure 2. Schematization of the heterodimer Gtr1-Gtr2 tethered to the budding yeast vacuolar surface via the Ego1-Ego2-Ego3 complex. The amino acids availability regulates the conformational changes of Gtr1 and Gtr2 upon GTP hydrolysis by Gtr1 and Gtr2 respectively. Taken from (Nicastro et al., 2017).

This action of amino acids on the Rag GTPases is mainly mediated by other regulators: a member of the HOPS complex, Vam6 (Binda et al., 2009), the leucyl-tRNA synthetase (LeuRS) (Bonfils et al., 2012), the Lst4/Lst7 complex (Péli-Gulli et al., 2015), and SEACAT and SEACIT complexes (Bar-Peled et al., 2013; Panchaud et al., 2013a, 2013b). All of these will be described in the following paragraphs.

2.2.1.1 EGO complex

The EGO complex is formed by five proteins: Ego1, Ego2, Ego3 (EGO-ternary complex, EGO-TC) and the two small Rag GTPases Gtr1 and Gtr2 (Binda et al., 2009; Dubouloz et al., 2005; Gao and Kaiser, 2006; Powis et al., 2015). The name EGO (Exit from rapamycin-induced GrOwth arrest) derives from a screening that identified mutants that could not recover from a rapamycin-induced growth arrest (Dubouloz et al., 2005).

The complex is tethered to the vacuole via Ego1, a protein that undergoes post-translational modifications such as N-terminal myristoylation and palmitoylation that allow the binding to the vacuolar membrane (Nadolski and Linder, 2009; Roth et al., 2006).

In mammals, a pentameric complex called Ragulator, exerts the same function of the yeast EGO-TC (Table 2) (Sancak et al., 2010). Although Ragulator has two more subunits compared to the EGO-TC and the sequence similarity of the other subunits

is not very high, the two complexes are highly related in terms of structure and function (Powis et al., 2015). Like the EGO-TC in *S. cerevisiae*, also Ragulator associates with Rag GTPases and functions as a scaffold to anchor the complete complex to the lysosome (Sancak et al., 2010).

EGO-TC	Ragulator
Ego1	LAMTOR1
Ego2	LAMTOR2 LAMTOR3
Ego3	LAMTOR4 LAMTOR5

Table 2. EGO-TC subunits and the corresponding subunits in the mammalian complex Ragulator.

However, it was also reported that Ragulator has an active role in mTORC1 regulation. In fact, this complex could function as a GTP exchange factor (GEF) for RagA/B in response to intra-lysosomal amino acids, interacting with the H^+-ATPase (v-ATPase, see below) (Bar-Peled et al., 2012).

2.2.1.2 GEFs and GAPs

Rag GTPases are fundamental for the amino acid signaling to the TORC1 pathway and their GTP/GDP-loading status reflects this signal.
Regulators of the Rag GTPases loading status can be classified into two categories: GTP exchange factors (GEFs), and GTPase activating proteins (GAPs) (Nicastro et al., 2017).
GTPases can bind GDP or GTP, but the G domain is more often associated with GTP because of the large intracellular abundance of this nucleotide compared with GDP. The GTPases hydrolyze GTP to GDP, but the exchange of GDP for GTP can be slow, so GEFs are required to accelerate this process. When a GEF binds the G domain of the GTPase, it promotes changes in conformation, the release of the cofactor Mg^{2+} ion (that coordinates the binding between the G domain and the nucleotide), and the consequent detachment of the GDP. Finally, the G domain of the GTPase accepts another guanine nucleotide and this binding displaces the GEF (Bos et al., 2007).

GAPs are required to increase the GTPase activity of those GTPases which have a naturally low GTP hydrolysis activity. Crystal structure analysis revealed that they support the orientation and polarization of a water molecule that can accept a phosphate group from the GTP, stabilizing the transition state of this process and increasing the efficiency of the GTPase activity (Bos et al., 2007; Vetter, 2001).
In the TORC1 pathway, several of such regulators of Rag GTPases have been identified.

2.2.2 SEACIT and SEACAT

Both SEACIT and SEACAT complexes are part of the octameric Seh1-Associated protein Complex SEAC. These complexes are evolutionarily conserved and correspond to GATOR1 and GATOR2 complexes in mammals, respectively.
SEACIT (SEAC Inhibiting TORC1) is a trimeric complex containing Npr2, Npr3 and Iml1 (NPRL2, NPRL3, and DEPDC5 in GATOR1) and SEACAT (SEAC Activating TORC1) is a pentameric complex formed by Seh1, Sec13, Rtc1/Sea2, Mtc5/Sea3, and Sea4 (Seh1L, Sec13, Wdr24, Wdr59, and Mios in GATOR2) (Bar-Peled and Sabatini, 2014; Bar-Peled et al., 2013; Panchaud et al., 2013a).
The first two proteins discovered were Npr2 and Npr3, identified in a screen as negative regulators of TORC1 (Neklesa and Davis, 2009). In 2011, Dokudovskaya and coworkers identified Iml1 as a component of the SEACIT complex and later, Panchaud and colleagues proposed that this complex, through Iml1, acts negatively on TORC1 by stimulating the Gtr1 GTPase activity and thus promoting its GDP-loaded status (Dokudovskaya et al., 2011; Panchaud et al., 2013b). Indeed, Iml1 (as well as its mammalian ortholog DEPDC5) is a GTPase activating protein (GAP) that exerts its activity on Gtr1 in response to the absence of amino acids, but the mechanism that regulates this response remains unknown (Nicastro et al., 2017; Panchaud et al., 2013b). The domain of Iml1 involved in the stimulation of the GTPase activity of Gtr1 *in vitro* has been identified as GAP domain. The Iml1 GAP domain ($Iml1^{GAP}$) includes the arginine 943 (Arg^{943}) that plays a significant role in the GAP activity of Iml1. In fact, a mutant in which this arginine is replaced by an alanine, shows a reduced inhibitory effect of Iml1 on TORC1 *in vivo* (Panchaud et al., 2013b).

It is published that methionine, promotes the activation of the type 2A protein phosphatase (PP2A) and consequentially supports the disruption of the SEACIT. Accordingly, this phosphatase dephosphorylates Npr2 that dissociates from Npr1 and Iml1, disassembling the SEACIT complex (Sutter et al., 2013).
SEACAT is the complex formed by the other five proteins of the SEA complex. Epistatic analysis revealed that this complex acts upstream of SEACIT, inhibiting its negative effect on Gtr1 in the presence of high levels of amino acids, but the molecular details of this mechanism remain elusive (Panchaud et al., 2013a).

2.2.3 Vam6

As mentioned, the mammalian Ragulator complex plays the role of GEF for RagA/B, while in yeast this function is carried out by Vam6 that exerts this task on Gtr1, alone or in combination with other molecules (Binda et al., 2009; Valbuena et al., 2012; Zhang et al., 2012). Vam6 (also known as Vps39) is a conserved protein, that localizes at the vacuole and is part of the HOmotypic fusion and vacuole Protein Sorting (HOPS/class C-Vps) complex in yeast (Caplan et al., 2001; Ostrowicz et al., 2008).
Binda and coworkers isolated Vam6 as a potential GEF for Gtr1 in a synthetic lethal screen in which the Gtr1 mutant with a reduced affinity for nucleotides ($Gtr1^{S20L}$) was overexpressed. The strongest growth defect phenotype was found in the *vam6Δ* and in *gtr1Δ* mutants. The same study also showed that Vam6 interacts *in vivo* with Gtr1 and stimulates *in vitro* the nucleotide exchange activity of this Rag GTPase (Binda et al., 2009).
Vam6 has a human homolog hVps39-1 (or hVam6), but it appears that this protein does not act as a GEF on RagA/B since does not interact with RagA *in vivo* and does not have GEF activity on RagB *in vitro* (Bar-Peled et al., 2012; Caplan et al., 2001; Messler et al., 2011).

2.2.4 FNIP1/2-FLCN and Lst4/Lst7 complexes

So far, we described regulators for Gtr1 (or RagA/B in mammals), but also regulators of Gtr2 (Rag C/D) were discovered.

The mammalian proteins FNIP1/2 and Folliculin (FLCN) interact with each other, forming a complex that is important for the proper lysosomal localization of TORC1 through Rag GTPases, in response to amino acid signals (Petit et al., 2013; Tsun et al., 2013).

The FNIP1/2-FLCN complex stimulates the GTPase activity of Gtr2, although it binds directly and mainly the GDP-loaded RagA/B in starved cells (Martina et al., 2014; Petit et al., 2013; Tsun et al., 2013).

Lst4 and Lst7 are two yeast proteins that are the orthologs of FNIP and Folliculin, respectively. They form a complex and, under amino acids starvation conditions, accumulate at the vacuolar surface. It was demonstrated that the Lst4-Lst7 complex poorly interacts with Rag GTPases in absence of amino acids, unlike FNIP-FLCN complex that binds Rag GTPases upon amino acid starvation (Péli-Gulli et al., 2015; Petit et al., 2013). The yeast complex, once at the vacuole, interacts strongly with GTP-loaded Gtr2 and acts as a GAP for this Rag GTPase only upon re-addition of nutrients, promoting its GDP-loaded status (Péli-Gulli et al., 2015).

The regulation of the GAP activity of Lst4-Lst7, mediated by the availability of amino acids, suggests the possibility that this complex is involved in a feedback loop mechanism to regulate the hyperactivation of TORC1 upon amino acid re-addition (Fig. 3). Although how amino acids are sensed by Lst4-Lst7 is still unknown, there are five amino acids that can effectively displace this complex from the vacuole. Indeed, the re-addition of anyone of these amino acids (methionine, cysteine, glutamine, asparagine, and aspartate) can also re-activate TORC1 after amino acid starvation (Péli-Gulli et al., 2015). Notably, all of these five amino acids can be converted to glutamate/glutamine, which are known to strongly activate TORC1 (Durán et al., 2012; Ljungdahl and Daignan-Fornier, 2012; Stracka et al., 2014).

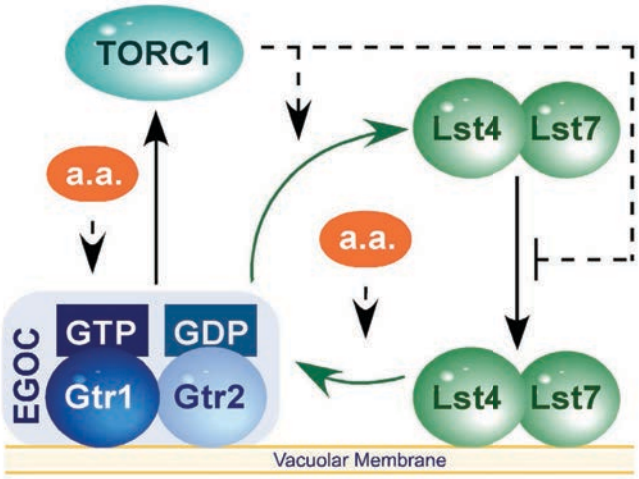

Figure 3. A TORC1-dependent feedback mechanism attenuates Lst4-Lst7 function. Schematization of the feedback loop depending on amino acid availability that regulates the Ls4-Lst7 vacuolar localization and GAP activity. Taken from (Péli-Gulli et al., 2015).

2.2.5 Leucyl-tRNA synthetase

The tRNA charging enzyme leucyl-tRNA synthetase (LeuRS, Cdc60 in *S. cerevisiae*) is an activator of TORC1 both in mammals and in yeast, signaling to Rag GTPases the level of cytosolic leucine or branched-chain amino acids (Bonfils et al., 2012; Han et al., 2012; Powis and De Virgilio, 2016). In budding yeast, Cdc60 interacts with Gtr1 (but not with Gtr2), promoting its GTP-loading status, in a leucine-dependent manner. This interaction takes place through the LeuRS editing domain, charged to recognize and remove the wrong amino acid from mischarged $tRNA^{Leu}$ (Tukalo et al., 2005). When leucine is abundant, Cdc60 and Gtr1 are bound and this probably preserves the binding of negative modulators of this Rag GTPase (Bonfils et al., 2012). Under shortage of cytosolic leucine, the probability of mischarged $tRNA^{Leu}$ is higher and the LeuRS editing domain changes its conformation, which disrupts its interaction with Gtr1 (Bonfils et al., 2012; Powis and De Virgilio, 2016).
In mammals, Han and colleagues proposed a GAP activity for the LeuRS on RagD, but this data is still controversial, since another study could not reproduce it and a recent publication defined the FNIP1/2-FLCN complex as the GAP for RagC/D (Han et al., 2012; Petit et al., 2013; Tsun et al., 2013).

2.2.6 V-ATPase

The activation of TORC1 via amino acids, in both yeast and mammals, occurs at the vacuolar/lysosomal membrane and involves both cytosolic and vacuolar/lysosomal amino acid bulks. Since amino acids and other compounds move between the cytosol and the vacuole/lysosome, the proton gradient across the membrane of these organelles changes and can be converted into a signal to evaluate the intracellular amino acid availability (Ljungdahl and Daignan-Fornier, 2012; Sekito et al., 2008). This gradient is established through the vacuolar/lysosomal H^+-ATPase (v-ATPase) that plays an important role in TORC1 regulation, in response to the presence of amino acids and the pH control (Forgac, 2007; Mellman et al., 1986).
The V-ATPase is a proton-pump that imports protons into the vacuole/lysosome, hydrolyzing ATP (Forgac, 2007; Mellman et al., 1986). In multicellular organisms, the V-ATPase has an active role directly interacting with the Ragulator-RagGTPases complex and promoting the GEF activity of Ragulator on RagA/B, although the mechanism remains unclear (Bar-Peled et al., 2012; Zoncu et al., 2011). In yeast, the V-ATPase role in TORC1 regulation is more related to its function in reporting the cytosolic pH, which gives a readout of the carbon source availability (Dechant et al., 2014).

2.2.7 TSC and RHEB

In budding yeast, the regulatory branch represented by Tuberous Sclerosis Complex (TSC) and RHEB is likely not present because it has no TSC complex ortholog and the RHEB homolog Rhb1 does not perform the same function as its homolog in mammals (González and Hall, 2017; Urano et al., 2000).
The TSC complex is a GAP for Rheb, a small GTPase, that directly binds and activates mTORC1 when GTP-loaded (Castro et al., 2003; Garami et al., 2003; Inoki et al., 2003b; Saucedo et al., 2003; Yamagata et al., 1994).
This branch is involved in the regulation of mTORC1 via hormonal signals (*e.g.* insulin) and it is required to properly activate mTORC1 at the lysosome (Nicastro et al., 2017; Sato et al., 2009).

2.2.8 Inhibitors

Over the years, several inhibitor molecules of TORC1, natural or artificial one, were identified. Among the artificial ones, the chemical compounds TORIN1 and TORIN2, and the most common WORTMANNIN have been developed (Brunn et al., 1996; Liu et al., 2011; Thoreen et al., 2009), while rapamycin and caffeine are two examples of natural TORC1 inhibitory compounds.

2.2.8.1 Rapamycin

The macrolide Rapamycin has allowed the discovery of the Tor kinases. This molecule is produced by the soil bacterium *Streptomyces hygroscopicus* that was recovered in 1972 from the Easter Islands (Sehgal et al., 1975; Vézina et al., 1975). Developed as an antifungal antibiotic, now it is commonly used in cancer treatment due to its antiproliferative properties (Ballou and Lin, 2008). Rapamycin inhibits specifically TORC1 when assembled in complex with the proline isomerase Fpr1 (yeast ortholog of the mammalian FKBP12). This complex binds the FRB domain of Tor1/2, inhibits its activity and causes cell growth arrest, mimicking the nutrient starvation response (Weisman, 2016). Yang and coworkers proposed that FRB domain of the mammalian mTOR has a role of gatekeeper for the catalytic domain of the kinase, both restricting the access to the catalytic pocket and being a specific substrate docking site (Yang et al., 2013). Thus, when rapamycin-FKBP12 complex binds to the FRB domain, the substrate recruitment is blocked and the active-site access is restricted (Yang et al., 2013). In yeast, the rapamycin-Fpr1 complex binds the FRB domain and causes restricted access of the substrates to the active site. Notably, rapamycin-Fpr1 complex inhibits specifically TORC1 and not TORC2 because the C-terminus of Avo3 subunit masks the FRB domain of Tor2, preventing the binding of the rapamycin-Fpr1 complex to this domain and, thus, the inhibition of TORC2 (Gaubitz et al., 2015).

2.2.8.2 Caffeine

Caffeine is a natural alkaloid that affects different cellular processes linked to cell growth, DNA metabolism, and cell cycle progression, and probably acts as a low-affinity ATP analog (Cortez, 2003; Kaufmann et al., 2003). Independent studies identified TORC1 mutants as being sensitive to caffeine, and indeed in 2006, it was reported that TORC1 is a target of caffeine (Levin, 2005; Martín et al., 2000; Reinke et al., 2004, 2006; Torres et al., 2002). Reinke and colleagues identified mutants in the FRB and the kinase domains of Tor1, that combined confer a significant resistance to caffeine *in vivo* and *in vitro*. The site mutated in FRB domain like that one in the kinase domain is highly conserved (Reinke et al., 2006). This direct negative effect of caffeine on TORC1 was also observed by Wanke and coworkers. They used particular strains in which the TORC1 or the TORC2 essential functions are bypassed, and verified that only TORC1 bypass cells were resistant to high doses of rapamycin or caffeine, confirming the specificity of these inhibitors for TORC1 (Wanke et al., 2008).

2.2.8.3 AUXIN

As part of the studies presented in this thesis, auxin (i.e. indole-3-acetic acid, IAA) has been identified as a TORC1 inhibitor in yeast (See Chapter III). The following paragraph therefore briefly presents an overview of the role of auxin in plants and yeast cells.

Indole-3-acetic acid (IAA), the most abundant compound in the auxin class, is a plant hormone well characterized for its involvement in plant elongation, division, and differentiation, like in the case of root and the shoot development (Abel and Theologis, 2010; Halliday et al., 2009; McSteen, 2010; Möller and Weijers, 2009; Scarpella et al., 2010; Sundberg and Østergaard, 2009; Teale et al., 2006). Beside its involvement in the development of plants, IAA is also considered important for the defense response, such as from the leaf pathogen *Pseudomonas syringae* in *Arabidopsis thaliana* (Navarro et al., 2006). IAA is also synthesized by some microbes, including bacteria and yeast (Basse et al., 1996; Gruen, 1959; Yamada et al., 1985). Few studies analyzed the role of microbial IAA as a signalling molecule

that mediates the interaction between plant and microorganism (Spaepen and Vanderleyden, 2011), and as a growth inhibitor, at high concentrations, in yeast cells (Liu et al., 2016; Prusty et al., 2004).

In plants, IAA regulates development at several levels. Both its metabolism and transport mediate the effect of this auxin on plant development (Enders and Strader, 2015; Petrasek and Friml, 2009; Vanneste and Friml, 2009).

IAA is synthesized *de novo* from tryptophan or by a tryptophan-independent pathway, through the conversion of pre-existing compounds and storage forms (Enders and Strader, 2015). IAA *de novo* biosynthesis is suggested to be a regulator of the tryptophan-independent pathway, while this latter influences IAA transport and sensitivity (Cohen and Bandurski, 1982; Korasick et al., 2013). Storage forms and the regulation of their conversion to IAA are also involved in several development processes, such as root production and elongation (Rampey, 2004; Strader et al., 2010).

IAA can move through the vascular system from one tissue to another or by diffusion from the outside to the inside of the plant cells in its protonated form (Zazímalová et al., 2010). Nevertheless, given its importance, IAA transport from the outside to the inside of the cell and vice versa is highly regulated by many transporters, as illustrated in Figure 4 (Zazímalová et al., 2010).

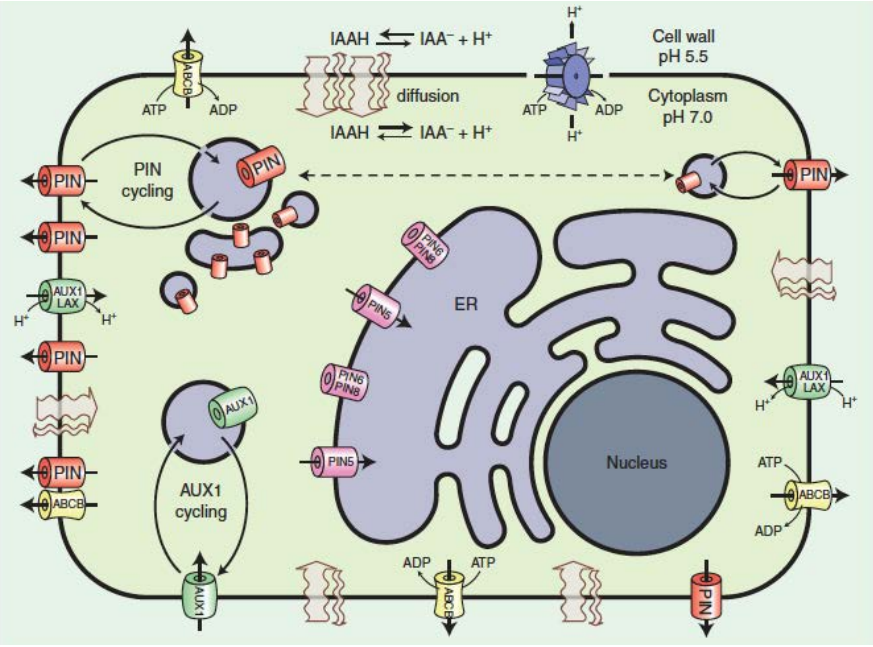

Figure 4. Organization of IAA transporters in *Arabidopsis* cell. Red PINs represent "long" PINs, pink PINs are the "short" PINs transporters. Taken from (Zazímalová et al., 2010).

For the uptake of IAA, the AUX1 and the Like AUX1 (LUX) permeases contribute to internalizing this compound with a H^+-symport mechanism (Kerr and Bennett, 2007). Concerning the efflux, two families of transporters are involved: the PIN transporters (Plant-specific pin-formed proteins) (Ga lweiler et al., 1998; Luschnig et al., 1998) and the ABCB transporters (Verrier et al., 2008).

The role of IAA in yeast cells is still under investigation, but some studies suggested that this molecule is secreted and may control the cell growth of competing fungi (Liu et al., 2016; Prusty et al., 2004; Rao et al., 2010). In *S. cerevisiae*, IAA inhibits filamentation, regulating the morphological transition from the vegetative to the pseudohyphal or filamentous form (Prusty et al., 2004). In the same study, the researchers tried several hormones or indoles, but only IAA was specifically recognized by cells, suggesting the involvement of specific transporters such as the Avt proteins in the IAA uptake (Prusty et al., 2004). They observed that IAA has a different effect depending on its concentration: at high concentrations, it inhibits growth, instead at low concentrations, it promotes filamentation and adhesion (Prusty et al., 2004). At lower concentrations, IAA acts on yeast morphogenesis through the Flo11 protein which is required for filamentation and invasive growth (Gagiano et al., 1999), a process up-regulated in the presence of IAA (Prusty et al., 2004). At higher IAA concentrations, cell growth is inhibited and this effect is dramatically enhanced in mutants devoid of the transcription factor Yap1 (*yap1-1*) (Prusty et al., 2004). Interestingly, the deletion of any of the Avt transporters reduces the hypersensitivity of the *yap1-1* mutant because of the reduced IAA uptake. This correlates with the observation that Avt proteins are homologous to Aux1, the plant permease that allows the internalization of IAA in Arabidopsis (Kerr and Bennett, 2007; Prusty et al., 2004).

Using gas-chromatography mass spectrometry (GC-MS), it was found that *S. cerevisiae* can synthesize IAA from tryptophan in a Trp-dependent pathway that involves two aldehyde dehydrogenases Ald2 and Ald3, but yeast can also produce IAA in a Trp-independent manner (Liu et al., 2016; Rao et al., 2010). Once produced, IAA is secreted into the environment, and likely acts as a regulator of filamentation that is a virulent trait for pathogenic fungi, suggesting a link between IAA and fungal virulence. Notably, in the human pathogen *C. albicans* IAA stimulates filamentation

independently from its filamentation pathway that involves MAP kinases and the PKA pathway (Rao et al., 2010).

Recently, another group proposed that *S. cerevisiae* developed a Trp-independent pathway to synthesize IAA, growing the cells in a medium lacking tryptophan and measuring the produced IAA (Liu et al., 2016). Moreover, it was observed that only three *Saccharomyces* strains can produce IAA in the absence of tryptophan, suggesting that this ability evolved differently among yeast strains (Liu et al., 2016). In addition, the capacity to produce IAA and the tolerance to this compound negatively correlate with each other, suggesting that yeasts produce IAA and secrete it to inhibit the growth of competitors (Liu et al., 2016).

2.3 Downstream signaling

The regulation of TORC1 occurs also through feedback loops, often caused by the effect of its targets or the processes regulated by this complex.

2.3.1 Sch9

Sch9 is a yeast AGC kinase and is the best-characterized target of TORC1. First reported as a phosphoprotein that lost its phosphorylation upon rapamycin treatment, later it was demonstrated to be directly phosphorylated by TORC1 on several residues in the C-terminal domain of the protein (Jorgensen et al., 2004; Urban et al., 2007).

Initially, the functional homolog of Sch9 in mammals was considered the S6 kinase (S6K), for their similar functions and their regulation by TORC1 (Urban et al., 2007). Later, studies pointed out that in yeast the AGC kinase Ypk3 may be the S6K homolog (Gonzalez et al., 2015; Yerlikaya et al., 2016).

Microarray analysis revealed that, through the phosphorylation of Sch9, TORC1 regulates the genes involved in ribosome biogenesis and ribosomal proteins (Urban et al., 2007). Sch9 is also involved in the entry into quiescence preventing the activation of the kinase Rim15 through its phosphorylation (Bontron et al., 2013; Pedruzzi et al., 2003; Wanke et al., 2008).

Finally, TORC1 regulates translation initiation partially via Sch9, affecting the phosphorylation of the initiation factor eIF2α (Urban et al., 2007).
The phosphorylation of Sch9 is commonly used as an *in vivo* readout of the TORC1 activity.

2.3.2 Tap42

Tap42 is a PP2A phosphatase associated protein. When phosphorylated by TORC1, it binds the PP2A and the PP2A-like phosphatase Sit4 catalytic subunit, inhibiting their phosphatase activity (Di Como and Arndt, 1996; Düvel et al., 2003; Jiang and Broach, 1999; Jiang and Carlson, 1996; Weisman, 2016). Upon nutrient starvation, Tap42 is dephosphorylated and dissociates from the phosphatases that are thus active. These phosphatases are responsible for the dephosphorylation of Gln3 and Gat1 proteins, two transcription factors that can thus enter into the nucleus and promote the transcription of the nitrogen catabolite repression (NCR) genes in response to the shortage of the preferred nitrogen sources (Beck and Hall, 1999; Cardenas et al., 1999; Tate et al., 2010).
Together with Sch9, Tap42 contributes to regulate ribosome biogenesis at transcriptional and posttranscriptional levels (Weisman, 2016).

2.3.3 Atg proteins and Autophagy

One of the most important processes regulated by TORC1 is autophagy, an extremely conserved process among eukaryotes, which allows the degradation of molecules and cellular organelles to survive in response to non-favorable growth conditions (Nakatogawa et al., 2009).
Autophagy is induced by nutrient depletion and other stimuli such as growth factors or hormones, but it can also be stimulated by the presence of pathogens, such as bacteria, or damaged organelles (Klionsky, 2007; Mizushima, 2007). Since this process is also linked to cellular and tissue homeostasis (Antonucci et al., 2015), longevity (Rubinsztein et al., 2011; Terman et al., 2007) and development (Mizushima and Levine, 2010), its disfunction is associated with cancer, inflammation, and aging (Yin et al., 2016).

Yeast remarkably helped researchers to understand the autophagy system, as the first mutants in autophagy were identified in this organism (Takeshige et al., 1992).
Autophagy induction is represented by one main event: the formation of the phagophore, a *de novo* formation structure with a double membrane that eventually evolves into a vesicle called autophagosome (Yin et al., 2016). This latter contains the cargo, all the proteins, molecules, and organelles that will be degraded or recycled into the vacuole/lysosome, to obtain energy and essential components (Yin et al., 2016).
Briefly, in yeast, to respond to nutrient starvation, the first step is the formation of the Atg1 complex (Atg1, Atg13, Atg17, Atg31, and Atg29) that is responsible for the recruitment of other Atg proteins to the Phagophore Assembly Site (PAS) (Papinski et al., 2014; Suzuki et al., 2007). Then, the phagophore maturates into the phagosome where the class III phosphatidylinositol 3-kinase complex produces phosphatidylinositol-3-phosphate, a phospholipid necessary for the localization to the PAS of other Atg proteins such as Atg18 and Atg2, which recruit Atg8, Atg9, and Atg12 (Burman and Ktistakis, 2010; Obara et al., 2008). Atg8 and Atg12 are two ubiquitin-like (Ubi) proteins, while Atg9 is a transmembrane protein that acts as a membrane transporter. These three proteins are implicated in the phagophore expansion (Kobayashi et al., 2012; Ohsumi, 2001; Reggiori et al., 2005; Yamamoto et al., 2012). Finally Atg4, a cysteine protease, mediates the deconjugation of Atg8 from the autophagosome membrane, cleaving the phosphatidylethanolamine (PE) from this protein. This process promotes the fusion of the vesicle with the vacuole and the release of the cargo from the autophagic body into the vacuolar lumen (Fig. 5) (Epple et al., 2001; Kirisako et al., 2000; Nair et al., 2012; Teter et al., 2001).

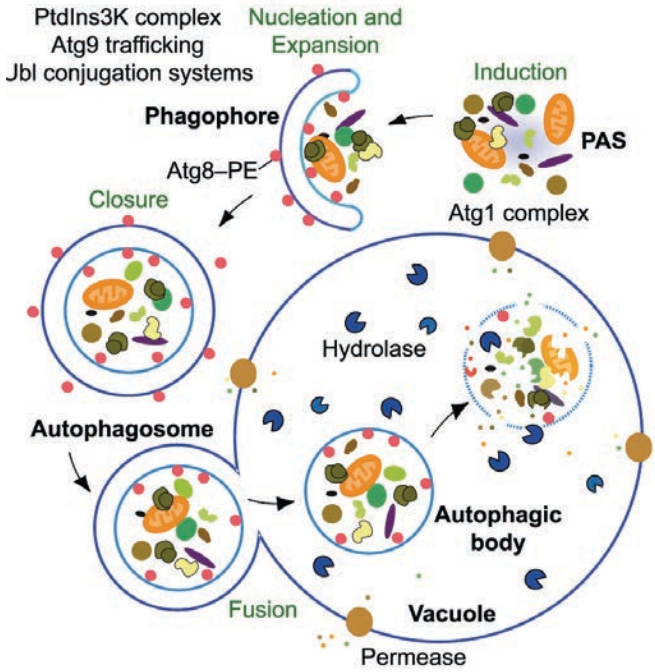

Figure 5. Autophagy machinery in yeast. Schematization of the most important steps required for the autophagy system in yeast. Taken from (Yin et al., 2016).

Three Atg proteins, Atg13/mAtg13 (in both yeast and mammals), Atg1/ULK1, and Atg14 (both only in mammals), were identified as direct TORC1 targets (Hosokawa et al., 2009; Kamada et al., 2010; Yuan et al., 2013).

In particular, Atg13 has a very peculiar role in the autophagy induction because this protein is part of the Atg1 complex (ULK1 complex in mammals). In yeast, this phosphoprotein, very rich in serines, can be phosphorylated by TORC1 but also by PKA, in both cases inhibiting autophagy (Kamada et al., 2010; Stephan et al., 2009). Atg13 interacts with Atg17, which is in a trimeric complex with Atg29 and Atg31. Upon nutrient starvation, TORC1 is inactive and this interaction is strengthened by the dephosphorylation of Atg13, allowing the formation of a multimeric complex and the binding with Atg1, favoring the formation of the PAS to initiate the autophagy (Fujioka et al., 2014; Yamamoto et al., 2016).

Atg1 is a protein kinase that has a basal activity under nutrient rich conditions, to initiate a selective kind of autophagy named the cytoplasm-to-vacuole (Cvt) pathway (Kamada et al., 2000). Under nutrient availability, TORC1 controls the activation of Atg1 through the phosphorylation of Atg13, disrupting its binding with the kinase. Indeed, upon starvation, Atg1 activity increases because of the interaction with dephosphorylated Atg13, allowing its auto-phosphorylation and the

phosphorylation of other Atg proteins, such as Atg9 (Kamada et al., 2000, 2010; Matsuura et al., 1997; Papinski et al., 2014).

Noda and coworkers proposed that, when TORC1 is active at the vacuolar membrane, Atg13 is phosphorylated and it has a cytosolic localization; upon shortage of amino acids, TORC1 is still localized at the vacuolar membrane but in $Gtr2^{GTP}$-dependent punctate structures, through the binding between Gtr2 and Kog1 (Kira et al., 2014, 2016; Noda, 2017). This punctate localization sequesters TORC1 that can not phosphorylate Atg13 anymore, allowing the recruitment of this protein to the PAS and the initiation of autophagy (Kamada et al., 2000; Noda, 2017).

In mammals, ULK1 and mAtg13 are associated even in the presence of nutrients, so the mechanism proposed is that mTOR binds ULK1-Atg13 in a nutrient condition-dependent manner, phosphorylating both Atg proteins upon nutrient availability, which inhibits autophagy (Hosokawa et al., 2009; Jung et al., 2009).

Another direct target of TORC1 identified in mammals is Atg14. This protein is part of the class III phosphatidylinositol 3-kinase complex that is essential for the recruitment of the Atg proteins to the PAS and for induction of autophagy. When phosphorylated, Atg14 does not interact with the rest of the complex, inhibiting its pro-autophagic activity (Yin et al., 2016; Yuan et al., 2013).

TORC1 inhibits autophagy also through gene expression regulation. Indeed, the expression of the ubiquitin-like protein Atg8, involved in the expansion of the autophagosome, considerably increases upon TORC1 inactivation (Huang et al., 2000; Kirisako et al., 1999; Noda, 2017).

AIM and OUTLINE

Aim and Outline

So far, few direct substrates of TORC1 have been identified, such as Sch9 (Urban et al., 2007), Tap42 (Di Como and Arndt, 1996; Düvel et al., 2003; Jiang and Broach, 1999), and Atg13 (Kamada et al., 2010), all involved in the translation of the effect of TORC1 activity on cell growth, in response to nutrients availability. In this context, the general aim of this thesis was to find new targets, as well as new regulators of TORC1.

In the first chapter of this thesis, we present the Lst4 protein as a new direct target of TORC1, which acts through a negative feedback mechanism to control the TORC1 activity homeostatically. Accordingly, Lst4, that is a GAP for Gtr2 together with Lst7 (Lst4-Lst7 complex) (Péli-Gulli et al., 2015), is phosphorylated by TORC1 on several residues within an unstructured region that splits the DENN domain of Lst4 into two parts (intra-DENN loop). Interestingly, the inta-DENN loop is sufficient and necessary for anchoring the Lst4-Lst7 complex to the vacuolar membrane where it exercises its GAP activity on Gtr2. In addition, the phosphorylation status of the intra-DENN loop of Lst4 regulates only the localization of the Lst4-Lst7 complex but does not influence its GAP activity. With the phosphorylation of Lst4 intra-DENN loop, TORC1 regulates its own activation by displacing Lst4-Lst7 complex from the vacuole, avoiding its hyperactivation in presence of amino acids.

In the second chapter of this thesis, we decided to find new substrates of TORC1 and we chose to focus on the cluster of proteins involved in the regulation of autophagy. To achieve this purpose, we screened all the Atg proteins as putative targets of TORC1. After the purification of the substrates, we coupled the TORC1 *in vitro* kinase assay with the mass spectrometry analysis and we found that five Atg proteins (i.e. Atg9, Atg13, Atg23, Atg29, and Atg33) are directly phosphorylated by TORC1. Notably, among the Atg proteins, we found Atg13 that was already described as a TORC1 target (Kamada et al., 2010). Further, we investigated the phosphorylation of one Atg protein in particular, Atg29. Purifying this protein from bacteria, we performed an *in vitro* kinase assay, which revealed several TORC1-dependent phosphosites on Atg29. We present in this part of the thesis

preliminary data as a proof of principle of a new method for the finding of new TORC1 targets. Further studies are necessary to clarify the physiological role of these phosphorylation events on the Atg proteins and in particular on Atg29 by TORC1.

In the third chapter of this thesis, we characterize a new direct inhibitor of TORC1, the plant hormone auxin or indole-3-acetic acid (IAA). It is known that IAA has a negative effect on cell growth (Liu et al., 2016; Prusty et al., 2004), but there are no studies that link the IAA-dependent growth inhibition to the inactivation of TORC1, so we decided to investigate this possibility. We observed the effect of IAA on growth, monitoring the cell proliferation and determining the doubling time of the cell population in the presence or in the absence of different concentrations of IAA. Accordingly, we show that IAA is an inhibitor of TORC1 (determining its IC_{50} *in vivo*) and we confirm that the inhibitory role of IAA on TORC1 is direct performing a TORC1 *in vitro* kinase assay in presence of different concentrations of this compound. Interestingly, we also perform a screening for the hypersensitive mutants to IAA observing a notable overlapping among these with rapamycin-sensitive mutants. Our data suggest that IAA is a physiologically important regulator of TORC1 in yeast.

CHAPTER I:

Feedback Inhibition of the Rag GTPase GAP complex Lst4-Lst7 Safeguards TORC1 from Hyperactivation by Amino Acid Signals

Own contribution to this chapter:

- **Fig. 2B**: TORC1 phosphorylates Lst4 *in vitro*;
- **Fig. 3D**: Lst4 variants combined with Lst7 have similar capacity to stimulate the GTPase activity of Gtr2

Report

Cell Reports

Feedback Inhibition of the Rag GTPase GAP Complex Lst4-Lst7 Safeguards TORC1 from Hyperactivation by Amino Acid Signals

Graphical Abstract

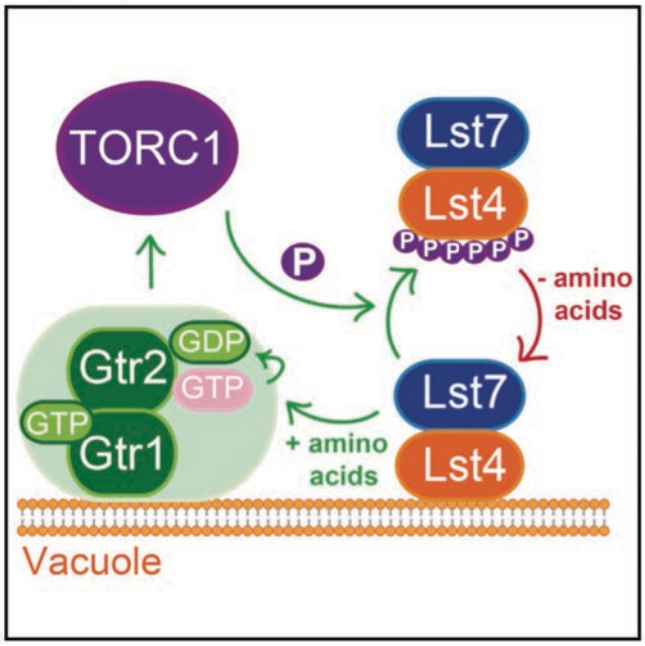

Authors

Marie-Pierre Péli-Gulli, Serena Raucci, Zehan Hu, Jörn Dengjel, Claudio De Virgilio

Correspondence

claudio.devirgilio@unifr.ch

In Brief

Amino acids activate Rag GTPase-TORC1 signaling in part through the conserved Lst4-Lst7 Rag GTPase GAP complex. Here, Péli-Gulli et al. show that the Lst4-Lst7 module is a direct TORC1 target and key node of a feedback mechanism that adjusts TORC1 activity to amino acid availability.

Highlights

- Amino acids activate the Lst4-Lst7-Rag GTPase-TORC1 branch at the vacuolar membrane
- The Lst4 intra-DENN loop is required and sufficient for its membrane tethering
- TORC1 phosphorylates this loop to disperse the Lst4-Lst7 complex from the vacuole
- This feedback inhibition prevents TORC1 hyperactivation and is relevant for growth

Péli-Gulli et al., 2017, Cell Reports *20*, 281–288
July 11, 2017
http://dx.doi.org/10.1016/j.celrep.2017.06.058

CellPress

Cell Reports
Report

Feedback Inhibition of the Rag GTPase GAP Complex Lst4-Lst7 Safeguards TORC1 from Hyperactivation by Amino Acid Signals

Marie-Pierre Péli-Gulli,[1,2] Serena Raucci,[1,2] Zehan Hu,[1] Jörn Dengjel,[1] and Claudio De Virgilio[1,3,*]
[1]Department of Biology, University of Fribourg, CH-1700 Fribourg, Switzerland
[2]These authors contributed equally
[3]Lead Contact
*Correspondence: claudio.devirgilio@unifr.ch
http://dx.doi.org/10.1016/j.celrep.2017.06.058

SUMMARY

Amino acids stimulate the eukaryotic target of rapamycin complex 1 (TORC1), and hence growth, through the Rag GTPases and their regulators. Among these, the yeast Lst4-Lst7 Rag GTPase GAP complex clusters, as we previously reported, at the vacuolar membrane upon amino acid starvation. In response to amino acid refeeding, it activates the Rag GTPase-TORC1 branch and is then dispersed from the vacuolar surface. Here, we show that the latter effect is driven by TORC1 itself, which directly phosphorylates several residues within the intra-DENN loop of Lst4 that, only in its non-phosphorylated state, tethers the Lst4-Lst7 complex to the vacuolar membrane. An Lst4 variant disrupting this feedback inhibition mechanism causes TORC1 hyperactivation and proliferation defects in cells grown on poor nitrogen sources. Thus, we identify Lst4 as a TORC1 target and key node of a homeostatic mechanism that adjusts TORC1 activity to the availability of amino acids.

INTRODUCTION

The eukaryotic target of rapamycin complex 1 (TORC1) is a homeostatic controller of cell growth that adjusts anabolic and catabolic processes to diverse environmental signals, and aberrant mammalian TORC1 (mTORC1) signaling contributes to the progression of human diseases such as cancer and diabetes (Albert and Hall, 2015; Eltschinger and Loewith, 2016; Saxton and Sabatini, 2017). Amino acids are important signals that control TORC1 function via the conserved, heterodimeric Rag family of GTPases (i.e., yeast Gtr1 combined with Gtr2 or mammalian RagA or RagB combined with RagC or RagD) (Binda et al., 2009; Jewell et al., 2013; Kim et al., 2008; Sancak et al., 2008; Sancak and Sabatini, 2009). Rag GTPase heterodimers stimulate TORC1 when they contain GTP-loaded Gtr1/RagA/B and GDP-loaded Gtr2/RagC/D, a configuration that is promoted in part by the GTPase activating protein (GAP) complex Lst4-Lst7 that acts on Gtr2 or the orthologous FNIP1/2-Folliculin (FLCN) complex that acts on RagC/D (Péli-Gulli et al., 2015; Petit et al., 2013; Tsun et al., 2013). How amino acids activate TORC1 through these GAP complexes is currently not known (Hatakeyama and De Virgilio, 2016).

Whereas much attention has been focused on the mechanisms by which amino acids activate (or by which their absence inactivates) the Rag GTPase-TORC1 branch (Powis and De Virgilio, 2016; Saxton and Sabatini, 2017), recent data indicate the presence of additional regulatory layers such as feedback control loops that allow cells to rapidly and dynamically adjust TORC1 activity to changing levels of extracellular amino acids. In mammalian cells, for instance, amino acid-mediated stimulation of the RagA-mTORC1 interaction (and consequently lysosomal membrane recruitment and activation of mTORC1 by Rheb; Saxton and Sabatini, 2017) is likely attenuated by a negative feedback through Skp2-dependent RagA ubiquitination, which recruits GATOR1 to prevent mTORC1 hyperactivation (Jin et al., 2015). Because amino acid stimulation results in transient, Gtr1-dependent hyperactivation of vacuolar membrane-resident TORC1 in cells pregrown on nitrogen-poor media (Stracka et al., 2014), an analogous mechanism may also exist in yeast. In addition, alternative feedback circuits may also act through the Lst4-Lst7 GAP complex, which exhibits only a short-lived preference for Gtr2-binding following re-stimulation of cells with glutamine (Péli-Gulli et al., 2015).

Here, we report on our finding that Lst4 is a bona fide target of TORC1 in yeast and that the TORC1-mediated phosphorylation events on Lst4 serve to disperse the Lst4-Lst7 GAP complex from the vacuolar membrane to attenuate its stimulatory effects on Gtr2 and consequently TORC1 itself in glutamine-fed cells. Replacement of Lst4 residues phosphorylated by TORC1 with alanines results in constitutive vacuolar-membrane recruitment of Lst4-Lst7, which causes TORC1 hyperactivation in glutamine-stimulated cells and growth defects when cells are cultivated on nitrogen-poor media. Conversely, an Lst4 variant mimicking its TORC1-phosphorylated state, despite being fully capable of forming a functional GAP complex with Lst7, is unable to deliver the complex to the vacuolar membrane and fails to mediate amino acid-dependent TORC1 activation. Thus, our study identifies a physiologically relevant negative feedback mechanism that restricts TORC1 signaling upon sustained glutamine stimulation.

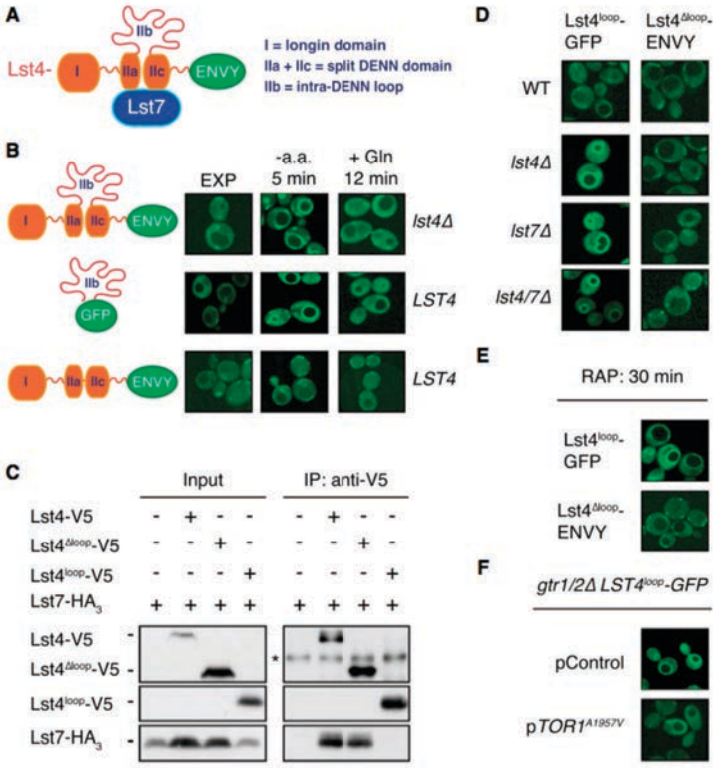

Figure 1. The Lst4 Intra-DENN Loop Is Necessary and Sufficient for Regulated Vacuolar Membrane Tethering

(A) Domain architecture of Lst4 (according to Pacitto et al., 2015). I, longin domain; IIa and IIc, Lst7-binding, split DENN domain; IIb, unstructured intra-DENN loop. Lst4 is represented fused to ENVY, a GFP moiety variant.

(B) Lst4^{loop}-GFP, but not Lst4$^{\Delta loop}$-ENVY, exhibits dynamic redistribution upon amino acid starvation and glutamine refeeding. Indicated strains genomically expressed Lst4-ENVY and Lst4$^{\Delta loop}$-ENVY from the *LST4* promoter or Lst4^{loop}-GFP from the *CYC1* promoter. Cells were cultured exponentially in SC medium (EXP), starved of amino acids for 5 min (-a.a.; 5 min), and restimulated with 3 mM glutamine for 12 min (+ Gln; 12 min).

(C) The Lst4^{loop} is dispensable for the interaction between Lst4 and Lst7. *lst7Δ* cells expressing plasmid-encoded Lst7-HA$_3$ and co-expressing (+) or not (-) the indicated plasmid-encoded Lst4-V5 variants were grown exponentially in SC. Lysates (input) and anti-V5 immunoprecipitates (IP: anti-V5) were analyzed by immunoblotting with anti-HA and anti-V5 antibodies. The asterisk denotes a cross-reacting band.

(D) Lst4^{loop}-GFP, but not Lst4$^{\Delta loop}$-ENVY, accumulates at the vacuolar surface of *lst4Δ*, *lst7Δ*, or *lst4/7Δ* cells. Indicated strains expressing either Lst4^{loop}-GFP or Lst4$^{\Delta loop}$-ENVY as in (B) were grown exponentially in SC. WT, wild-type.

(E) Lst4$^{\Delta loop}$-ENVY is not recruited to the vacuolar membrane following rapamycin treatment. Lst4^{loop}-GFP- or Lst4$^{\Delta loop}$-ENVY-expressing wild-type cells were grown exponentially in SC and then treated with rapamycin for 30 min.

(F) Expression of hyperactive *TOR1*^{A1957V} disperses the Lst4^{loop}-GFP from the vacuolar membrane in *gtr1Δ gtr2Δ* cells. Cells (indicated genotype) expressing or not (pControl) plasmid-encoded *TOR1*^{A1957V} (*pTOR1*^{A1957V}) were grown exponentially in SC.

RESULTS AND DISCUSSION

The Intra-DENN Loop Is Necessary and Sufficient for Regulated Vacuolar Membrane Targeting of Lst4

We previously observed that the Lst4-Lst7 heterodimer, like mammalian FNIP1/2-FLCN, clusters at and is released from the vacuolar membrane upon amino acid starvation and refeeding, respectively (Péli-Gulli et al., 2015; Petit et al., 2013; Tsun et al., 2013). To address the mechanistic basis of this dynamic regulation of the Lst4-Lst7 complex localization, we initially studied the potential role in this process of the unstructured loop within the DENN (differentially expressed in normal and neoplastic cells) domain of Lst4 (encompassing amino acids 400–600 of Lst4 and referred to as Lst4^{loop} hereafter), which splits the Lst7-interacting DENN domain of Lst4 into two halves (Pacitto et al., 2015) (Figure 1A). Like Lst4-ENVY (or Lst4-GFP; see Péli-Gulli et al., 2015), the Lst4^{loop}-GFP construct localized mainly within the cytoplasm of exponentially growing cells, was rapidly recruited to the vacuolar membrane upon starvation of cells for amino acids, and dispersed back to the cytoplasm upon refeeding of cells with glutamine, which is specifically potent for that matter (Figure 1B). An Lst4 ENVY-fusion protein lacking the Lst4^{loop} region (Lst4$^{\Delta loop}$-ENVY), in contrast, remained constitutively cytoplasmic in similar experiments, indicating that the Lst4^{loop} is both necessary and sufficient to mediate the amino acid starvation-induced vacuolar membrane recruitment of Lst4. Of note, control co-immunoprecipitation experiments revealed that the Lst4^{loop} was not required for Lst4 to associate with Lst7 (Figure 1C), as also described earlier (Pacitto et al., 2015). Combined with the fact that Lst7 depends on Lst4 for its vacuolar membrane recruitment (Péli-Gulli et al., 2015), the Lst4^{loop} appears therefore to primarily function in dynamically regulating the localization, but not the Gtr2 GAP function per se (see also below), of the entire Lst4-Lst7 complex.

Previously published data suggested that TORC1 antagonizes the vacuolar enrichment of the Lst4-Lst7 complex by a mechanism that remained unexplored (Péli-Gulli et al., 2015). We suspected therefore that TORC1 might exert its effect on the localization of Lst4-Lst7 by regulating (directly or indirectly) the function of the Lst4^{loop}. In support of this idea, we found interventions that reduce TORC1 activity, such as individual or combined loss of Lst4 and Lst7, combined loss of Gtr1 and Gtr2, and rapamycin treatment to trigger the enrichment of the Lst4^{loop}-GFP, but not that of the Lst4$^{\Delta loop}$-GFP, at the vacuolar membrane

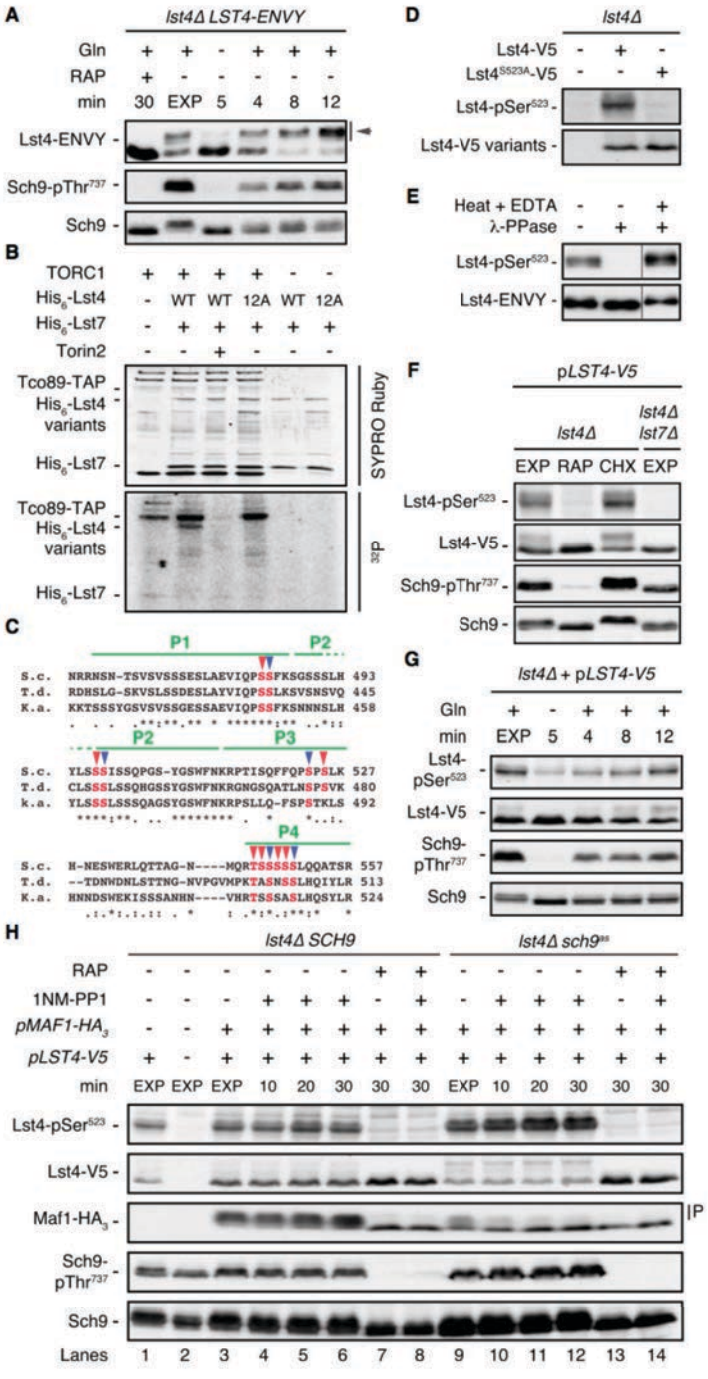

Figure 2. Lst4 Is Phosphorylated In Vivo and In Vitro by TORC1

(A) Lst4-ENVY phosphorylation mirrors TORC1 activation. Lst4-ENVY-expressing *lst4Δ* cells were grown in SC. They were either left untreated (EXP), treated with rapamycin for 30 min (RAP; 30 min), or starved of amino acids for 5 min (-; 5 min) and re-stimulated with 3 mM glutamine for the indicated times (+ Gln; 4–12 min). Phosphorylation of Lst4-ENVY was analyzed on a phostag gel followed by immunoblotting with anti-GFP antibodies. For comparison, phosphorylation of the TORC1 target residue Thr^{737} within Sch9 (Urban et al., 2007) was monitored by immunoblot analysis using anti-Sch9-$pThr^{737}$ and anti-Sch9 antibodies. The arrow points to hyperphosphorylated isoforms of Lst4-ENVY.

(B) TORC1 phosphorylates Lst4 in vitro. Purified recombinant His_6-Lst4/His_6-Lst7 (WT) and His_6-$Lst4^{12A}$/His_6-Lst7 (12A) were subjected to in vitro phosphorylation by TORC1 (purified from yeast) in the absence (-) or presence (+) of the TOR inhibitor Torin2. Representative SYPRO Ruby staining and autoradiography (^{32}P) blots are shown.

(C) TORC1 phosphorylates multiple residues within the intra-DENN loop of Lst4. A multiple sequence alignment of a part of the intra-DENN loop of Lst4 from *S. cerevisiae* (S.c.), *Torulaspora delbrueckii* (T.d.), and *Kazachstania africana* (K.a.) is shown. Mass spectrometric analysis of Lst4, which has been phosphorylated in vitro by purified TORC1, identified four different phosphopeptides (P1–4) with 12 potentially phosphorylated Ser (S)/Thr (T) residues (arrowheads; see Table S3). The 12 Ser/Thr residues that were mutated to Ala in the $Lst4^{12A}$ allele are marked with red or blue arrowheads, while the 5 Ser residues mutated to Asp in the $Lst4^{5D}$ allele are indicated only with blue arrowheads.

(D) Specificity of the anti-Lst4-$pSer^{523}$ antibodies. *lst4Δ* expressing, or not (-), plasmid-encoded Lst4-V5 or $Lst4^{S523A}$-V5 (+) were grown exponentially in SC, and the respective extracts were assayed by immunoblot analysis using anti-Lst4-$pSer^{523}$ and anti-V5 antibodies.

(E) Lst4-ENVY was immunoprecipitated from exponentially growing *lst4Δ* cells and then treated (+), or not (-), with λ-phosphatase (λ-PPase), which was (+), or was not (-), inactivated by heat (65°; 30 min) in the presence of EDTA prior to use. Immunoprecipitates were analyzed by immunoblotting using anti-Lst4-$pSer^{523}$ and anti-GFP antibodies.

(F) Lst4 phosphorylation on Ser^{523} (Lst4-$pSer^{523}$) mirrors TORC1 activation and requires the presence of Lst7. *lst4Δ* or *lst4Δ lst7Δ* strains expressing plasmid-encoded Lst4-V5 were grown exponentially in SC (EXP) and then treated with rapamycin (RAP) or cycloheximide (CHX) for 30 min. Lst4-$pSer^{523}$ and Sch9-$pThr^{737}$ were analyzed as in (D) and (A), respectively.

(G) Amino acid starvation and glutamine refeeding decrease and induce, respectively, the phosphorylation of Ser^{523} in Lst4. Cells (*lst4Δ*) expressing plasmid-encoded Lst4-V5 were treated as in (A). Lst4-$pSer^{523}$ and Sch9-$pThr^{737}$ were analyzed as in (F). See also Figure S1.

(H) Phosphorylation of Ser^{523} in Lst4 does not require Sch9. *lst4Δ SCH9* cells and *lst4Δ sch9Δ* cells that expressed the plasmid-encoded,

(legend continued on next page)

(Figures 1D and 1E). The expression of the hyperactive *TOR1*^{A1957V} allele (Reinke et al., 2006), in contrast, dispersed the Lst4^{loop}-GFP from the vacuolar membrane in *gtr1/2Δ* cells (Figure 1F). The vacuolar membrane recruitment of the Lst4^{loop}-GFP occurs therefore independently of the presence of Lst4-Lst7 or Gtr1-Gtr2 and is negatively regulated by TORC1.

The Lst4^{loop} Harbors Multiple TORC1 Phosphorylation Sites

Phostag gel electrophoresis separated Lst4-ENVY from extracts of exponentially growing wild-type cells into two roughly equal populations of fast and slowly migrating isoforms (Figure 2A). The levels of the latter, which we assumed corresponded to hyperphosphorylated variants of Lst4-ENVY, closely correlated with TORC1 activity, being barely detectable in rapamycin-treated and amino acid-starved cells but rapidly induced upon readdition of glutamine to starved cells (Figure 2A). To test whether Lst4 is a direct substrate of TORC1, a model we deemed feasible on the basis of both our present results and the reported spatial proximity of Lst4 and TORC1 at the vacuolar membrane (Binda et al., 2009; Péli-Gulli et al., 2015; Sturgill et al., 2008), we asked whether Lst4 could be a substrate of TORC1 in vitro. Indeed, TORC1 (purified from yeast) phosphorylated recombinant Lst4 (co-purified with Lst7) in the absence but not in the presence of the ATP-competitive TOR inhibitor Torin2 (Liu et al., 2013) (Figure 2B). Mass spectrometry (MS) analysis of the respective phosphorylated Lst4 protein allowed us to identify 4 non-overlapping phosphopeptides covering neighboring amino acid stretches within the intra-DENN loop of Lst4 with 12 potential phospho-Ser/Thr residues (see Table S3), many of which appeared to be conserved in closely related yeast species (Figure 2C). Because TORC1 was unable to phosphorylate in vitro an Lst4^{12A} variant in which these 12 Ser/Thr residues were substituted with Ala (Figure 2B), these 12 residues encompass the majority of residues in Lst4 that are modified by TORC1. To determine whether TORC1 also phosphorylates Lst4 in vivo, we used antibodies that recognized 1 of these 12 residues in Lst4 (i.e., Ser^{523}) specifically in its phosphorylated state (Figures 2D and 2E). Accordingly, we found that rapamycin-mediated TORC1 inhibition abolished whereas cycloheximide-mediated TORC1 activation (Binda et al., 2009) induced the phosphorylation of Ser^{523} within Lst4 (Lst4-pSer^{523}), as observed for the bona fide TORC1 target residue Thr^{737} in Sch9 (Sch9-pThr^{737}) (Urban et al., 2007) (Figure 2F). In addition, physiological interventions such as starvation for amino acids and glutamine refeeding also decreased and induced, respectively, both Lst4-pSer^{523} and Sch9-pThr^{737} levels with similar dynamics (Figure 2G). Moreover, glutamine refeeding failed to stimulate Lst4-Ser^{523} phosphorylation in the presence of rapamycin and did not significantly alter the levels of Lst4 (Figures S1A and S1B).

Although our in vitro and in vivo experiments pinpointed Lst4 as a direct TORC1 target, we considered it still formally possible that TORC1 controls Lst4 phosphorylation indirectly via Sch9. To address this point, we performed additional control experiments using a strain that expressed an ATP analog (1NM-PP1) sensitive Sch9^{as} variant (Huber et al., 2009). Because of the hypomorphic nature of this mutant allele (Huber et al., 2009), exponentially growing cells of the respective strain showed decreased basal phosphorylation levels of the Sch9 target Maf1 (i.e., lower levels of the slowly migrating, hyperphosphorylated Maf1 isoforms; compare lanes 3 and 9 in Figure 2H) that could be further reduced by 1NM-PP1 treatment (Figure 2H, lanes 10–12). Remarkably, however, *sch9*^{as} cells exhibited strongly increased basal levels of both Lst4-pSer^{523} and Sch9-pThr^{737} that were even further boosted by 1NM-PP1 treatment (Figure 2H, lanes 10–12). These results not only imply that Sch9 downregulation triggers TORC1 activation via a hitherto undescribed feedback mechanism but also exclude the involvement of Sch9 in direct phosphorylation of Lst4 (see also Figure S2). All of our data combined therefore confirm Lst4 as a bona fide target of TORC1.

Lst4 and Lst7 depend on each other for their assembly on the vacuolar membrane (Péli-Gulli et al., 2015). On the basis of our present observations and recent structural studies of Lst4 (Pacitto et al., 2015), this is likely explained by the fact that Lst7 binds to and consequently reunites the separated parts of the Lst4 split DENN domain, thereby also ensuring the proper folding of the intra-DENN loop of Lst4, which drives the joint recruitment of Lst4 and Lst7 to the vacuolar membrane (Figure 1A). Our results therefore predicted that loss of Lst7 should deprive the vacuolar membrane-resident TORC1 of its potential to gain access to and phosphorylate Lst4. This was indeed the case, as we could not detect any phosphorylation of Lst4-Ser^{523} in the absence of Lst7, while TORC1 was still able, albeit with reduced activity as expected, to phosphorylate Sch9-Thr^{737} in the same strain (Figure 2F).

TORC1 Phosphorylation Sites Critically Control Lst4 Localization

To analyze the role of TORC1-dependent phosphorylation of Lst4, we next studied the properties of Lst4, Lst4^{12A}, and the Lst4^{5D} variant, which carried phosphomimetic Asp (D) substitutions of those 5 Ser residues (i.e., Ser^{484}, Ser^{498}, Ser^{523}, Ser^{547}, and Ser^{550}) that our mass spectrometry analyses identified as the most probable TORC1-dependent phosphorylation sites within Lst4 (Figure 2C). In line with our previous results (Péli-Gulli et al., 2015), amino acid starvation (or rapamycin treatment) rapidly provoked a strong enrichment of Lst4-ENVY at the vacuolar membrane, which was reversed in starved cells when refed with glutamine (Figure 3A). Under the same conditions, Lst4^{12A}-ENVY was found constitutively enriched at, while Lst4^{5D} was invariably absent from the vacuolar membrane (Figure 3A). Importantly, both variants Lst4^{12A} and Lst4^{5D} associated normally with Lst7 within cells (Figure 3B). Moreover, they dictated the localization of Lst7, as Lst7-GFP was constitutively tethered to the vacuolar membrane in Lst4^{12A}-expressing cells, while it was unable to reach the vacuolar membrane

1NM-PP1 ATP analog-sensitive *sch9*^{as} allele (*lst4Δ sch9*^{as}) co-expressed (+), or not (-), Lst4-V5 and the Sch9 substrate Maf1-HA$_3$ from plasmids. Cells were grown exponentially (EXP) in SC and then subjected (+), or not (-), to rapamycin (RAP) and/or 1NM-PP1 treatments for the indicated times. Lst4-pSer^{523}, Lst4-V5, Maf1-HA$_3$, Sch9-pThr^{737}, and Sch9 were monitored by immunoblot analysis using anti-Lst4-pSer^{523}, anti-V5, anti-HA$_3$, anti-Sch9-pThr^{737}, and anti-Sch9 antibodies, respectively. P, phosphorylated isoforms of Maf1-HA$_3$. See also Figure S2.

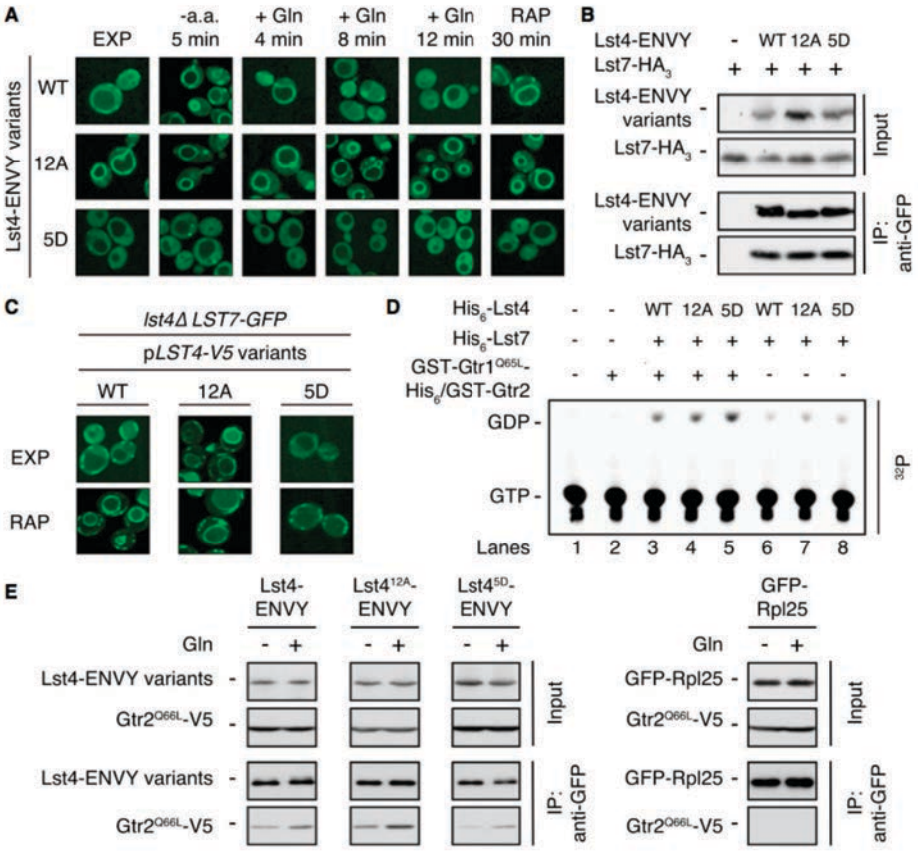

Figure 3. TORC1 Phosphorylation Sites Critically Control Lst4 Localization

(A) Lst4^{12A}-ENVY (12A) is stably enriched at, while Lst4^{5D}-ENVY (5D) is unable to reach the vacuolar surface. Cells (*lst4Δ*) expressing the indicated Lst4-ENVY variants from their genomes were grown exponentially in SC (EXP), treated with rapamycin (RAP), or starved of amino acids (-a.a.) and refed with 3 mM glutamine (+ Gln) for the indicated times.

(B) Lst4^{12A} and Lst4^{5D} normally associate with Lst7. Cells (*lst4Δ lst7Δ*) expressing, or not (-), Lst4-ENVY (WT), Lst4^{12A}-ENVY (12A), or Lst4^{5D}-ENVY (5D) from their genomes together with plasmid-encoded Lst7-HA$_3$ (+) were grown exponentially in SC. Lysates (input) and anti-GFP immunoprecipitates (IP: anti-GFP) were analyzed by immunoblotting using anti-HA and anti-GFP antibodies.

(C) Lst4 phospho-variants dictate Lst7-GFP localization. Cells (*lst4Δ LST7-GFP*) expressing plasmid-encoded Lst4-V5, Lst4^{12A} -V5, or Lst4^{5D}-V5 were grown exponentially (EXP) in SC or treated with rapamycin for 30 min (RAP).

(D) Lst4 (WT), Lst4^{12A} (12A), and Lst4^{5D} (5D) stimulate the GTPase activity of Gtr2 to a similar extent when combined with Lst7. Purified GST-Gtr1^{Q65L}-His$_6$/GST-Gtr2 (200 nM) were pre-loaded with (α-^{32}P) GTP and incubated for 20 min in the presence (WT, +; 12A, +; 5D, +; lanes 3–5) or absence (-, -; lane 2) of the different Lst4-Lst7 heterodimers (each 100 nM). The extent of (α -^{32}P) GTP hydrolysis to (α-^{32}P) GDP was measured by thin-layer chromatography (TLC), of which one representative autoradiograph is shown. In control experiments, (α-^{32}P) GTP was incubated alone (lane 1) or only together with the Lst4-Lst7 heterodimer variants (lanes 6–8). Notably, Lst4-Lst7, Lst4^{12A}-Lst7, and Lst4^{5D}-Lst7 did not significantly differ in their capacities to enhance the GTP hydrolytic activity of Gtr2, as the respective GAP-mediated fold increase of GTP hydrolysis was 31.5 ± 2.7 for Lst4-Lst7, 38.5 ± 12.0 for Lst4^{12A}-Lst7, and 41.4 ± 16.6 for Lst4^{5D}-Lst7 (n = 3; ±SD).

(E) Exponentially growing *lst4Δ gtr1Δ gtr2Δ* and *gtr1Δ gtr2Δ* cells expressing the Lst4-ENVY variants and GFP-Rpl25 (control), respectively, as well as Gtr1-HA$_3$ and Gtr2^{Q66L}-V5, were starved for amino acids (5 min; -) and then restimulated with glutamine (4 min; Gln; +). Lysates (input) and anti-GFP immunoprecipitates (IP: anti-GFP) were analyzed by immunoblotting using anti-GFP and anti-V5 antibodies. The corresponding interactions with wild-type Gtr2 were similar to, but overall weaker than, the ones with the preferred Lst4 substrate Gtr2^{Q66L} (Péli-Gulli et al., 2015; data not shown).

even in rapamycin-treated, Lst4^{5D}-expressing cells (Figure 3C). Interestingly, all heterodimeric variants normally stimulated the GTPase activity of Gtr2 when assayed in vitro (Figure 3D). Within cells, however, glutamine refeeding expectedly over-stimulated the interaction between Lst4^{12A} and GTP-locked Gtr2^{Q66L}, while Lst4^{5D} was significantly compromised in its

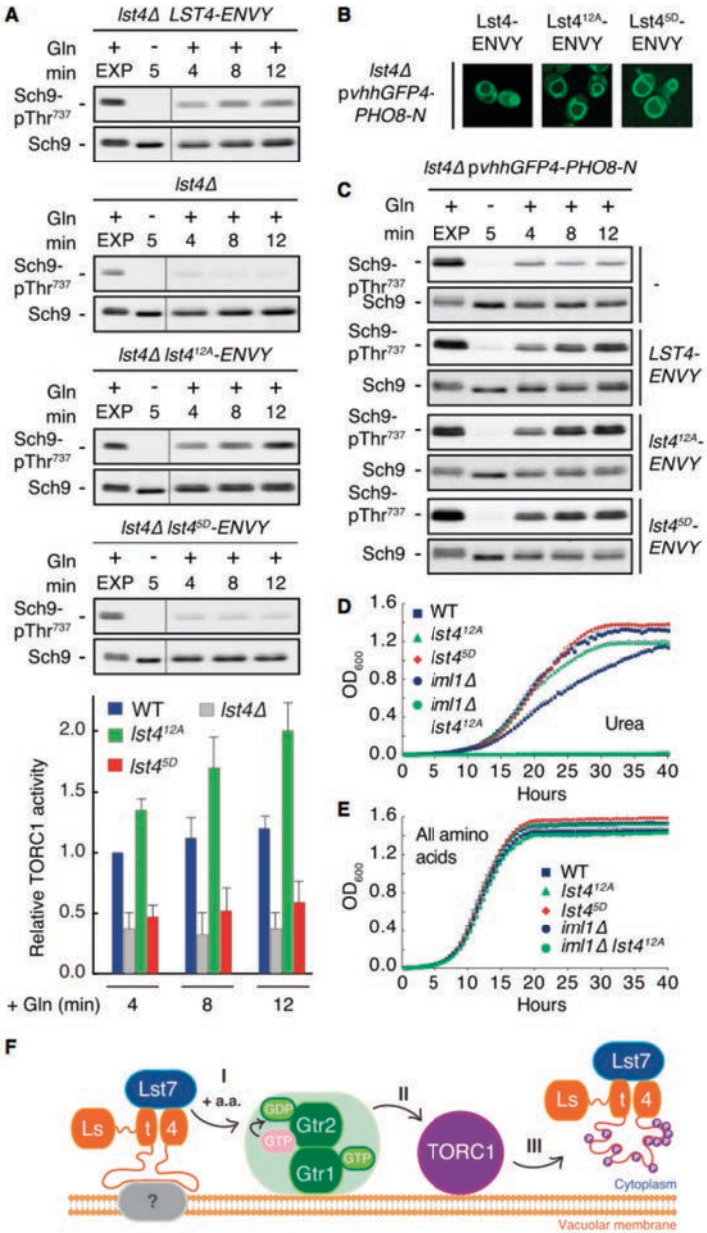

Figure 4. Homeostatic Control of TORC1 in Response to Amino Acids Relies on Feedback Inhibition of the Rag GTPase GAP Complex Lst4-Lst7

(A) Lst4, Lst4^{12A}, and Lst4^{5D} exhibit distinct TORC1 activation properties in vivo. Cells (*lst4Δ*) expressing, or not, the indicated Lst4-ENVY variants from their genomes were grown and tested for their TORC1 activities as in Figure 2A. Relative TORC1 activities were determined as the ratio of Sch9-pThr^{737}/Sch9 in *lst4Δ LST4-ENVY* (WT), *lst4Δ*, *lst4Δ lst4^{12A}-ENVY* (*lst4^{12A}*), and *lst4Δ lst4^{5D}-ENVY* (*lst4^{5D}*) cells, normalized to that of WT cells after 4 min of glutamine (Gln) refeeding, and presented in a bar graph as mean ± SD (n = 3).

(B) Artificial vacuolar membrane anchorage of Lst4-ENVY variants. Vacuolar membrane tethering of Lst4-ENVY variants in *lst4Δ* cells (grown exponentially on SC) was achieved through overexpression of the Pho8 N terminus fused to vhhGFP4, an anti-GFP single-domain antibody fragment (Caussinus et al., 2011).

(C) Constitutive vacuolar membrane tethering of Lst4^{5D}-ENVY suppresses its defect in mediating TORC1 activation by amino acid. Cells (*lst4Δ*) overexpressing vhhGFP4-Pho8-N and co-expressing, or not (-), the indicated Lst4-ENVY variants were cultured and assayed for TORC1 activation as in (A).

(D and E) Expression of the Lst4^{12A} variant impairs growth on nitrogen-poor medium. Growth curves of *lst4Δ* cells expressing Lst4-ENVY, Lst4^{12A}-ENVY, or Lst4^{5D}-ENVY, or of *iml1Δ lst4Δ* cells expressing Lst4-ENVY or Lst4^{12A}-ENVY from their genomes (relevant genotypes are indicated). Strains were either grown in SD containing 2.5 mM urea instead of ammonium sulfate (D) or in SC containing a mixture of all amino acids (E) as nitrogen source. Growth was monitored using a Bioscreen C reader set at 30°C with readings (OD_{600}) taken every 30 min. The experiments were performed independently three times with technical quadruplicates. Data are means + SD.

(F) TORC1 feedback inhibits Lst4-Lst7. For details, see text.

capacity to bind Gtr2^{Q66L} under the same conditions (Figure 3E). Taken together, our results are all consistent with a model in which TORC1-dependent phosphorylation of Lst4 primarily serves to dislodge the Lst4-Lst7 GAP complex from the vacuolar membrane.

TORC1-Mediated Control of Lst4 Localization Is Part of a Negative Feedback Mechanism

Given that the Lst4-Lst7 complex is critical for amino acid-dependent TORC1 activation, we reasoned that the aberrant subcellular localization of Lst4^{12A} or Lst4^{5D} might affect TORC1 activity in vivo. Indeed, the Lst4^{12A} mutant allele significantly hyperstimulated TORC1 in glutamine-refed cells (Figure 4A). Conversely, cells expressing the Lst4^{5D} allele exhibited, like *lst4Δ* cells, a strong defect in TORC1 reactivation when refed with glutamine subsequent to amino acid starvation (Figure 4A). As expected on the basis of our in vitro GAP assays (Figure 3D), both Lst4 alleles (i.e., Lst4^{12A} and Lst4^{5D}) were equally competent in vivo to reactivate TORC1 upon glutamine refeeding when they were

artificially and constitutively tethered to the vacuolar membrane (Figures 4B and 4C). Thus, the vacuolar membrane localization of Lst4 (combined with Lst7) is a pivotal process that is required for Rag GTPase-dependent activation of TORC1 by amino acids, and TORC1 inhibits (in a feedback loop) the Lst4-Lst7 Rag GTPase GAP primarily by favoring its dispersal from the surface of the vacuole.

Homeostatic control of TORC1 activity is important for the adaptation of cells to changing environments. Accordingly, a downshift in the quality of the nitrogen source coordinately downregulates TORC1 to induce, for instance, the expression of specific amino acid permeases and catabolic enzymes, and failure to do so (e.g., when cells express hyperactive Rag GTPases) results in cell proliferation defects on nitrogen-poor media (Binda et al., 2009; Neklesa and Davis, 2009). Consistent with this notion and the observed TORC1 activities in our *lst4* mutants (Figure 4A), we found *lst4*^{12A} cells, but not wild-type or *lst4*^{5D} cells, to exhibit a moderate but statistically significant cell proliferation defect when grown on the poor nitrogen source urea, while all strains grew equally well on a preferred nitrogen source (i.e., a mixture of all amino acids; Figures 4D and 4E). Moreover, loss of the Gtr1 GAP Iml1, which causes Gtr1 to be predominantly in its TORC1-activating GTP-bound state (Panchaud et al., 2013), caused a similar growth defect when cells were grown on urea (Figure 4D). Remarkably, the combination of *iml1Δ* (sustaining Gtr1^{GTP}) and *lst4*^{12A} (sustaining Gtr2^{GDP}) caused a dramatic synthetic growth defect that rendered cells unable to grow on urea, while they grew normally on amino acid-rich medium (Figures 4D and 4E). Appropriate feedback inhibition of the Lst4-Lst7 module by TORC1 is therefore part of a physiologically relevant adaptation program.

Taken together, our work advocates a model in which amino acid limitation triggers, through a still largely elusive mechanism, TORC1 downregulation, thereby favoring dephosphorylation and recruitment of the GAP complex Lst4-Lst7 to the vacuolar membrane (Figure 4F). In addition to being tethered proximally to Gtr2, the Lst4-Lst7 GAP further requires the presence of amino acids to be able to act on Gtr2 (Figure 4F, I), which then, in association with Gtr1, stimulates TORC1 (Figure 4F, II). Subsequent feedback inhibition of Lst4-Lst7 (Figure 4F, III), as revealed in this study, is a central element that secures the dynamic adjustment of TORC1 activity in response to amino acids. Further refinement of this model will undoubtedly depend on the identification of the protein(s) that dock Lst4 to the vacuolar membrane (Figure 4F, question mark). While we deem it possible that such a protein(s) may also be implicated in local amino acid-driven activation of the Lst4-Lst7 complex toward Gtr2, we speculate that the multiple TORC1 target residues in Lst4 might additively dictate the recognition of such a protein(s) and hence provide an additional regulatory layer to fine-tune graded TORC1 feedback responses. Finally, human FNIP1/2, like Lst4, contain a split DENN domain (Pacitto et al., 2015), and FLCN reportedly concentrates at the lysosomal surface upon mTORC1 inactivation in a human retinal pigment epithelial cell line (ARPE-19) (Martina et al., 2014), indicating that mTORC1 may use a feedback mechanism in higher eukaryotes that is analogous to the one in yeast.

EXPERIMENTAL PROCEDURES

Strains, Plasmids, and Growth Conditions

Saccharomyces cerevisiae strains and plasmids used in this study are listed in Tables S1 and S2, respectively. Exclusively prototrophic yeast strains were used throughout this study. Unless stated otherwise, yeast cells were pre-grown in synthetic dropout (SD; 0.17% yeast nitrogen base, 0.5% ammonium sulfate [AS], 0.2% dropout mix [USBiological], and 2% glucose) medium to maintain plasmids, spun and diluted in synthetic complete medium (SC; SD with all amino acids, but without AS), starved of amino acids and restimulated with 3 mM glutamine as previously reported (Péli-Gulli et al., 2015). Rapamycin (LC Laboratories), cycloheximide (Sigma), and 1 NM-PP1 (Cayman Chemicals) were used at 200 ng ml^{-1}, 25 μg ml^{-1}, and 200 nM, respectively, for the times indicated.

In Vivo and In Vitro TORC1 Activity Assays

In vivo TORC1 activity was monitored as previously described (Péli-Gulli et al., 2015), making use of phosphospecific anti-Sch9-pThr^{737} and anti-Sch9 antibodies (GenScript) to probe endogenous Sch9. For in vitro kinase assays, TORC1 was TAP-purified from a Tco89-TEV-TAP-expressing yeast strain grown in YPD and treated for 10 min with cycloheximide. The extraction buffer (50 mM HEPES/NaOH [pH 7.5], 5 mM CHAPS, 400 mM NaCl, 1 mM EDTA, 0.5 mM DTT, 400 μM Pefabloc, 1× Roche complete protease inhibitor-EDTA) was used to resuspend cells that were subjected to cryogenic disruption with an MM 400 Mixer Mill (Retsch). The cleared lysate was incubated with IgG-coupled Dynabeads (Dynabeads M-270 Epoxy; Invitrogen) for 2 hr at 4°C. After washes, the TORC1 complex was eluted using 5% TEV protease. Recombinant His$_6$-tagged Lst4 variants (600 ng/30 μl reaction) were co-purified with His$_6$-tagged Lst7 and used as in vitro substrates in TORC1 kinase reactions performed according to Urban et al. (2007). Briefly, reactions were performed in kinase buffer (50 mM HEPES/NaOH [pH 7.5], 5 mM CHAPS, 400 mM NaCl, 0.5 mM DTT, phosphatase inhibitors), started by adding the ATP Mix (4.2 mM $MgCl_2$, 300 μM ATP, and 3.3 μCi [γ-^{32}P]-ATP [Hartmann Analytic, SRP-501]) and stopped by adding SDS-PAGE sample buffer. Proteins were separated by SDS-PAGE, stained with Sypro Ruby (Sigma), and analyzed using a phosphorimager (Typhoon FLA 9500; GE Healthcare).

Mass Spectrometry Analyses

Mass spectrometric measurements were performed on a Q Exactive Plus mass spectrometer coupled to an EasyLC 1000 (Thermo Fisher Scientific). Prior analysis phosphopeptides were enriched by TiO_2. The mass spectrometry raw data files were analyzed using MaxQuant software (Cox and Mann, 2008), version 1.4.1.2, using a Uniprot *S. cerevisiae* database from March 2016 containing common contaminants such as keratins and enzymes used for in-gel digestion.

Miscellaneous

GAP assays were performed as previously detailed (Péli-Gulli et al., 2015). Co-immunoprecipitation and fluorescence microscopy experiments were also carried out as described before (Panchaud et al., 2013). Phosphorylated forms of tagged-Lst4 were detected by electrophoresis on a 6% SDS-PAGE gel containing 20 μM Phos-tag (Wako) followed by immunoblotting with anti-GFP antibodies (Roche) or by classical SDS-PAGE and immunoblotting using anti-Lst4-pSer^{523} antibodies generated by GenScript and anti-V5 antibodies (Thermo Fisher Scientific). A standard protocol was applied to in vitro dephosphorylate immunoprecipitated Lst4-ENVY with λ-phosphatase (New England Biolabs).

SUPPLEMENTAL INFORMATION

Supplemental Information includes two figures and three tables and can be found with this article online at http://dx.doi.org/10.1016/j.celrep.2017.06.058.

AUTHOR CONTRIBUTIONS

Conceptualization, M.-P.P.-G., S.R., and C.D.V.; Methodology, M.-P.P.-G., S.R., Z.H., J.D., and C.D.V.; Investigation, M.-P.P.-G., S.R., and Z.H.;

Writing – Original Draft, C.D.V.; Writing – Review & Editing, M.-P.P.-G., J.D., and C.D.V.; Funding Acquisition, Resources, & Supervision, J.D. and C.D.V.

ACKNOWLEDGMENTS

We thank Floriane Jacquier, Hélène Bloechlinger, and Yvan Meier for technical assistance and Robbie Loewith, Dieter Kressler, and Riko Hatakeyama for plasmids. This research was supported by the Canton of Fribourg and the Swiss National Science Foundation (J.D. and C.D.V.).

Received: April 10, 2017
Revised: June 2, 2017
Accepted: June 21, 2017
Published: July 11, 2017

REFERENCES

Albert, V., and Hall, M.N. (2015). mTOR signaling in cellular and organismal energetics. Curr. Opin. Cell Biol. *33*, 55–66.

Binda, M., Péli-Gulli, M.P., Bonfils, G., Panchaud, N., Urban, J., Sturgill, T.W., Loewith, R., and De Virgilio, C. (2009). The Vam6 GEF controls TORC1 by activating the EGO complex. Mol. Cell *35*, 563–573.

Caussinus, E., Kanca, O., and Affolter, M. (2011). Fluorescent fusion protein knockout mediated by anti-GFP nanobody. Nat. Struct. Mol. Biol. *19*, 117–121.

Cox, J., and Mann, M. (2008). MaxQuant enables high peptide identification rates, individualized p.p.b.-range mass accuracies and proteome-wide protein quantification. Nat. Biotechnol. *26*, 1367–1372.

Eltschinger, S., and Loewith, R. (2016). TOR complexes and the maintenance of cellular homeostasis. Trends Cell Biol. *26*, 148–159.

Hatakeyama, R., and De Virgilio, C. (2016). Unsolved mysteries of Rag GTPase signaling in yeast. Small GTPases *7*, 239–246.

Huber, A., Bodenmiller, B., Uotila, A., Stahl, M., Wanka, S., Gerrits, B., Aebersold, R., and Loewith, R. (2009). Characterization of the rapamycin-sensitive phosphoproteome reveals that Sch9 is a central coordinator of protein synthesis. Genes Dev. *23*, 1929–1943.

Jewell, J.L., Russell, R.C., and Guan, K.L. (2013). Amino acid signalling upstream of mTOR. Nat. Rev. Mol. Cell Biol. *14*, 133–139.

Jin, G., Lee, S.W., Zhang, X., Cai, Z., Gao, Y., Chou, P.C., Rezaeian, A.H., Han, F., Wang, C.Y., Yao, J.C., et al. (2015). Skp2-mediated RagA ubiquitination elicits a negative feedback to prevent amino-acid-dependent mTORC1 hyperactivation by recruiting GATOR1. Mol. Cell *58*, 989–1000.

Kim, E., Goraksha-Hicks, P., Li, L., Neufeld, T.P., and Guan, K.L. (2008). Regulation of TORC1 by Rag GTPases in nutrient response. Nat. Cell Biol. *10*, 935–945.

Liu, Q., Xu, C., Kirubakaran, S., Zhang, X., Hur, W., Liu, Y., Kwiatkowski, N.P., Wang, J., Westover, K.D., Gao, P., et al. (2013). Characterization of Torin2, an ATP-competitive inhibitor of mTOR, ATM, and ATR. Cancer Res. *73*, 2574–2586.

Martina, J.A., Diab, H.I., Lishu, L., Jeong-A, L., Patange, S., Raben, N., and Puertollano, R. (2014). The nutrient-responsive transcription factor TFE3 promotes autophagy, lysosomal biogenesis, and clearance of cellular debris. Sci. Signal. *7*, ra9.

Neklesa, T.K., and Davis, R.W. (2009). A genome-wide screen for regulators of TORC1 in response to amino acid starvation reveals a conserved Npr2/3 complex. PLoS Genet. *5*, e1000515.

Pacitto, A., Ascher, D.B., Wong, L.H., Blaszczyk, B.K., Nookala, R.K., Zhang, N., Dokudovskaya, S., Levine, T.P., and Blundell, T.L. (2015). Lst4, the yeast Fnip1/2 orthologue, is a DENN-family protein. Open Biol. *5*, 150174.

Panchaud, N., Péli-Gulli, M.P., and De Virgilio, C. (2013). Amino acid deprivation inhibits TORC1 through a GTPase-activating protein complex for the Rag family GTPase Gtr1. Sci. Signal. *6*, ra42.

Péli-Gulli, M.P., Sardu, A., Panchaud, N., Raucci, S., and De Virgilio, C. (2015). Amino acids stimulate TORC1 through Lst4-Lst7, a GTPase-activating protein complex for the Rag family GTPase Gtr2. Cell Rep. *13*, 1–7.

Petit, C.S., Roczniak-Ferguson, A., and Ferguson, S.M. (2013). Recruitment of folliculin to lysosomes supports the amino acid-dependent activation of Rag GTPases. J. Cell Biol. *202*, 1107–1122.

Powis, K., and De Virgilio, C. (2016). Conserved regulators of Rag GTPases orchestrate amino acid-dependent TORC1 signaling. Cell Discov. *2*, 15049.

Reinke, A., Chen, J.C., Aronova, S., and Powers, T. (2006). Caffeine targets TOR complex I and provides evidence for a regulatory link between the FRB and kinase domains of Tor1p. J. Biol. Chem. *281*, 31616–31626.

Sancak, Y., and Sabatini, D.M. (2009). Rag proteins regulate amino-acid-induced mTORC1 signalling. Biochem. Soc. Trans. *37*, 289–290.

Sancak, Y., Peterson, T.R., Shaul, Y.D., Lindquist, R.A., Thoreen, C.C., Bar-Peled, L., and Sabatini, D.M. (2008). The Rag GTPases bind raptor and mediate amino acid signaling to mTORC1. Science *320*, 1496–1501.

Saxton, R.A., and Sabatini, D.M. (2017). mTOR signaling in growth, metabolism, and disease. Cell *168*, 960–976.

Stracka, D., Jozefczuk, S., Rudroff, F., Sauer, U., and Hall, M.N. (2014). Nitrogen source activates TOR (target of rapamycin) complex 1 via glutamine and independently of Gtr/Rag proteins. J. Biol. Chem. *289*, 25010–25020.

Sturgill, T.W., Cohen, A., Diefenbacher, M., Trautwein, M., Martin, D.E., and Hall, M.N. (2008). TOR1 and TOR2 have distinct locations in live cells. Eukaryot. Cell *7*, 1819–1830.

Tsun, Z.Y., Bar-Peled, L., Chantranupong, L., Zoncu, R., Wang, T., Kim, C., Spooner, E., and Sabatini, D.M. (2013). The folliculin tumor suppressor is a GAP for the RagC/D GTPases that signal amino acid levels to mTORC1. Mol. Cell *52*, 495–505.

Urban, J., Soulard, A., Huber, A., Lippman, S., Mukhopadhyay, D., Deloche, O., Wanke, V., Anrather, D., Ammerer, G., Riezman, H., et al. (2007). Sch9 is a major target of TORC1 in *Saccharomyces cerevisiae*. Mol. Cell *26*, 663–674.

Cell Reports, Volume *20*

Supplemental Information

Feedback Inhibition of the Rag GTPase GAP Complex Lst4-Lst7 Safeguards TORC1 from Hyperactivation by Amino Acid Signals

Marie-Pierre Péli-Gulli, Serena Raucci, Zehan Hu, Jörn Dengjel, and Claudio De Virgilio

Supplemental Information

Supplemental Figures

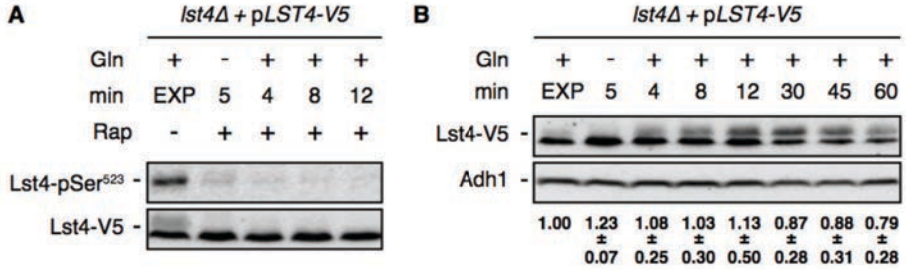

Figure S1. Glutamine Refeeding Fails to Stimulate Lst4-Ser^{523} Phosphorylation in the Presence of Rapamycin and Does Not Significantly Alter Lst4 Levels, Related to Fig. 2G

(A) TORC1 inhibition prevents glutamine-stimulated phosphorylation of Ser^{523} in Lst4. Cells (*lst4*Δ) expressing plasmid-encoded Lst4-V5 were treated as in Figure 2G, except that rapamycin (200 ng ml^{-1}) was added at the beginning of the amino acid starvation and maintained throughout the glutamine restimulation period.

(B) Amino acid starvation and glutamine refeeding do not significantly affect Lst4-V5 levels. Cells (as in [A]) were treated as in Figure 2G, including additional sampling time points up to 60 min following glutamine refeeding. Representative anti-V5 and anti-Adh1 immunoblots are shown together with respective values of the Lst4-V5 levels that were calculated as the mean ratio of Lst4-V5/Adh1 (n =3; ± SD) and normalized to the respective ratio in exponentially growing (EXP) cells (set to 1.0).

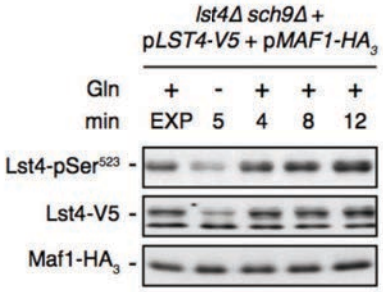

Figure S2. Phosphorylation of Ser^{523} in Lst4 Does Not Require Sch9, Related to Fig. 2H

Exponentially growing *lst4*Δ *sch9*Δ cells expressing plasmid-encoded Lst4-V5 and Maf1-HA$_3$ were starved for amino acids and refed with glutamine and analyzed for the phosphorylation levels of Ser^{523} in Lst4, for the total levels of Lst4-V5, and, in an additional control, for the extent of hyperphosphorylation of the Sch9 target Maf1-HA$_3$ (as in Figure 2H). As judged from the relative levels of the slowly migrating Lst4-V5 versus the respective faster migrating ones, and in line with the results in Figure 2H, loss of Sch9 appeared to result in Lst4 hyperphosphorylation in non-starved cells. Notably, while Maf1-HA$_3$ migrated in multiple phosphorylated isoforms in exponentially growing cells expressing functional Sch9 (Figure 2H), no such isoforms were detected in the absence of Sch9 (neither in exponentially growing nor in glutamine-refed *sch9*Δ cells).

Supplemental Tables

Table S1. Strains Used in This Study

Strain	Genotype	Source	Figure
KT1961	*MATa; his3, leu2, ura3-52, trp1*	[1]	
KP09	[KT1961] *MATa; lst4Δ::KanMX*	[2]	2D; 2F-H; 4A, C; S1A, B
KP10	[KT1961] *MATa; lst7Δ::KanMX*	[2]	1C; 3B
MP372-2D	[KT1961] *MATa; LST7-GFP::HIS3MX, lst4Δ::KanMX*	[2]	3C
MP412-1C	[KT1961] *MATa; lst4Δ::KanMX, lst7Δ::KanMX*	This study	2F
MP4469	[KT1961] *MATa; lst4Δ::KanMX, URA3::LST4p-LST4-ENVY*	This study	1B; 2A, E; 3A; 4A-C
MP4509	[KT1961] *MATa; lst4Δ::KanMX, URA3::LST4p-lst4^{12A}-ENVY*	This study	3A; 4A-C
MP4510	[KT1961] *MATa; lst4Δ::KanMX, URA3::LST4p-lst4^{5D}-ENVY*	This study	3A; 4A-C
MP4569	[KT1961] *MATa; URA3::CYC1p-lst4^{loop}-GFP*	This study	1B; 1D, E
MP4570	[KT1961] *MATa; lst4Δ::KanMX, URA3::CYC1p-lst4^{loop}-GFP*	This study	1D
MP4571	[KT1961] *MATa; lst7Δ::KanMX, URA3::CYC1p-lst4^{loop}-GFP*	This study	1D
MP4572	[KT1961] *MATa; lst4Δ::KanMX, lst7Δ::KanMX, URA3::CYC1p-lst4^{loop}-GFP*	This study	1D
MP4573	[KT1961] *MATa; gtr1Δ::natMX, gtr2Δ::natMX, URA3::CYC1p-lst4^{loop}-GFP*	This study	1F
MP4638	[KT1961] *MATa; lst4Δ::KanMX, sch9Δ::natMX, pRS414-SCH9^{T492G}, pRS416-LST4p-LST4-V5-HIS$_6$*	This study	2H
MP4680	[KT1961] *MATa; lst4Δ::KanMX, lst7Δ::KanMX, URA3::LST4p-LST4-ENVY*	This study	3B
MP4684	[KT1961] *MATa; lst4Δ::KanMX, lst7Δ::KanMX, URA3::LST4p-lst4^{12A}-ENVY*	This study	3B
MP4688	[KT1961] *MATa; lst4Δ::KanMX, lst7Δ::KanMX, URA3::LST4p-lst4^{5D}-ENVY*	This study	3B
MP268-2B	[KT1961] *MATa; gtr1Δ::NatMX, gtr2Δ::NatMX*	[2]	3E
MP4704	[MP268-2B] *MATa; lst4Δ::KanMX, URA3::LST4p-LST4-ENVY*	This study	3E
MP4708	[MP268-2B] *MATa; lst4Δ::KanMX, URA3::LST4p-lst4^{12A}-ENVY*	This study	3E
MP4709	[MP268-2B] *MATa; lst4Δ::KanMX, URA3::LST4p-lst4^{5D}-ENVY*	This study	3E
MP4847	[KT1961] *MATα; iml1Δ::KanMX, lst4Δ::KanMX, URA3::LST4p-LST4-ENVY*	This study	4D, E
MP4849	[KT1961] *MATα; iml1Δ::KanMX, lst4Δ::KanMX, URA3::LST4p-lst4^{12A}-ENVY*	This study	4D, E
MP4642	[KT1961] *MATa; lst4Δ::KanMX, sch9Δ::KanMX, pRS416-LST4p-LST4-V5-HIS$_6$*	This study	S2
MP4693	[KT1961] *MATa; lst4Δ::KanMX, lst7Δ::KanMX, URA3::LST4p-lst4^{Δloop}-ENVY*	This study	1D
MP4697	[KT1961] *MATa; URA3::LST4p-lst4^{Δloop}-ENVY*	This study	1B; 1D, E
MP4698	[KT1961] *MATa; lst4Δ::KanMX, URA3::LST4p-LST4-ENVY*	This study	4D, E
MP4699	[KT1961] *MATa; lst4Δ::KanMX, URA3::LST4p-lst4^{Δloop}-ENVY*	This study	1D
MP4700	[KT1961] *MATa; lst4Δ::KanMX, URA3::LST4p-lst4^{12A}-ENVY*	This study	4D, E
MP4510	[KT1961] *MATa; lst4Δ::KanMX, URA3::LST4p-lst4^{5D}-ENVY*	This study	4D, E
MP4703	[KT1961] *MATa; lst7Δ::KanMX, URA3::LST4p- lst4^{Δloop}-ENVY*	This study	1D
TB50a	*MATa; trp1 his3 ura3 leu2 rme1*	[3]	
RL170-2C	[TB50a] *MATa; TCO89-TAP::TRP1*	[4]	2B

Table S2. Plasmids Used in This Study

Plasmid	Genotype	Source	Figure
pRS413	CEN, ARS, *HIS3*	[5]	1B-F; 2A; 2D, E; 2H; 3A, B, E; 4A; 4D; S2
pRS414	CEN, ARS, *TRP1*	[5]	1B; 1D-F; 2A; 2D-H; 3A; 3D; 4A-D, S1A, B; S2
pRS415	CEN, ARS, *LEU2*	[5]	1B-F; 2A; 2D-H; 3A, B; 3D; 4A-D; S1A, B
pRS416	CEN, ARS, *URA3*	[5]	1C; 2D; 2F-H; 3B; 4A; 4C; S1A, B
pMP3008	[pRS413] *LST4p-LST4-V5-HIS$_6$*	This study	2D; 2F, G; S1A, B
pMP3055	[pRS413] *LST4p-lst4^{S523A}-V5-HIS$_6$*	This study	2D
pMP2576	[pRS414] *LST7p-LST7-HA$_3$*	This study	1C; 3B
pAH145	[pRS414] *sch9^{T492G}*	[6]	2H
pPL155	[pRS415] *HA$_3$-TOR1^{A1957V}*	[7]	1F
p1392	[pRS415] *MAF1-HA$_3$*	[6]	2H; S2
pMP2780	[pRS416] *LST4p-LST4-V5-HIS$_6$*	This study	1C; 2H; 3C; S2
pMP3143	[pRS416] *CYC1p-lst4^{loop}-V5-HIS$_6$*	This study	1C
pMP3147	[pRS416] *LST4p-lst4$^{\Delta loop}$-V5-HIS$_6$*	This study	1C
pMP3149	[pRS416] *LST4p-lst4^{5D}-V5-HIS$_6$*	This study	3C
pMP3165	[pRS416] *LST4p-lst4^{12A}-V5-HIS$_6$*	This study	3C
pRS306	integrative, *URA3*	[8]	
pMP3042	[pRS306] *LST4p-LST4-ENVY*	This study	1B; 2A, E; 3A; 4A-C
pMP3062	[pRS306] *LST4p-lst4^{12A}-ENVY*	This study	3A; 4A-C
pMP3064	[pRS306] *LST4p-lst4^{5D}-ENVY*	This study	3A; 4A-C
pMP3077	[pRS306] *CYC1p-lst4^{loop}-GFP*	This study	1B; 1D-F
pSIVu	integrative, *URA3*	[9]	
pMP3166	[pSIVu] *LST4p-LST4-ENVY*	This study	2A; 2E; 3A, B; 4A-D
pMP3167	[pSIVu] *LST4p-lst4$^{\Delta loop}$-ENVY*	This study	1B; 1D, E
pMP3168	[pSIVu] *LST4p-lst4^{12A}-ENVY*	This study	3A, B; 4A-D
pMP3169	[pSIVu] *LST4p-lst4^{5D}-ENVY*	This study	3A, B; 4A-D
pRS423	2μ, *HIS3*	[10]	
pRH2953	[pRS423] *VAC8p-vhhGFP4-PHO8N*	R. Hatakeyama	4B, C
pAS2570	[pET28b$^+$] *HIS$_6$-LST4*	[2]	2B; 3D
pAS2571	[pET15b$^+$] *HIS$_6$-LST7*	[2]	2B; 3D
pMP3057	[pET28b$^+$] *HIS$_6$-lst4^{12A}*	This study	2B; 3D
pMP3058	[pET28b$^+$] *HIS$_6$-lst4^{5D}*	This study	2B; 3D
pNP2038	[pET-24d] *GST-TEV-GTR2*	[11]	3D
pJU1046	[pGEX-6P] *GST-TEV-gtr1^{Q65L}-HIS$_6$*	R. Loewith	3D
p3285	pYEGFP-GAC111-*RPL25*	D. Kressler	3E
pMP2789	[pRS415] *GTR1p-GTR1-HA$_3$*	This study	3E
pMP2337	[pRS416] *GTR1p-GTR1-HA$_3$*	[2]	3E
pMP2782	[pRS414] *GTR2p-gtr2^{Q66L}-V5-HIS$_6$*	[2]	3E

Table S3. TORC1-Controlled Phosphorylation Sites in Lst4[a]

No.	Position	PEP	Score	Phospho (ST) Probabilities
P1	484	1.00E-02	303.5	NSNTSVSVSSSESLAEVIQPS(0.044)S(0.956)FK
P2	498	1.00E-02	173.0	SGSSSLHYLS(0.009)S(0.039)S(0.901)IS(0.047)SQPGSYGSWFNK
P3	523	5.30E-57	126.8	RPTISQFFQPS(0.997)PS(0.003)LK
P3	525	8.75E-29	101.9	RPTISQFFQPS(0.166)PS(0.834)LK
P4	547	8.12E-08	74.4	TS(0.003)S(0.983)S(0.013)SSLQQATSR
P4	549	2.21E-108	162.4	TSSS(0.003)S(0.752)S(0.244)LQQATSR
P4	550	2.27E-56	131.4	TSSSS(0.029)S(0.969)LQQATSR

[a] Peptides are numbered according to Figure 2. The position of the most likely phosphorylated amino acid residue as identified by MS-analysis is indicated (see also respective phosphosite localization probabilities). Sites marked in red (*i.e.* probability > 0.001) were exchanged to alanine and sites marked in blue (*i.e.* probability > 0.9) were exchanged to alanine and/or phospho-mimetic aspartate. In addition, we also included the conserved Thr^{545}, which is adjacent to a serine cluster, in these analyses. PEP: posterior error probability; Score: Andromeda score.

Supplemental References

1 Pedruzzi I, Dubouloz F, Cameroni E *et al.* TOR and PKA signaling pathways converge on the protein kinase Rim15 to control entry into G_0. *Mol Cell* 2003; **12**:1607-1613.

2 Péli-Gulli MP, Sardu A, Panchaud N, Raucci S, De Virgilio C. Amino Acids Stimulate TORC1 through Lst4-Lst7, a GTPase-Activating Protein Complex for the Rag Family GTPase Gtr2. *Cell Rep* 2015; **13**:1-7.

3 Beck T, Hall MN. The TOR signalling pathway controls nuclear localization of nutrient-regulated transcription factors. *Nature* 1999; **402**:689-692.

4 Shimada K, Filipuzzi I, Stahl M *et al.* TORC2 signaling pathway guarantees genome stability in the face of DNA strand breaks. *Mol Cell* 2013; **51**:829-839.

5 Brachmann CB, Davies A, Cost GJ *et al.* Designer deletion strains derived from *Saccharomyces cerevisiae* S288C: a useful set of strains and plasmids for PCR-mediated gene disruption and other applications. *Yeast* 1998; **14**:115-132.

6 Huber A, Bodenmiller B, Uotila A *et al.* Characterization of the rapamycin-sensitive phosphoproteome reveals that Sch9 is a central coordinator of protein synthesis. *Genes Dev* 2009; **23**:1929-1943.

7 Reinke A, Chen JC, Aronova S, Powers T. Caffeine targets TOR complex I and provides evidence for a regulatory link between the FRB and kinase domains of Tor1p. *J Biol Chem* 2006; **281**:31616-31626.

8 Sikorski RS, Hieter P. A system of shuttle vectors and yeast host strains designed for efficient manipulation of DNA in Saccharomyces cerevisiae. *Genetics* 1989; **122**:19-27.

9 Wosika V, Durandau E, Varidel C, Aymoz D, Schmitt M, Pelet S. New families of single integration vectors and gene tagging plasmids for genetic manipulations in budding yeast. *Molecular genetics and genomics : MGG* 2016; **291**:2231-2240.

10 Christianson TW, Sikorski RS, Dante M, Shero JH, Hieter P. Multifunctional yeast high-copy-number shuttle vectors. *Gene* 1992; **110**:119-122.

11 Panchaud N, Péli-Gulli MP, De Virgilio C. Amino acid deprivation inhibits TORC1 through a GTPase-activating protein complex for the Rag family GTPase Gtr1. *Sci Signal* 2013; **6**:ra42.

CHAPTER II:

In vitro kinase assay and Mass Spectrometry analysis approach to discover new TORC1 targets

2.1 Introduction

The known TORC1 substrates in yeast are involved in the regulation of different processes, such as transcription (Gln3 or Sfp1) (Bertram et al., 2000; Lempiäinen et al., 2009) , nitrogen starvation response (Tap42) (Di Como and Arndt, 1996; Jiang and Broach, 1999; Li et al., 2017; Yan et al., 2006), ribosome biogenesis (Sch9 or Ypk3) (Urban et al., 2007; Yerlikaya et al., 2016) and autophagy (Atg13) (Kamada et al., 2010; Klionsky et al., 2003).

The discovery of new targets of TORC1 is particularly important to investigate the role of this complex in the regulation of other pathways and to resolve the mechanisms of these regulations.

In the first chapter, we demonstrate that Lst4 is a hitherto unknown target of TORC1 and we underline the importance of this target as part of a feedback mechanism that controls TORC1 in a homeostatic manner.

The difficulty to discover new TORC1 targets is mainly due to the need to test the putative TORC1 substrates *in vitro*, to verify their direct phosphorylation by the kinase complex. For this approach, it is necessary to purify the candidate proteins as well as TORC1, which imply various technical hurdles.

In this chapter, we combined the TORC1 *in vitro* kinase assay using purified TORC1 and putative target proteins isolated from yeast, with mass spectrometry analysis with the aim to discover new TORC1-dependent phosphosites.

2.2 Results

2.2.1 The purification of substrates

We decided to identify possible TORC1 substrates with two different approaches, both involving mass spectrometry analysis: the SILAC technique and the *in vitro* protein kinase assay combined with mass spectrometry. The first approach was used to perform a high throughput screening of all the yeast proteins in order to have a large scale data set (data not shown) to, later, focus on a cluster of proteins studied with the second approach. Notably, for the SILAC technique we used a particular yeast strain lacking the *ARG4* and *LYS2* genes, which were grown in the

presence or absence of the heavy isotopes of arginine (Arg^{10}) and lysine (Lys^{8}). We treated the cells with rapamycin for 30 minutes before pelleting and we prepared the lysates that were analyzed by mass spectrometry, comparing the phosphoproteome of the rapamycin-treated cells to the one of the untreated cells (in the presence or absence of heavy amino acids for both conditions) to find the TORC1-dependent phosphosites.

Based on the SILAC results, we decided to choose a group of proteins involved in the same biological process, to investigate the role of TORC1. Among the detected phosphosites, we noticed that several within Atg proteins (i.e. Atg4, Atg13, Atg20, Atg29, and Atg33) were less phosphorylated when analysed in lysates from rapamycin-treated cells. Thus, we decided to further analyse the entire family of Atg proteins. It is known that TORC1 phosphorylates Atg13 to negatively regulate autophagy (Kamada et al., 2010; Klionsky et al., 2003), but we wanted to study if this kinase complex is able to regulate this process at different levels, through the phosphorylation of other Atg proteins.

The first step included the purification of all the Atg proteins present in yeast (Table 2.1).

Protein name	Alternative protein name	Systematic gene name	Ptotein name	Alternative protein name	Systematic gene name
Atg 1		YGL180W	Atg 19		YOL082W
Atg 2		YNL242W	Atg 20		YDL113C
Atg 3		YNR007C	Atg 21		YPL100W
Atg 4		YNL223W	Atg 22		YCL038C
Atg 5		YPL149W	Atg 23		YLR431C
Atg 6	also called Vps30	YPL120W	Atg 24	also called Snx4	YJL036W
Atg 7		YHR171W	Atg 26		YLR189C
Atg 8		YBL078C	Atg 27		YJL178C
Atg 9		YDL149W	Atg 29		YPL166W
Atg 10		YLL042C	Atg 31		YDR022C
Atg 11		YPR049C	Atg 32		YIL146C
Atg 12		YBR217W	Atg 33		YLR356W
Atg 13		YPR185W	Atg 34		YOL083W
Atg 14		YBR128C	Atg 36		YJL185C
Atg 15		YCR068W	Atg 38		YLR221C
Atg 16		YMR159C	Atg 39		YLR312C
Atg 17		YLR423C	Atg 40		YOR152C
Atg 18		YFR021W	Atg 41		YPL250C

Table 2.1 List of all Atg proteins present in *S.cerevisiae*.

The 36 Atg proteins were purified from yeast cells belonging to two different yeast collections, which expressed epitope-tagged proteins under the control of the *GAL1* promoter. As shown in Figure 2.1, plasmids allowed either the expression of GST-tagged protein (from the pEG(KG) vector) or of TAP-tagged protein (from the BG1085 vector).

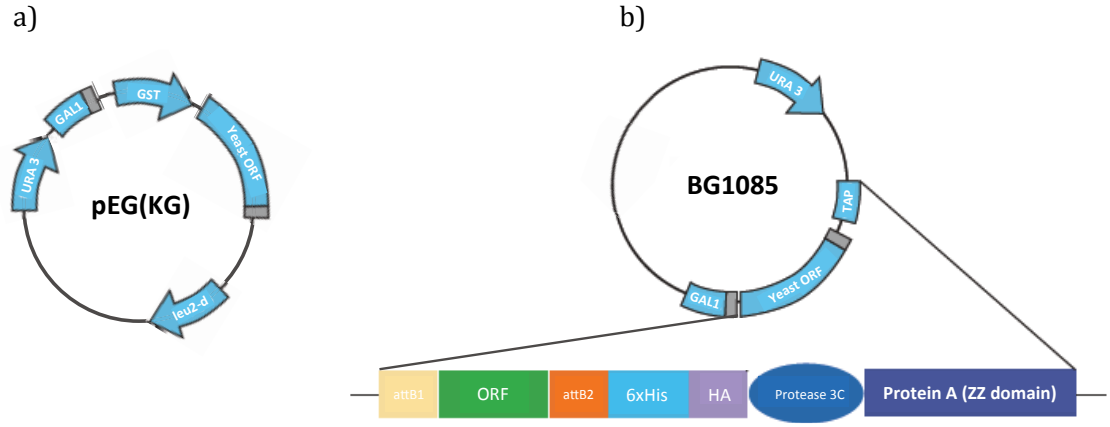

Figure 2.1 Schematic presentation of the plasmids for the overexpression of GST-tagged proteins (a) (Zhu et al., 2000) and TAP-tagged proteins (b) (Gelperin et al., 2005).

For both GST and 6His (TAP) purifications, we grew the cells in a synthetic medium supplied with raffinose and sucrose as carbon sources and then, for the induction, cells were diluted in YP Galactose 2% and grown for 6 hours. The cells were treated for 30 minutes with rapamycin before pelletting to minimize the TORC1-dependent phosphorylation events in these cells. The proteins were purified in groups of two, thus each flask contained two strains carrying each a plasmid for the overexpression of two different Atg proteins (Fig. 2.2).

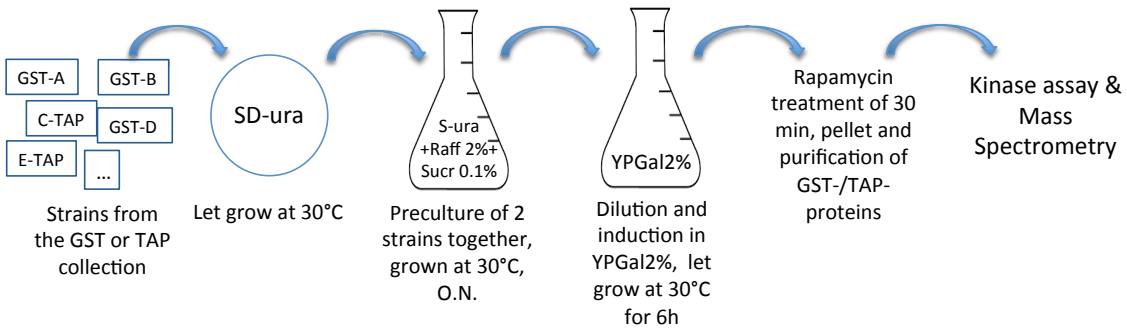

Figure 2.2 Schematic presentation of the protocol for the purification of the Atg proteins that were either GST- or TAP-tagged.

In Figure 2.3 we show the western blots obtained, in which we detected the GST-tagged and the TAP-tagged proteins using anti-GST and anti-HA antibodies, respectively:

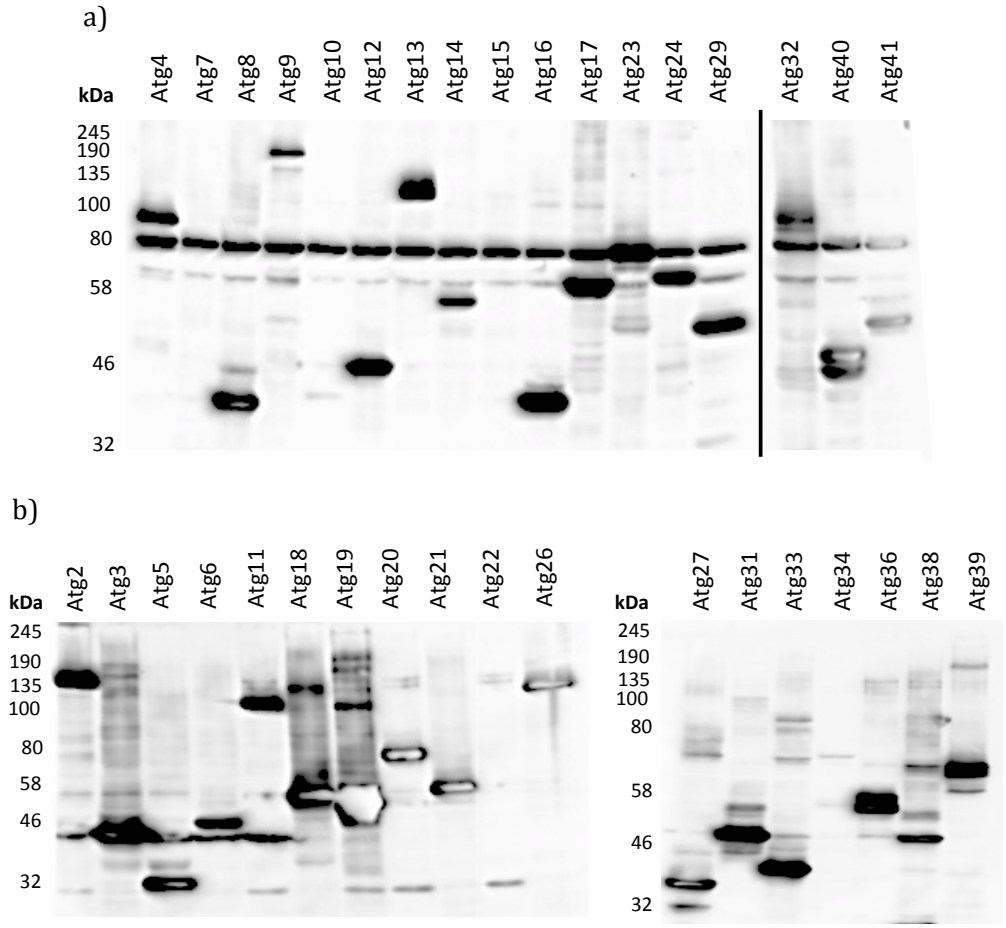

Figure 2.3 Induction of Atg proteins upon growth on galactose. Cells were grown in S-URA 2% Raffinose 0.1% Sucrose medium. The induction was done adding 2% galactose, for 6 h. The total extract of each strain was analyzed on a SDS-Page gel followed by immunoblotting with anti-GST (a) or anti-HA (b) antibodies to control the Atg proteins expression.

Even though some Atg proteins were less expressed than others, the mass spectrometry analysis revealed that all the proteins could be purified in sufficient amounts (except Atg15; the respective clone in the GST collection carries a STOP codon just before the *ATG15* ORF).

Notably, we intentionally did not include Atg1 in the list of the purified Atg proteins as substrates, being Atg1 itself a kinase, to avoid issues in interpreting the results because of the presence of another kinase.

2.2.2 TORC1 *in vitro* kinase assay

Once the candidates that we wanted to test as TORC1 substrates were purified, we needed to purify also the kinase complex. For this purpose, we used a yeast strain in which the TORC1 subunit Tco89 was genomically TAP-tagged (Shimada et al., 2013). Briefly, we grew the cells in YPD medium, then we supplied the high density culture with more nutrients (YPD powder) in order to avoid starvation, and we let the cells grow for 1 hour to obtain an even higher cell density (OD_{600} between 3 and 4). We treated the cells with cycloheximide for 10 minutes to hyperactivate TORC1 and finally we pelleted the cells by filtration. The cells were broken and the complex was purified pulling down Tco89-TAP using magnetic beads coupled with IgG. The complex was eluted cleaving the TAP tag with the TEV protease (Fig. 2.4).

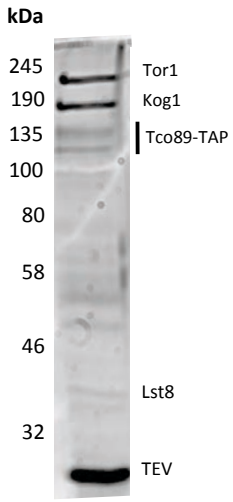

Figure 2.4 TOR Complex 1 purified from yeast. Representative SYPRO Ruby staining of the TOR Complex 1 purified and eluted with TEV protease.

At this point, we performed several kinase assays, using purified TORC1 as kinase and groups of 6 purified Atg proteins as substrates for each kinase assay, supplying γ-[$^{18}O_4$]-ATP (heavy ATP) to distinguish the phosphorylation events during the kinase assay from the ones that were already carried out within the cells (Zhou et al., 2007). In addition, we used wortmannin, a PI3K inhibitor that also potently inhibits TORC1 (Brunn et al., 1996; Yano et al., 1993), as control to verify that the phosphorylations during the kinase assay were TORC1-dependent and not due to

the presence of another kinase that co-purified with TORC1 or with one of the Atg proteins.

In Table 2.2 we summarized the performed kinase assays, each done in triplicate and in the presence or absence of 6 μM Wortmannin, followed by the mass spectrometry analysis of the phosphosites:

Assay 1	TORC1 +	Atg 4	**Assay 4**	TORC1 +	Atg 11
		Atg 7			Atg 21
		Atg 8			Atg 26
		Atg 9			Atg 31
		Atg 10			Atg 36
		Atg 14			Atg 39
Assay 2	TORC1 +	Atg 15	**Assay 5**	TORC1 +	Atg 3
		Atg 16			Atg 5
		Atg23			Atg 6
		Atg 24			Atg 32
		Atg 29			Atg 34
		Atg 40			Atg 41
Assay 3	TORC1 +	Atg 2	**Assay 6**	TORC1 +	Atg 12
		Atg 19			Atg 17
		Atg 20			Atg 18
		Atg 22			Atg 27
		Atg 33	**Assay 7**	TORC1 +	Atg 13
		Atg 38			

Table 2.2 List of the TORC1 Kinase assays using Atg proteins as substrates. Each assay was done in triplicate and in presence or absence of 6 μM Wortmannin.

We added at least 1 μg of each Atg protein and approximately an amount of TORC1 of 10 μg. The kinase assay reactions were done in columns containing a protein filter with a cutoff of 10 kDa and incubated at 30°C for 2h, in the presence of kinase buffer and a solution of $MgCl_2$ and heavy ATP. Notably, we intentionally performed the kinase assay with Atg13 as substrate separately from other Atg proteins to avoid the possibility that Atg1, that strongly interacts with Atg13, could be present in the assay, distorting the interpretation of the results.

2.2.3 Samples preparation & mass spectrometry analysis

After the incubation, the samples were centrifuged to stop the reaction, to eliminate the kinase buffer, and to resuspend the proteins in 8 M Urea for protein denaturation. Then, we exchanged the buffer (ABC buffer) for trypsin protease

treatment. Once the peptides were obtained they were eluted by centrifugation, acidified with trifluoroacetic acid (TFA) and incubated with TiO_2 beads for phosphopeptide enrichment. Thus, the phosphopeptides were separated from the rest of the peptides, that we used to quantify the amount and sequence coverage of each protein. The mass spectrometric measurements were performed using a Q Exactive Plus mass spectrometer (Thermo Fisher Scientific) coupled to an EASY-nLC 1000 nanoflow-HPLC (Thermo Fisher Scientific). The raw MS data were analyzed using MaxQuant version 1.4.1.2 and the same software was used for the quantification of peptides and proteins (Cox and Mann, 2008). Searches were performed against the UniProt yeast FASTA database (March 2016). The results are summarized in Table 2.3, in which we report the sites phosphorylated by TORC1 on different Atg proteins. These sites were not, or significantly less, phosphorylated in the presence of wortmannin and were normalized on the total amount of each protein.

Gene	Positions within proteins	TORC1_wo/w_1	TORC1_wo/w_2	TORC1_wo/w_3	Localization prob	Modified sequence
ATG9	250	>100	n.d.	>100	1.00	FTGS(p)PLNNTNR
ATG13	351	>100	>100	>100	1.00	SLSLS(p)PCT(p)R
	355	9.82	19.37	16.39	1.00	ANS(p)FEPQS(p)WQKK
	360	>100	>100	>100	1.00	ANS(p)FEPQS(p)WQKK
	379	>100	>100	>100	1.00	VGS(p)IGSQS(p)ASR
	382	>100	>100	>100	1.00	VGS(p)IGS(p)QSASR
	384	>100	>100	>100	0.99	VGS(p)IGSQS(p)ASR
	393	>100	>100	>100	1.00	NPSNSS(p)FFNQPPVHR
	429	n.d.	>100	>100	0.94	YSSS(p)FGNIR
	454	>100	>100	n.d.	1.00	AVKS(p)PLQPQESQEDLMDFVK
	496	>100	>100	>100	0.99	KTSGNNPPNINISDS(p)LIR
	541	n.d.	>100	>100	0.96	SDSHSPLPSIS(p)PSMHYGS(p)LNSR
	548	>100	>100	>100	0.99	SDSHSPLPSISPSMHYGS(p)LNSR
	554	>100	>100	>100	1.00	MS(p)QGANASHLIAR
	571	>100	>100	>100	0.87	GGGNSS(p)TSALNSR
	573	>100	>100	>100	0.96	GGGNSSTS(p)ALNSR
	604	>100	>100	>100	0.94	QGM(ox)SGLPPIFGGESTS(p)YHHDNK
	637	>100	>100	>100	0.97	LLNQMGNS(p)ATK
	644	>100	>100	>100	0.98	FKSS(p)IS(p)PR
	646	>100	>100	>100	1.00	FKSS(p)IS(p)PR
	649	2.02	>100	>100	1.00	S(p)IDS(p)ISS(p)SFIK
	656	>100	>100	>100	0.96	SIDSISSS(p)FIK
	671	>100	>100	>100	0.98	QPYHYS(p)QPTTAPFQAQAK
ATG23	420	>100	>100	n.d.	0.85	QPST(p)PSFLVASK
	422	n.d.	>100	>100	0.98	QPSTPS(p)FLVASK
	429	>100	>100	n.d.	0.96	QPSTPSFLVASKS(p)PPK
	438	>100	>100	0.71	1.00	IGISES(p)VVNANK
ATG29	115	>100	>100	n.d.	0.96	YTPT(p)LQNDNLLNVSASPLTTER
ATG33	129	n.d.	>100	>100	1.00	LAASELSDS(p)IIDLGEDNHASENTPR

Table 2.3 Summary of the mass spectrometry analysis results for the TORC1-dependent phosphosites on Atg proteins. The experiments were done in triplicate, in presence or absence of Wortmannin 6 μM. The ratio between the phosphosites intensity in absence (TORC1_wo) and presence (TORC1_w) of Wortmannin is indicated as >100 in case no peptides were found in the samples with Wortmannin. All the phosphosites were detected in at least two out of three replicates with a minimum fold change of greater than 10.

Notably, we obtained a good sequence coverage of each Atg protein when analyzing the non-phosphorylated peptides (Fig. 2.5):

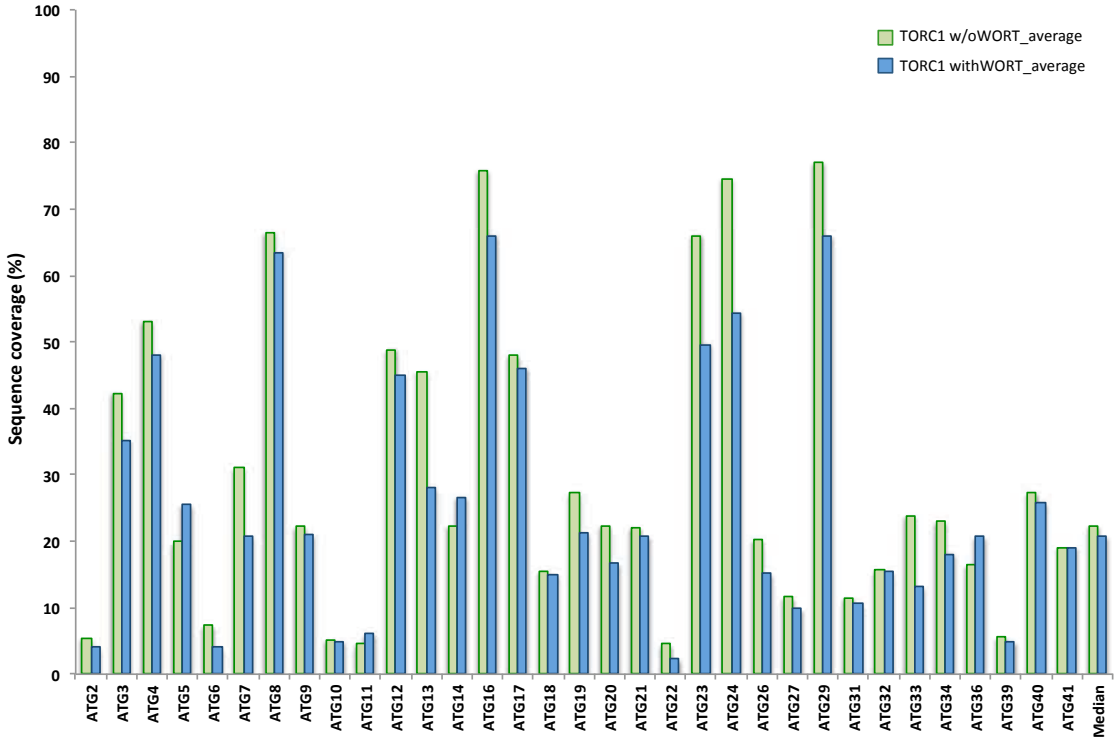

Figure 2.5 Sequence coverage (%) of all Atg proteins. The mean sequence coverage percentage for each Atg protein is represented. Data were obtained from triplicates of the kinase assays in the presence (TORC1 w/oWORT, blue) or absence (TORC1 withWORT, green) of 6 μM Wortmannin.

From these results, we observed that TORC1 can phosphorylate, at least *in vitro*, other Atg proteins, such as Atg9, Atg23, Atg29, and Atg33 in addition to the known TORC1 target Atg13, which was phosphorylated on several residues. Among these sites on Atg13, serines 496, 541, 646, and 649 were already described as TORC1 targets (Kamada et al., 2010), supporting the validity of our results. Excluding the five detected Atg proteins, we did not detect other phosphopeptides in other Atg

proteins, indicating that TORC1 retains a certain specificity towards substrates *in vitro*.

Among the Atg proteins phosphorylated by TORC1, we decided to further investigate Atg29, which in our assay was phosphorylated on threonine 115. Notably, this protein, together with Atg17, Atg31, Atg13 and Atg1, forms the Atg1 complex, the first complex that is assembled in response to nutrient starvation to initiate the autophagic process (Papinski et al., 2014; Suzuki et al., 2007). Interestingly, a study proposed that Atg29 is a phosphoprotein that plays a critical role for the activation of autophagy resulting from the phosphorylation on its C-terminus (Mao et al., 2013).

2.2.4 Study of Atg29 phosphorylation *in vitro* by TORC1

In order to analyze with a better resolution the TORC1-dependent phosphorylation sites on Atg29, we decided to purify this protein from bacteria, optimizing the sequence of the *ATG29* yeast gene for expression in the Rosetta *E.coli* strain.

The results, summarized in Table 2.4, revealed several additional residues on Atg29 that were directly phosphorylated by TORC1.

Protein	Position	TORC1 vs Ctrl	Localization prob	Modified sequence
ATG29	106	1.39	1.00	YSNDQVNEGMS(p)DLIHK
	115	67.31	1.00	YTPT(p)LQNDNLLNVSASPLTTER
	125	>100	1.00	YTPTLQNDNLLNVS(p)ASPLTTER
	127	>100	1.00	YTPTLQNDNLLNVSAS(p)PLTTER
	166	0.55	1.00	TSDS(p)ENKPNDKLDK
	187	>100	0.97	EMECGS(p)SDDDLSSSLSVSK
	188	>100	1.00	EMECGSS(p)DDDLSSSLSVSK
	193	>100	0.85	EMECGSSDDDLS(p)SSLSVSK
	194	>100	0.88	EMECGSSDDDLSS(p)SLSVSK
	195	>100	0.99	EMECGSSDDDLSSS(p)LSVSK
	201	510.29	1.00	S(p)ALEEALMDR

Table 2.4 Summary of the mass spectrometry analysis results regarding the TORC1-dependent phosphosites on Atg29. The experiments were done in triplicate, in presence or absence of Wortmannin 6 μM (Ctrl). The ratio between the phosphosites intensity in the absence and presence of Wortmannin (TORC1 vs Ctrl) is indicated as >100 in case no peptides were found in the samples with wortmannin. All the phosphosites were detected in at least two out of three replicates.

As observed in the presented data set, threonine 115 of Atg29 was detected being phosphorylated using both Atg29 purified from yeast and from bacteria, while other phosphosites were detected only using the Atg29 purified from bacteria. These differences may be due to the fact that the Atg proteins purified from yeast may have already been partially phosphorylated within the cells, despite the 30 minutes treatment with rapamycin before the collection for the purification. Thus, there was the possibility that more TORC1-dependent phosphosites on Atg29 existed, as the results obtained with Atg29 purified from bacteria suggest.

We observed that there were several sites phosphorylated by TORC1 at the C-terminus of Atg29. Among these sites, we detected serine 201, that has been hypothesized to be phosphorylated together with serine 197 and serine 199 by the Atg1 kinase to activate autophagy (Mao et al., 2013). Despite its proposed role in the literature, our results showed the direct phosphorylation of serine 201 by TORC1, suggesting that this residue, once phosphorylated, could have a negative role in autophagy activation. In order to complete our data set on the phosphorylation of this Atg protein, we also performed a kinase assay in which we used purified Atg1 as kinase and Atg29 purified from bacteria as substrate (data not shown). Notably, we used the Atg1 kinase-dead allele (Atg1-KD) as control. The results showed that Atg1 phosphorylates Atg29 on several residues including serine 201. The ratio between the S201 phosphosite intensity in the presence of Atg1 divided by the S201 phosphosite intensity in the presence of the Atg1-KD allele was much lower (Atg1 vs Atg1 KD = 8.41) compared to that one obtained using TORC1 as kinase in the presence or absence of Wortmannin (TORC1 vs Ctrl = 510.29). In this case, we can conclude that, at least *in vitro*, the serine 201 on Atg29 can be phosphorylated by both kinases. To elucidate which kinase acts on this residue *in vivo*, further *in vivo* experiments are necessary.

2.3 Discussion

In this study we proposed a method to identify new targets of TORC1. In particular, our data show that TORC1 phosphorylates several Atg proteins, confirming the prominent role of this kinase complex in the regulation of autophagy.

Our work was focused on the study of the group of Atg proteins (purified from yeast) that we used as substrates in TORC1 *in vitro* kinase assays and which we analyzed by mass spectrometry. Mass spectrometry is commonly used for kinase-substrates analysis and in general, after the kinase assay reaction, the samples are loaded on SDS-PAGE gels and further treated for the MS analysis. In this study, we did not use the classical SDS-PAGE gel method for the preparation of the mass spectrometry analysis samples, but we performed the kinase assays directly on molecular weight cutoff filters in which we could directly exchange the buffers and treat the samples with trypsin. With the SDS-PAGE gel method, after the kinase assay reaction, the sample had to be loaded on an acrylamide gel and, after a coomassie staining, all the bands corresponding to the different proteins had to be cut and undergo a time consuming procedure to proceed with the trypsine digestion. The several steps required for the SDS-PAGE method also resulted in loss of material. The new technique that we used has two important advantages: (i) the possibility to collect and analyze the phosphopeptides coming from all the proteins phosphorylated during the reaction (including the auotphosphorylation events on the TORC1 kinase complex, such as those on Tco89), which minimize the loss of material and (ii) the fact that trypsin digestion could be done in solution on the filter, which allowed easy exchange of the kinase buffer with that one compatible for the MS analysis. In addition, using the γ-[$^{18}O_4$]-ATP (heavy ATP) we could discriminate the phosphorylation events during the kinase assay from the phosphosites already phosphorylated in the cells (Zhou et al., 2007).

We confirmed the validity of this method with our results on Atg13 and we identified also other Atg proteins such as Atg9, Atg23, Atg29, and Atg33 as novel substrates of TORC1, at least *in vitro.*

Proteins purified from yeast may already be phosphorylated and hence we may miss some important phosphorylation events. This problem can be solved by purifying the target protein from bacteria, as we have done with Atg29. We have choosen this protein because of its peculiar role in the activation of autophagy (Mao et al., 2013; Papinski et al., 2014; Suzuki et al., 2007) and we identified 11 residues on Atg29 that were highly phosphorylated by TORC1 (Table 2.4).

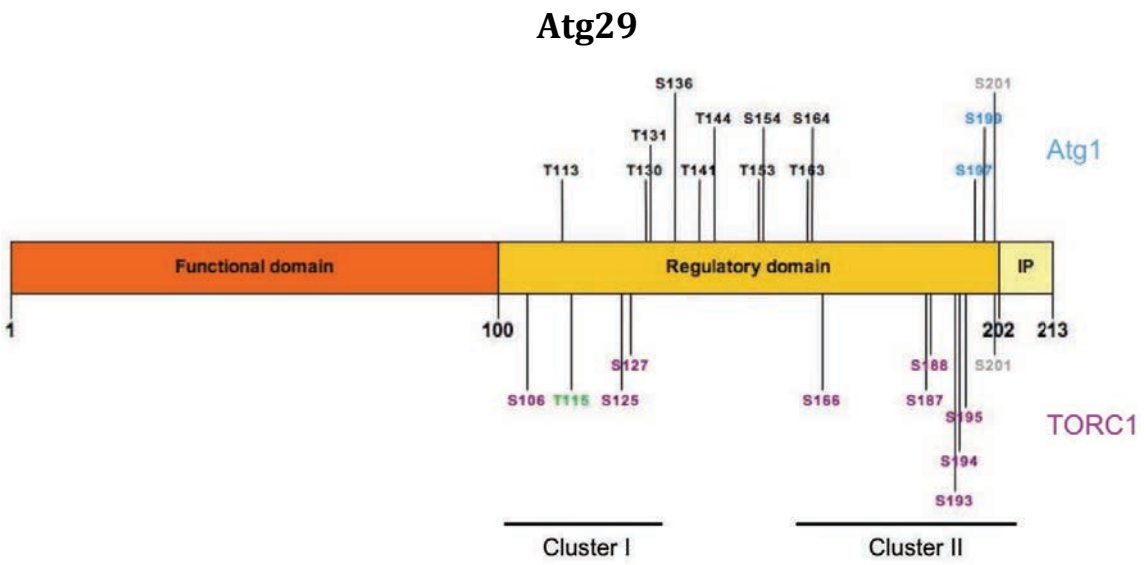

Figure 2.6 Map of the residues phosphorylated by TORC1 and Atg1 on Atg29. The TORC1-dependent phosphosites identified using Atg29 purified from the bacterial Rosetta strain are indicated in violet; the residue in green (T115) represents the TORC1-dependent phosphosite identified using both Atg29 purified from yeast and bacteria. The Atg1-dependent phosphosites are indicated in blue and the S201 residue that could be both a TORC1- and Atg1-dependent phosphosite is indicated in gray. The other phosphorylatable residues on Atg29 are indicated in black. The domains of Atg29 are indicated in different colours: Functional domain in orange, regulatory domain in yellow and inhibitory peptide (IP) in light yellow. Modified from (Mao et al., 2013).

Notably, it was shown that the C-terminus of Atg29 represent the regulatory domain of this protein in which there are 23 phosphorylatable residues (serines and threonines; Fig. 2.6). According with our results, we could identify two main clusters of phosphorylated residues, both in the regulatory domain of Atg29: one in the N-terminal part of the regulatory domain and another in the C-terminus. Threonine 115, detected using both Atg29 purified from yeast and from bacteria, was part of the N-terminal cluster sites, togheter with serines 106, 125, and 127. The phosphorylated residues in the very C-terminus of Atg29 included serine 201 (Fig.2.6). The result with respect to this serine is in contrast with what was observed previously. Mao and coworkers proposed that this site could be phosphorylated by Atg1 to promote autophagy (Mao et al., 2013). They mutated this serine in alanine together with serine 197 and serine 199 (Atg29 S3A) and performed an autophagy assay. They observed a decrease in autophagy activation of 45% in the Atg29 S3A mutant compared to the WT and they concluded that these three sites on Atg29 could be Atg1 targets (Fig. 2.6). This reduction in autophagy

activation could be due to the alanine mutations in the residues S197 and S199, thus it could be possible that the S201 is not responsible for this phenotype. Notably, the authors did not show any data about the autophagy activation in the mutant $Atg29^{S201A}$ or in the mutant $Atg29^{S197AS199A}$. In our study, we provided evidence that serine 201 is directly phosphorylated by TORC1 *in vitro*, suggesting that its TORC1-dependent phosphorylation would likely inhibit autophagy, although our experiment using Atg1 as kinase reveals that this residue could also be an Atg1 target *in vitro*. To better elucidate the discrepancy between our data and the results of Mao et al., further studies are necessary such as autophagy assays to clarify the physiological role of this phosphosite *in vivo*, as well as the importance of the other residues phosphorylated by TORC1. Notably, it could be also important to verify these phosphorylation events *in vitro* with an alternative experiment such as the autoradiography technique that involes the use of radioactive ATP during the kinase assay or *in vivo* using phospho-specific antibodies against one or more residue(s) of Atg29 upon nutrients availability or nitrogen starvation. Thus, we could verify at the same time the autophagy activation in these two conditions with an autophagy assay. We would expect that, upon favorable growth conditions, TORC1 is active and can phosphorylate Atg29 and thereby inhibit the autophagy, while, upon nitrogen starvation, TORC1 is inactive, the TORC1-dependent phosphosites on Atg29 are not phosphorylated and autophagy is activated. Expectedly, given that TORC1 and Atg1 regulate autophagy in general in an opposite manner, TORC1- and Atg1-dependent phosphorylation events should implicate different residues within their shared target proteins. It is therefore likely that the S201 on Atg29 is only a target of either TORC1 or Atg1, which would indicate that one of these kinases may be less specific when assayed *in vitro*.

Another protein that could be interesting to analyze in more detail is Atg9. This protein is considered a membrane transporter and it is a known Atg1 target phosphorylated by this kinase on several residues to regulate the expansion of the autophagosome (Papinski et al., 2014; Reggiori et al., 2005; Yamamoto et al., 2012). In our study Atg9 is phosphorylated by TORC1 on serine 250. Our data suggest that, in the context of autophagy, the kinases Atg1 and TORC1 could share some targets for the regulation of this process phosphorylating different sites of the Atg proteins

to promote (Atg1-dependent phosphorylations) or inhibit (TORC1-dependent phosphorylations) autophagy.

In conclusion, this method in which we combined the TORC1 *in vitro* kinase assay followed by mass spectrometry analysis allowed us to identify new targets of TORC1 belonging to the autophagy pathway, suggesting that this could be a useful approach to investigate other protein clusters studying the role of TORC1 in their regulation. Thus, one could also exploit this method for a more ambitious high throughput study purifying all the yeast proteins and using them as substrates in a TORC1 *in vitro* kinase assay.

CHAPTER III:

Study of the effect of IAA on TORC1 and cell growth

3.1 Introduction

TORC1 responds to several stimuli coming from the environment, and among them there are also some compounds that have a negative role in its regulation, such as rapamycin and caffeine, two inhibitors of TORC1 activity and cell growth. Both these molecules are natural compounds, rapamycin being a macrolide produced by soil bacteria, and caffeine being an alkaloid produced by different plants (such as coffee and cacao). Both compounds can affect several cellular processes such as cell growth and DNA metabolism (Heitman et al., 1991; Reinke et al., 2006; Sehgal et al., 1975; Vézina et al., 1975; Wanke et al., 2008).

The study of new TORC1 inhibitors is important as they could be used as therapeutics to negatively regulate cell growth in order to control proliferation in diseases like cancer.

In this contest, our own study (see below) indicated that indole-3-acetic acid (IAA) may be a natural compound that could impinge on TORC1.

IAA is the most common plant hormone of the auxins class and it is involved in regulation of plant development (Teale et al., 2006). Besides the naturally occurring members of the auxin family, some synthetically created molecules have a similar biological activity as IAA (Tan and Zheng, 2009). These include the 1-naphthaleacetic acid (NAA), which is slightly different in structure when compared to IAA (Figure 3.1), and which is highly used in commercial rooting powders.

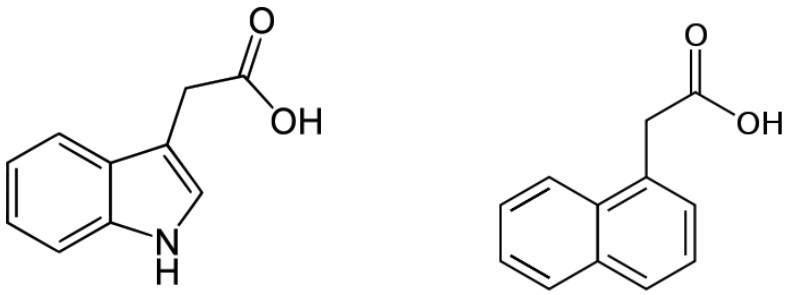

Indole-3-acetic acid **IAA**

1-Naphthaleneacetic acid **NAA**

Figure 3.1 Chemical structures of IAA and NAA. Taken and modified from (Tan and Zheng, 2009).

IAA is most well studied in plants, but it is also produced by other organisms such as bacteria and yeasts (Basse et al., 1996; Gruen, 1959; Yamada et al., 1985). This compound has been described as an inhibitor of yeast cell growth at high concentrations (EC_{50} 250 μM), and a stimulator of filamentation and adhesion at low concentrations (50 μM) (Prusty et al., 2004).

In this chapter, we investigated the possibility that the effect of IAA on yeast cell growth could be due to a role of this compound in the negative regulation of TORC1 activity. Although we found NAA to more potently inhibit yeast cell growth (not shown), we focus in this chapter on the natural auxin IAA and its potential role as a TORC1 inhibitor in yeast.

3.2 Results

3.2.1 The effect of IAA on cell growth

To study the effect of IAA on yeast growth, we tested different concentrations of this compound, in a drop spot assay, using different mutants involved in the TORC1 pathway and comparing them to the WT (BY4741/2 background). We tested the effect of this compound on two media: YPD and SD medium lacking all amino acids (to avoid the possible interference of the amino acids in the IAA uptake) (Fig. 3.2).

Because 1 mM IAA had little effect on growth of WT cells, we studied the effect of this compound in *tco89Δ* and *gtr1Δ* mutants that have intrinsically low TORC1 activity. Unfortunately, on YPD plates as well as on SD plates, we did not detect any effect on growth using IAA on all the tested mutants (which also included the *fpr1Δ* and *iml1Δ* strains) (Fig. 3.2).

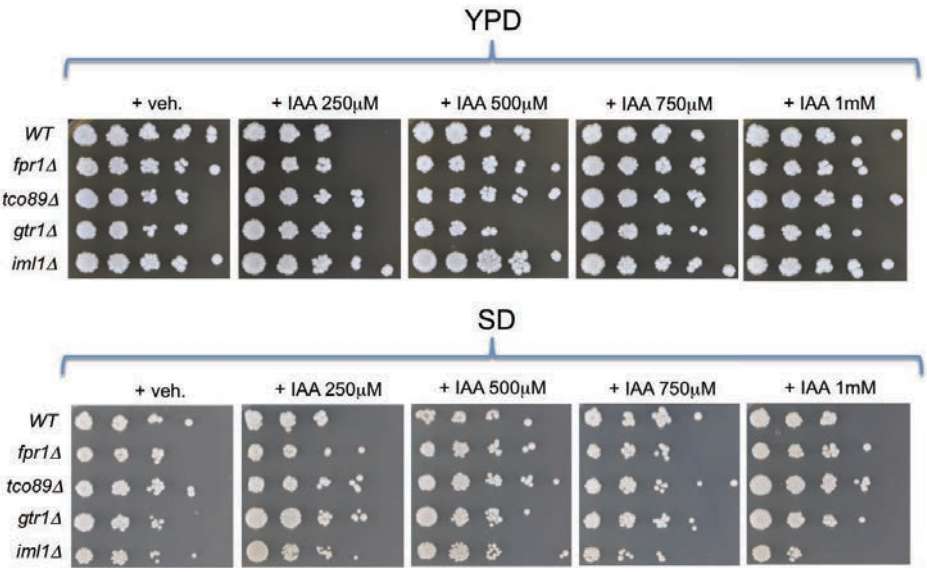

Figure 3.2 IAA (<1 mM) does not affect growth in both YPD and SD solid medium. Spotting 10-fold dilutions of these cells onto YPD or SD plates containing drug vehicle or different concentrations of IAA indicates that the WT as well as all the mutants tested are not inhibited in growth at none of these concentrations. Prototrophic cells were spotted on SD medium. Vehicle: ethanol 90% Tween 10%. The cells grew at 30°C for 2 days.

Since we could not reproduce an effect by IAA on yeast growth on solid medium, we decided to perform our experiments in liquid cultures, in which the cellular metabolism may differ when compared to growth on solid media (Váchová et al., 2012). Perhaps, we speculated, the distribution of IAA may be more homogeneous in liquid cultures when compared to the solid medium.

Therefore, we performed another growth assay in liquid medium (Bioscreen assay) that gave us the possibility to quantify the effect on growth by calculating the doubling time of the cultures treated with different concentrations of IAA. To verify that the inhibitory effect on growth implicated the TORC1 pathway, we also included a particular strain in which the TORC1 pathway is genetically bypassed by expressing a plasmid carrying an allele of the TORC1 target Sch9 that mimics its TORC1-phosphorylated state ($Sch9^{2D/3E}$), combined with the deletions of *GLN3* and *GAT1* (Urban et al., 2007; Wanke et al., 2008). Since this strain is not in the BY4741/2 background, we also compared the two WT strains (BY and TB50) to verify that they had the same growth phenotype in the presence of IAA (Fig. 3.3):

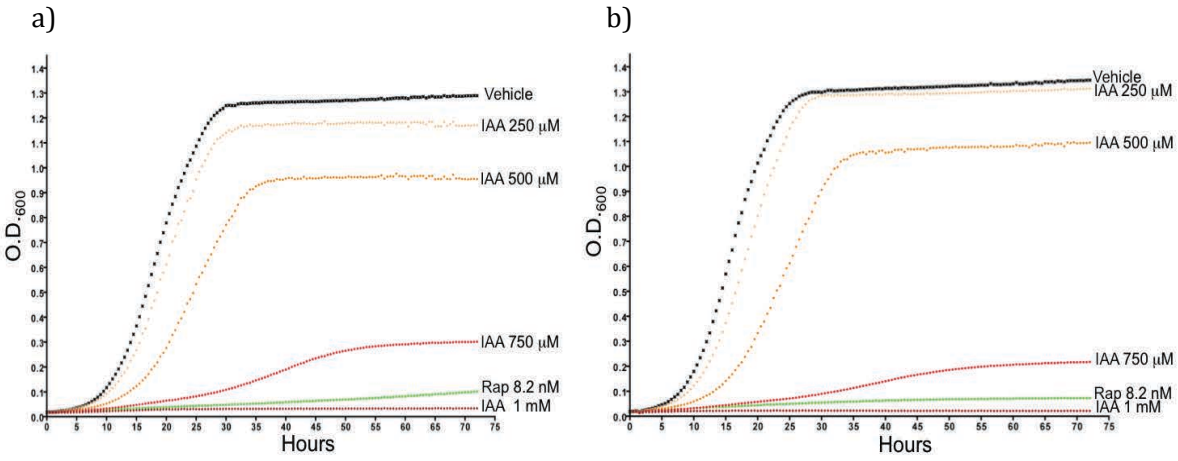

Figure 3.3 WT BY and WT TB50 respond to auxin in a similar way. Growth curves of WT BY (a) and WT TB50 (b) in absence or presence of different concentrations of IAA. As control, rapamycin was used at a concentration of 8.2 nM. Vehicle: ethanol 90% Tween 10%. All assays were carried out in triplicate and expressed as mean + SD.

From these results, we concluded that growth of both WT strains was dramatically inhibited by similar concentrations of IAA (750 μM) (Fig. 3.3).

We proceeded, therefore, to the analysis of the TORC1 bypass strain (TORC1bp) comparing its growth in the presence of IAA with that one of the WT TB50. We observed that the TORC1 bypass strain was partially protected from the growth inhibitory effect of IAA, starting to be sensitive to this compound at a higher concentration (1 mM) when compared to the WT (Fig. 3.4). Notably, the TORC1bp strain was fully resistent to rapamycin, as aspected.

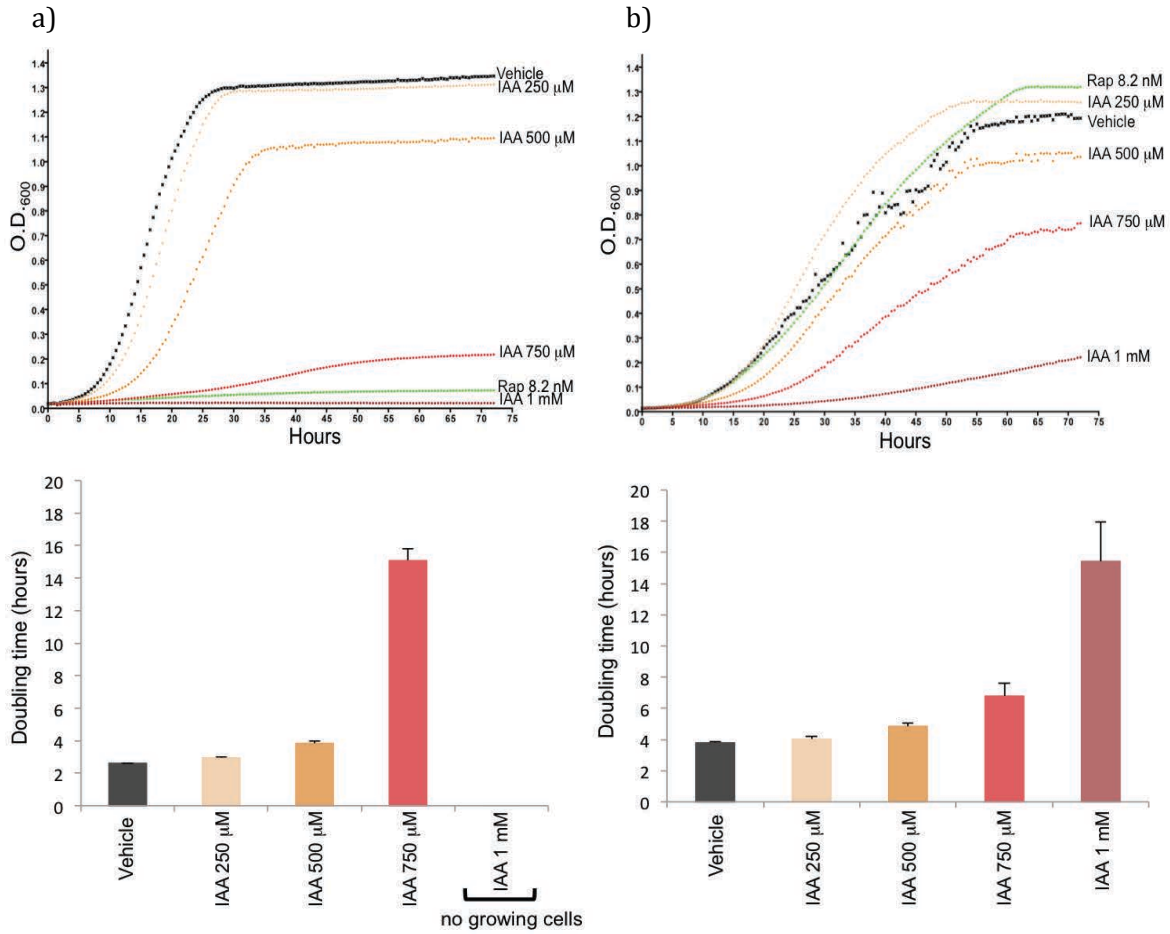

Figure 3.4 Bypassing TORC1 pathway, cells are more resistant to IAA. Growth curves and doubling time of WT TB50 (a) and TORC1bp (b) in absence or presence of different concentrations of IAA. As control, rapamycin was used at a concentration of 8.2 nM. Vehicle: ethanol 90% Tween 10%. The doubling time was calculated according to the exponential growth curves in their linear range. All assays were carried out in triplicate and expressed as mean + SD.

From these results, we infer that IAA mediates growth inhibition only in part via TORC1, since TORC1bp cells were still sensitive to 1 mM IAA. This compound has likely additional growth-limiting targets within cells.

We also calculated the half maximal effective concentration (EC_{50}) of IAA in WT (EC_{50}: 0.58 mM), but we could not calculate the EC_{50} in TORC1bp cells because, with the tested IAA concentrations, we could not obtain a sigmoid curve for the growth rate of this strain (Fig. 3.5). The fact that the highest concentration of IAA tested (1 mM) could not completely inhibit cell growth in TORC1bp strain, while it did in WT cells supported the hypothesis that TORC1 is an important target of IAA.

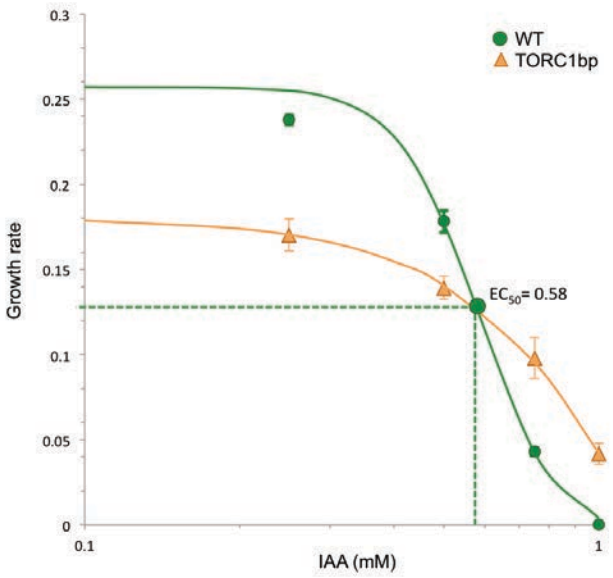

Figure 3.5 EC_{50} of IAA calculated on WT cells and the growth rate curve of the TORC1bp cells. In green is represented the growth rate depending on the concentrations of IAA of WT cells; in orange is represented the growth rate depending on the concentrations of IAA of TORC1bp cells. The growth rates were calculated according with the exponential growth curves in their linear range. All assay points were done in triplicate and expressed as mean +- SD.

Notably, our WT strain appears less sensitive to IAA (EC_{50}: 580 μM) than a previously reported strain (EC_{50}: 250 μM) (Prusty et al., 2004). The reason for this difference is likely the different capacities of the respective cells to take up IAA from the medium.

3.2.2 IAA inhibits TORC1 *in vivo*

The results shown above suspect that the effect of IAA on growth could be due to an inhibitory effect of IAA on TORC1. To verify this hypothesis, we performed a TORC1 activity assay *in vivo*, testing different concentrations of IAA. For this purpose, we quantified the *in vivo* phosphorylation of two direct substrates of TORC1: Sch9 (Urban et al., 2007) and Lst4 (see Chapter 1) (Fig. 3.6).

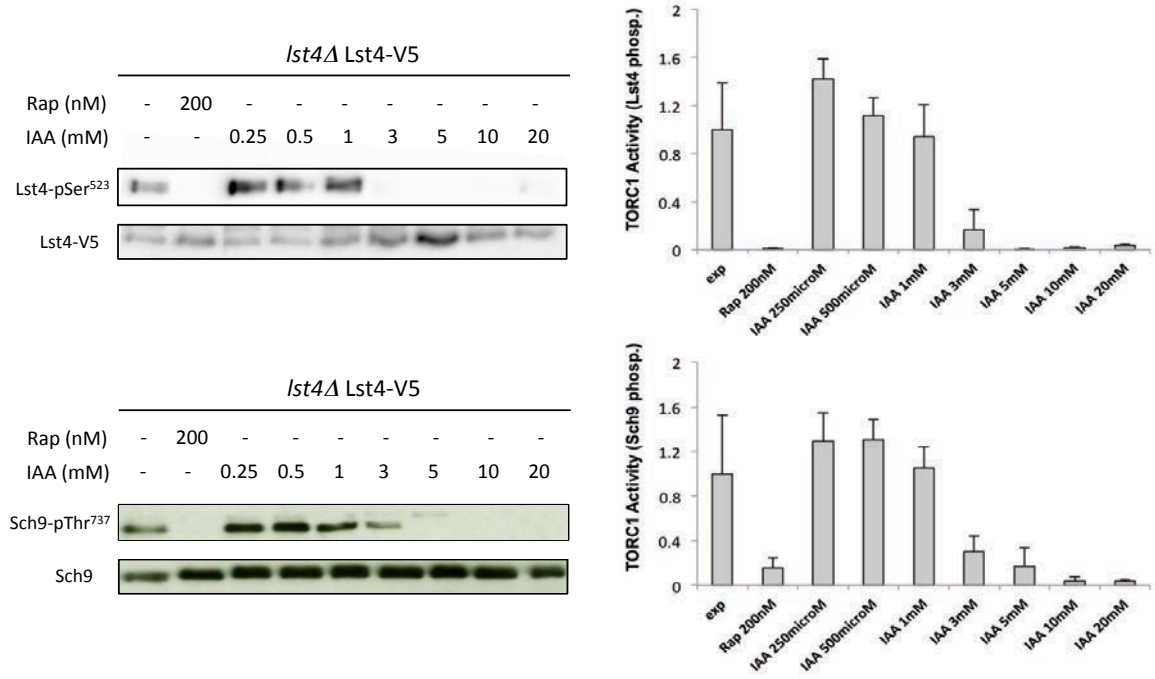

Figure 3.6 IAA inhibits TORC1 *in vivo*. Lst4-V5-expressing *lst4Δ* cells were grown in SD medium, depleted of all amino acids. They were either left untreated (-), treated with rapamycin for 30 min (Rap; 200 nM), or treated with different concentrations of auxin IAA for 30 min (IAA; 0.25, 0.5, 1, 3, 5, 10, 20 mM). Phosphorylation of Lst4-V5 and endogenous Sch9 were analyzed on a SDS-Page gel followed by immunoblotting with anti-Lst4-pSer^{523} and anti-V5 antibodies to monitor the Lst4 phosphorylation, and anti-Sch9 and anti-Sch9-pThr^{737} antibodies to monitor the Sch9 phosphorylation. All assays were carried out in triplicate and expressed as mean + SD.

We observed that IAA could inhibit TORC1 *in vivo* with an IC_{50} = 1.55 mM using Lst4 as substrate, and an IC_{50} = 2 mM if we considered Sch9 as a read-out of TORC1 activity (Fig. 3.7). This slight difference of IC_{50} using these two substrates could be due to the different activity of the (unknown) phosphatases dephosphorylating the two TORC1 targets.

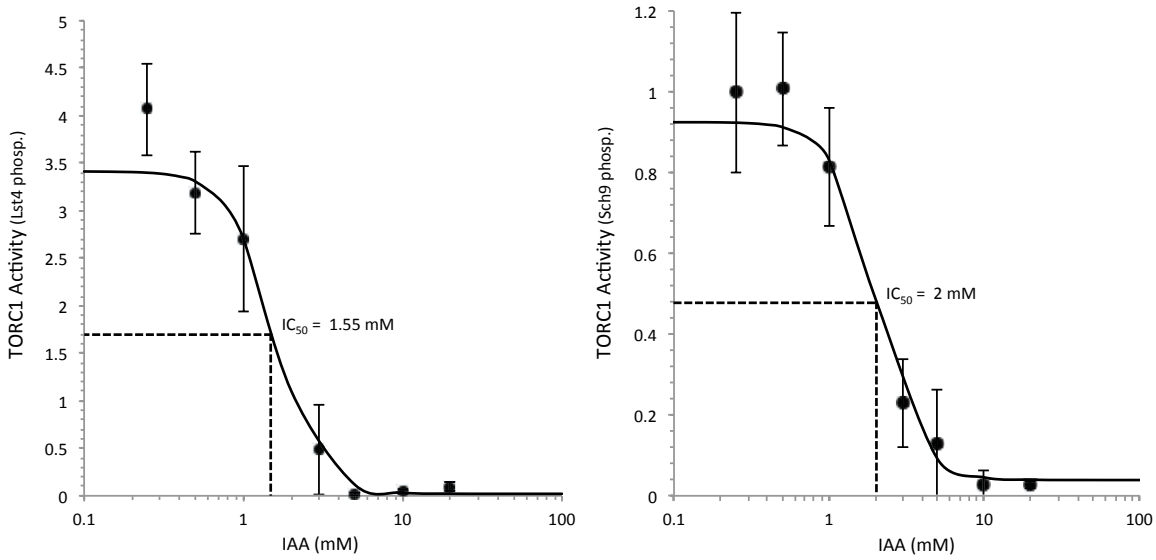

Figure 3.7 IC_{50} of IAA calculated on Lst4 phosphorylation and Sch9 phosphorylation. *In vivo* TORC1 kinase assay with Lst4 and Sch9 as substrates was used to determine the IC_{50} of IAA. All assay points were done in triplicate and expressed as mean +-SD.

The concentration of IAA that affects TORC1 activity *in vivo* is significantly higher compared to rapamycin ($IC_{50\text{-in vivo}}$: 10.7 nM), but it is in a similar range as caffeine ($IC_{50\text{-}in\ vivo}$: 5.5 mM) (Wanke et al., 2008).

3.2.3 IAA inhibits TORC1 *in vitro*

To test whether IAA could directly inhibit TORC1, we studied its inhibitory effect in TORC1 *in vitro* kinase assays. For this purpose, we used as substrate a small part of the Lst4 protein, a direct target of TORC1 (see Chapter 1), that is phosphorylated by this kinase on several residues.

Stikingly, IAA inhibits TORC1 *in vitro*, confirming our hypothesis that IAA is a direct inhibitor of TORC1 (Fig. 3.8).

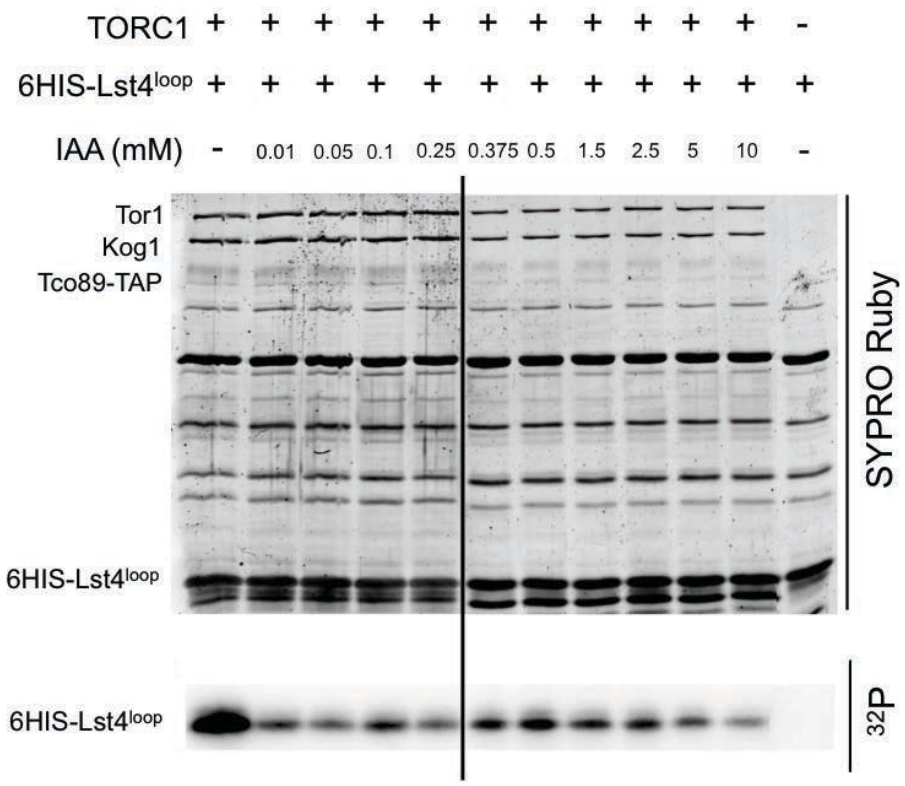

Figure 3.8 IAA directly inhibits TORC1 *in vitro*. Purified recombinant His6-Lst4^{loop} was subjected to *in vitro* phosphorylation by TORC1 (purified from yeast) in the absence (-) or presence (+) of different concentrations of IAA. Representative SYPRO Ruby staining and autoradiography (^{32}P) blots of triplicates are shown.

With this experiment we were able to confirm that IAA directly inhibits TORC1. We observed that already at the lowest concentration tested (10 μM) the phosphorylation of Lst4^{loop} was reduced by 50% when compared to the control sample (Fig. 3.9). It is important to specify that, with the tested IAA concentrations, we could not obtain a sigmoid curve and so we could not calculate properly the IC_{50}. This is the reason why we did not define 10 μM of IAA as the IC_{50} of IAA on TORC1 activity *in vitro*, but we described this concentration as the concentration of IAA already sufficent to decrese *in vitro* the TORC1 activity of the half. Thus, it is likely that IAA inhibits TORC1 activity at lower concentrations. Further analysis should reveal whether IAA inhibits TORC1 in a non-competitive manner.

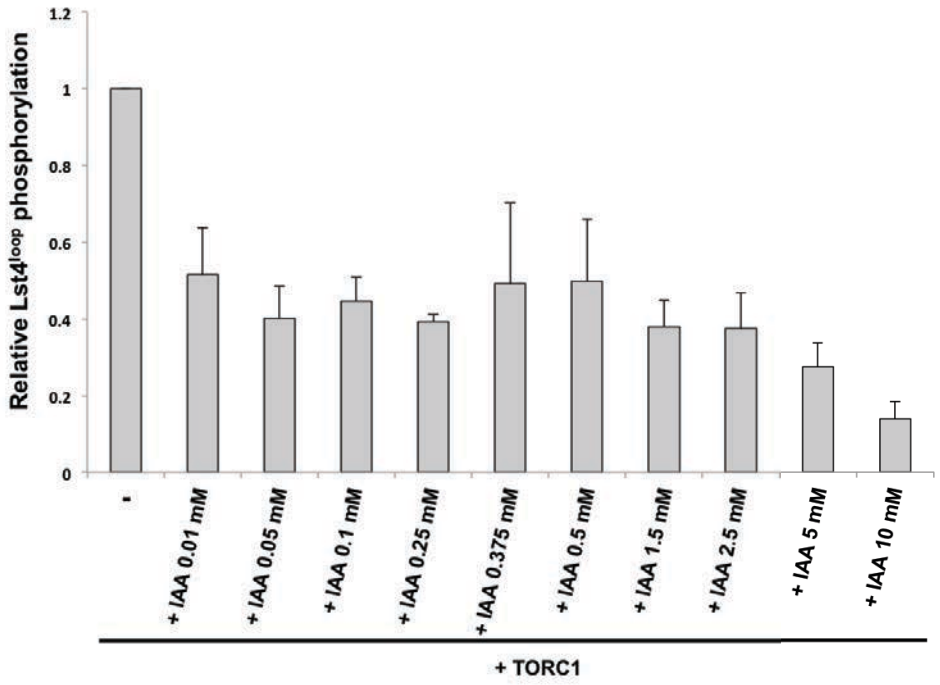

Figure 3.9 IAA inhibits TORC1 activity *in vitro*. Quantification of the relative Lst4^{loop} phosphorylation *in vitro* by TORC1 in absence (-) or in presence of different concentrations of IAA determined according with the P^{32} autoradiography result.. All assay points were done in triplicate and expressed as mean + SD.

3.2.4 Genetic screening using IAA and rapamycin reveals common sensitive mutants

The high throughput approach studying a new compound is normally a useful experiment to have more information about the pathways involved in the response to that particular molecule. In our study, the aim was to investigate a putative role of IAA on the TORC1 pathway, so we decided to screen the entire knock out (KO) yeast collection to find mutants sensitive to IAA, verifying if we could obtain an overlap doing the same screening using rapamycin.

The KO yeast collection is the set of all the viable mutants of *S. cerevisiae* in the BY4742 background, organized in plates of 384 wells each. To this aim we used a robot that automatically spots the different strains on solid medium with or without IAA or rapamycin.

First, we focused on searching for the ideal concentrations of the two drugs to detect the sensitive mutants. For this purpose, we spotted the WT and the *gtr1Δ* mutant on SD complete medium in the presence of different concentrations of IAA or

rapamycin. For the robotic screening procedures, we chose 3mM concentration of IAA and 4 nM concentration of rapamycin (Fig. 3.10), which allowed visibly to discern the growth difference between WT and *gtr1Δ* cells.

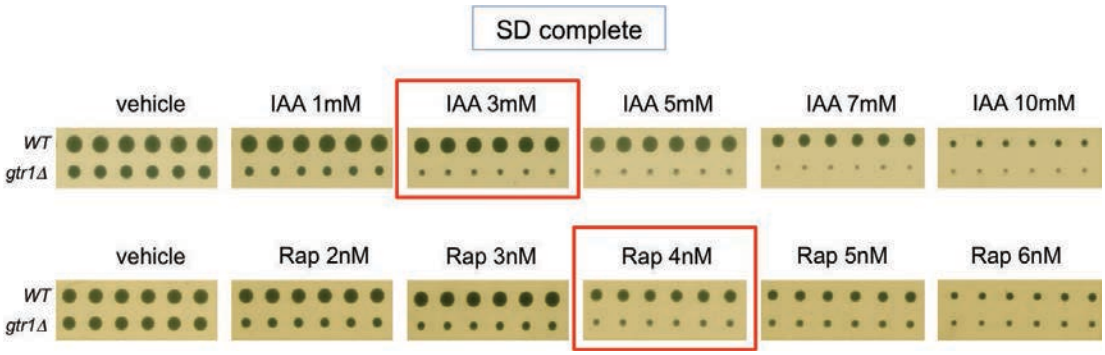

Figure 3.10 Choice of the concentrations of IAA and rapamycin for the KO collection screening. The WT and the *gtr1Δ* mutant were spotted on SD complete medium in presence or absence of different concentrations of IAA or rapamycin. For each condition, the spots represent repetitions of the same amount of cells. Red squares indicate the chosen concentrations for the KO collection screening. Vehicle: ethanol 90% Tween 10%.

To perform the screening with the selected concentrations of the drugs, the first step was to transform each plate of the collection from a 384 format into a 1536 format to be able to have 4 replicates of each strain. Then, we could use this collection and the robot to screen all the yeast mutants on plates without drugs, and on plates with IAA or rapamycin. For each plate and each mutant, the robot spotted the same amount of cells on the vehicle plate as well as on the plates containing 3 mM of IAA or 4 nM of rapamycin (an example in Fig. 3.11).

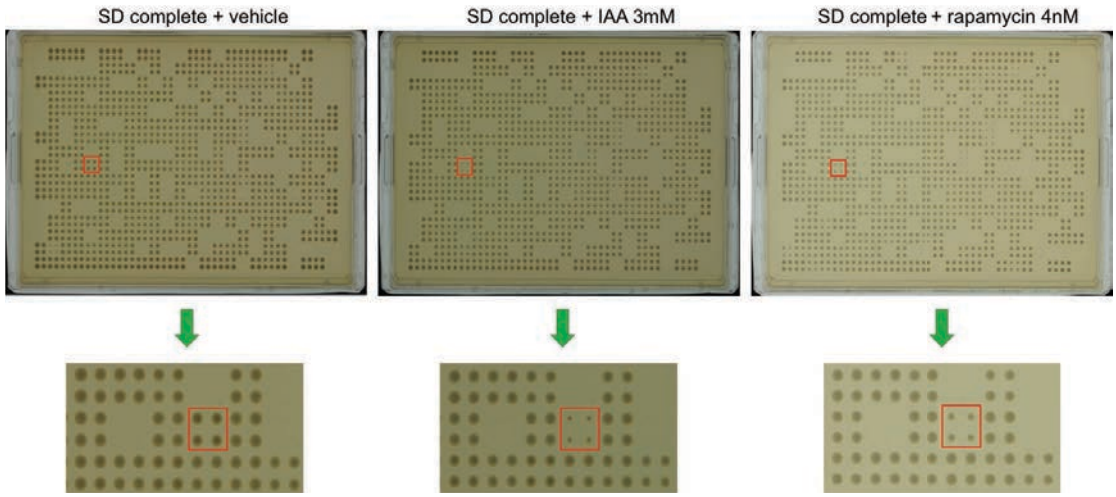

Figure 3.11 Example of plates spotted using the robot. The quadruplicate of each mutant was spotted on SD complete + vehicle (Control plate) and on SD complete + 3 mM IAA or + 4 nM rapamycin. Vehicle: ethanol 90%, Tween 10%. The cells grew at 30°C for 2 days.

The analysis was carried out using a dedicated platform on the Rothstein Laboratory website. Briefly, this tool allows to process all the plates (CONTROL and DRUG) analyzing the colony size of each mutant. The software compares the size of the four colonies corresponding to the same mutant in the control plate and in the plate with IAA or rapamycin, calculating a P-value for the difference among the size of the spot in the control and the size of the spot in the treatment plate. Among all the results for each mutant, only those with a P-value <0.05 were considered mutants with a significant growth defect in presence of the drugs.
Strikingly, several mutants were found to be sensitive to both drugs, and among those were also some known mutants of genes involved in the TORC1 pathway (Table 3.1). The detected rapamycin-sensitive mutants were 275, while the mutants conferring IAA-sensitivity were 161, with an overlap between the two categories of 86 hits (Fig. 3.12).

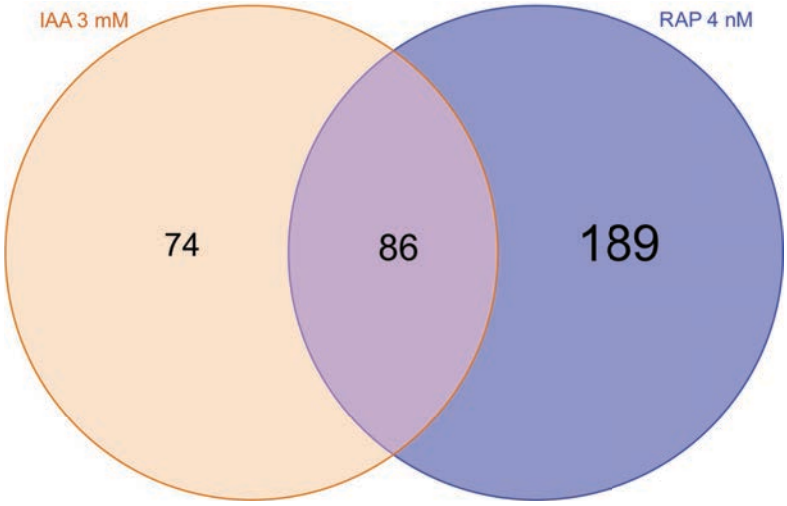

Figure 3.12 IAA and rapamycin share several sensitive mutants. Venn diagram represents all the knock out mutants sensitive to IAA (3 mM) and/or rapamycin (4 nM). The complete list of the mutated genes sensitive to rapamycin and/or IAA is in Table 3.1 and Table 3.2.

According to the Gene Ontology analysis (SGD, GO TermFinder platform), the mutants conferring sensitivity to both drugs belong to different categories such as vesicle-mediated transport, cellular and RNA metabolic processes, lipids and

ergosterol biosynthesis and, strikingly, the TORC1 pathway (Fig. 3.13; Table 3.1). Interestingly, the rapamycin-sensitive mutants, more numerous than those susceptible to IAA, included more GO clusters such as pH regulation, gene expression and transcription regulation, and protein modification (Fig. 3.13; Table 3.2).

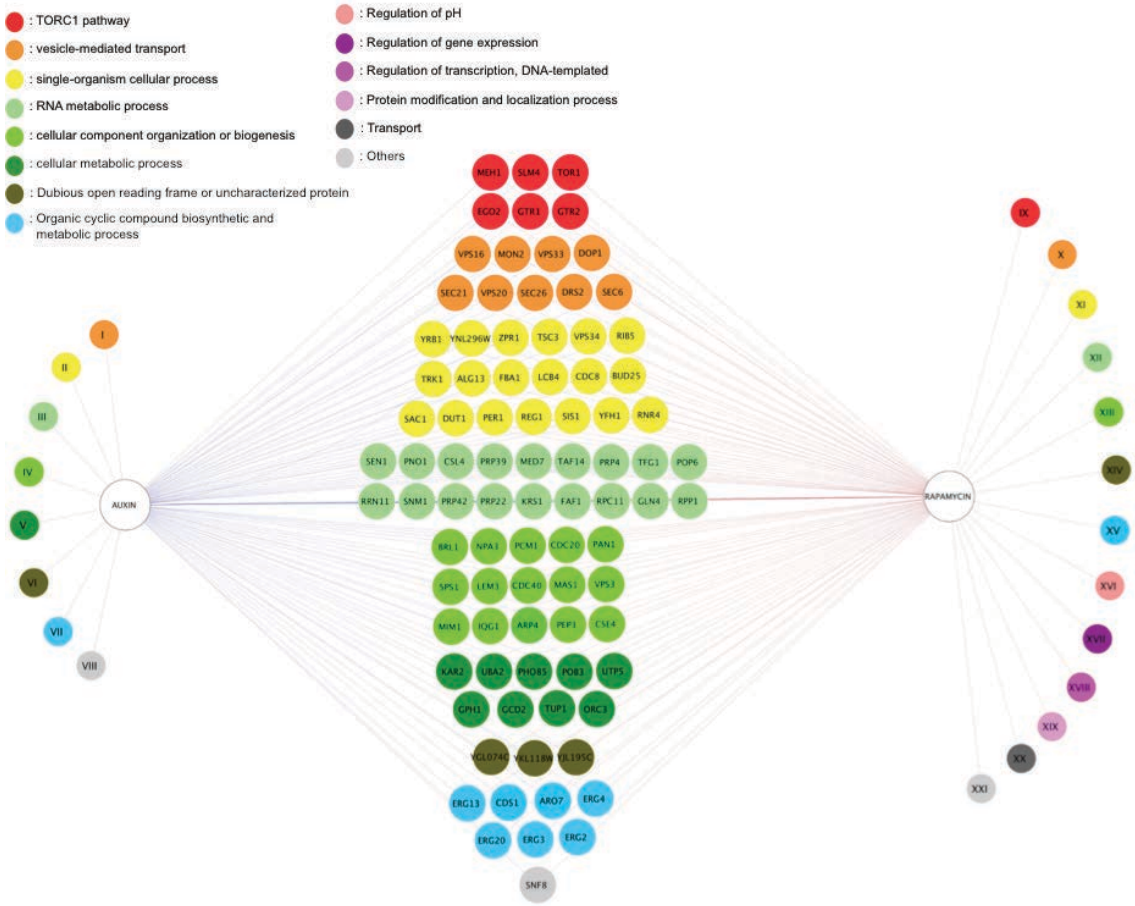

Figure 3.13 Overlap between the rapamycin-sensitive mutants and the IAA-sensitive mutants, organized in GO clusters. Edges indicate the chemical interaction and nodes represent either compounds or genes. The gene nodes color-coded correspond to defined GO categories. For the mutants collected in the different groups corresponding to the roman numbers (I-XXI), see Table 3.1 and Table 3.2.

With this screening we were able to corroborate our *in vivo* and *in vitro* data that indicate a role of IAA in direct inhibition of TORC1. Neverthless, it appears that IAA also affects other pathways that are important for growth. This is in line with our data in which the TORC1bp strain was found to be only partially resistant to IAA (Fig. 3.4).

We also tried to get IAA-resistant mutants (using 10 mM of IAA), but unfortunately we could not obtain any mutant resistant to this concentration of this compound.

3.3 Discussion

In this chapter, we reported growth assay data that confirmed the inhibitory role of IAA on yeast cell growth described in the literature (Prusty et al., 2004). It is important to underline that we could be able to see a clear effect on growth treating the cells with IAA only when cells were grown in liquid medium and no effects were detected on plates. We could not elucidate the reason of these different results using plates or liquid medium, but we hypothesize that the cells could have a different response to this compound and a different uptake efficiency in liquid culture compared to solid medium. Our results on the effect of IAA on growth also confirmed another recent study in which the authors analyzed the effect of exogenous IAA on growth of different yeast strains (Liu et al., 2016). In this study, among the strains significantly inhibited in growth in the presence of high IAA concentration (5 mM), there was the S288C, the ancestor of the BY4741/2 (Liu et al., 2016). This correlates with our findings using the BY4741/2 and TB50 backgrounds.

In our study, we showed an effect of IAA on cell growth with an EC_{50} of 0.58 mM on WT cells and a partial resistant phenotype for the TORC1bp strain compared to the WT, suggesting the involvement of the TORC1 pathway in the response to IAA treatment. Notably, the TORC1bp strain was still sensitive to 1 mM IAA, pointing out that this compound has other pathway targets for the inhibition of cell growth.

The partial resistance obtained with the TORC1bp strain motivated us to investigate the possibility that IAA could affect TORC1 activity more directly, so we performed *in vivo* and *in vitro* assays that supported our hypothesis that IAA is a direct inhibitor of TORC1. Our data revealed an $IC_{50\text{-}in\ vivo}$ of IAA of 1.55-2 mM and we observed that *in vitro* TORC1 reduces its activity of the half in presence of 10 μM of IAA. To find the $IC_{50\ in\text{-}vitro}$ requires testing IAA concentrations lower than 10 μM in order to identify the sigmoid curve that describe the dose-dependent effect of IAA on TORC1 activity.

To strengthen our findings, we essayed all the yeast viable knock out mutants for growth on IAA or rapamycin in order to test the predicted existence of mutants that are sensitive to both drugs. Indeed, among the latter mutants there were some that are known to exhibit low TORC1 activity such as *tor1Δ*, *gtr1Δ*, *gtr2Δ*, *ego1Δ*, *ego2Δ* mutants.

It is known that yeast can produce IAA per se, although different *Saccharomyces* strains have a different capacity in IAA production, with a range from 1.6 mM to 80 μM (Liu et al., 2016; Rao et al., 2010). The production of IAA by microorganisms is linked to the inhibition of the growth of competitors, indeed it was observed that strains, that can produce high amounts of IAA, are tolerant to this compound (Liu et al., 2016). Among the strains that could produce IAA, there was the S288C strain, but this yeast is still sensitive to this molecule (Liu et al., 2016). We also found several mutants that were sensitive to IAA, but we could not find any of them that were resistant to this compound (10 mM). Among the sensitive mutants, we found genes involved in cell wall integrity such as *cdc1Δ* and *psa1Δ* that could suggest a more efficient IAA uptake conferring the hypersensitivity to this compound compared to other mutants.

As described above, yeast produces IAA and considering our findings concerning the direct inhibitory role of this compound on TORC1, these data together could suggest a mechanism to regulate the homeostasis of TORC1 activity avoiding its hyperactivation. It will be interesting to verify that the effective intracellular concentrations of IAA may be in a range that enables it to act as a physiologically important regulator of TORC1 within cells.

Drugs	Sensitive genes	GeneOntology
IAA 3 mM & Rap 4 nM	SLM4, GTR1, GTR2, MEH1, TOR1, EGO2	TORC1 pathway
	DOP1, DRS2, MON2, SEC21, SEC26, SEC6, VPS16, VPS20, VPS33	vesicle-mediated transport
	ALG13, BUD25, CDC8, CDS1, DUT1, FBA1, PER1, REG1, RIB5, RNR4, SAC1, SIS1, SPS1, TRK1, TSC3, VPS34, YFH1, YNL296, WYRB1, ZPR1	single-organism cellular process
	CSL4, FAF1, GLN4, KRS1, MED7, ORC3, PNO1, POP6, PRP22, PRP39, PRP4, PRP42, RPC11, RPP1, RRN11, SEN1, SNM1, TAF14, TFG1	RNA metabolic process
	BRL1, CDC20, CDC40, CSE4, IQG1, KAR2, LEM3, MAS1, MIM1, NPA3, PAN1, PCM1, PEP3, VPS3	cellular component organization or biogenesis
	YGL074C, YJL195C, YKL118W	dubious open reading frame
	ARP4, GCD2, GPH1, PHO85, POB3, TUP1, UBA2, UTP5	cellular metabolic process
	ARO7, ERG13, ERG2, ERG20, ERG3, ERG4	organic cyclic compound biosynthetic and metabolic process

Table 3.1 List of genes (grouped to GO terms) which render cells sensitive to both IAA and rapamycin when deleted.

Drugs	Group	Sensitive genes	GeneOntology
IAA 3 mM	I	GCS1, GLO3, SEC31, VPS17, VPS5, VTI1	vesicle-mediated transport
	II	YNL277w-A, ACB1, CHS1, PDR12	single-organism cellular process
	III	CBF5, GCD10, GCD14, GRC3, MES1, MSL5, PRP2, PRP21, RPR2, SIN4, SSL1, TAD2, TBF1	RNA metabolic process
	IV	CDC28, CIK1, CKS1, DBF2, END3, FPK1, IRR1, MCD1, MEX67, SAC6, SGD1, SLA1, SLG1, ULP2, VAM10, VRP1	cellular component organization or biogenesis
	V	CDC1, CDC27, GND1, HOM2, MRP4, PFK1, PFK2, PHA2, PRE1, PSA1, PTC1, RFC5, RPL32, RPT5, RRD1, SAP190, SAS10, SSQ1, VPS25, WAR1, SPT7	cellular metabolic process
	VI	YGL069C, YGR190C	dubious open reading frame
	VII	ERG12, ERG24, ERG6	organic cyclic compound biosynthetic and metabolic process
	VIII	SPT14, FEN1, KEI1, SUR4, TSC13, MCM2, ORC1, PSF3, YRA1	other
Rap 4 nM	IX	LST7, VAM6	TORC1 pathway
	X	APL2, APM1, ARL3, BRE5, BST1, DID4, PEP12, RET3, SEC3, SNF7, SRO7, VAM3, VAM7, VPS24	vesicle-mediated transport
	XI	APC11, FES1, FYV6, IRC8, ANP1, APQ12, ARL1, BUR2, CHO1, CKA2, CLB2, EPS1, ESA1, ETR1, GAA1, GLC7, GUP1, HOM3, HSL7, ILV5, IME4, INP53, JAC1, KIN3, KRE6, LCB4, MNN10, NAT3, NBP2, NDE1, NUC1, OCA5, OST4, PIB2, PKP1, PKR1, PPE1, PRS3, RTS1, SIC1, SPO22, SSN8, TEF4, TEM1, TIF35, UGP1, YGR064W, YJL018W, YNL190W	single-organism cellular process
	XII	DBP9, ELP2, ELP3, GON7, IKI1, KTI11, KTI12, LSM1, LSM7, NCS6, NPL3, PAT1, POP2, PRP40, RET1, RPB11, RPB4, RPB8, TAD3, THP1	RNA metabolic process
	XIII	ARP6, CDC24, ECM33, GAS1, GVP36, NOC2, NUP145, POC4, RHO4, RRS1, SOF1, SWC5, TEL2, TIF3, TMA108, VMA21, VPS72	cellular component organization or biogenesis
	XIV	YAR040C, YBL094C, YBR134W, YCL007C, YDL152W, YDR433W, YER119C-A, YIL141W, YJL135W, YLR317W, YMR031W-A, YOR331C, YPL238C, YPR170C, YCL002C, YHL037C, YIL029C, YJL016W, YKL077W, YKL096c-B, YLR358C, YMR001c-A	dubious open reading frame and uncharacterized protein
	XV	ERG26, ERG5	organic cyclic compound biosynthetic and metabolic process
	XVI	VMA1, VMA11, VMA13, VMA16, VMA2, VMA22, VMA3, VMA4, VMA5, VMA7, VMA8, VMA9, VPH2, YHR039C-B	regulation of pH
	XVII	CCR4, CDC73, CTR9, DHH1, SBP1, TOP1	regulation of gene expression
	XVIII	CTK2, CTK3, DST1, HTZ1, NOT5, SET2, SFP1, SNF2, SPT4, SUS1	regulation of transcription, DNA-templated
	XIX	GGA2, STP22, YRB2, PEP8, SEM1, RPP1A, UBA4, UBP3, YDJ1, YUR1	protein modification and localization process
	XX	MCH5, MUP3, OPT2, PMP2, RAV1, VPS27, VPS28, VPS29, VPS36, VPS4, VPS52, VPS54, VPS71, YHL008C, YIA6	transport
	XXI	RSC1, ATG11, KRE28, YAF9, YNG2, RHR2, VID28, YPK1	other

Table 3.2 List of genes (grouped to GO terms) which render cells either sensitive to IAA or to rapamycin when deleted (groups I-XXI).

General Discussion

Future perspectives to improve the knowledge about the role of Lst4-Lst7 complex in the regulation of TORC1 activity homeostasis

After the identification of the regulators of the Gtr1 Rag GTPase (Iml1 as a GAP and Vam6 as a potential GEF), the discovery of the Lst4-Lst7 complex as a GAP for Gtr2 started to elucidate the regulation of this Rag GTPase (Péli-Gulli et al., 2015). It has been reported that the Lst4-Lst7 complex is recruited to the vacuolar membrane in an amino acid availability-dependent manner and that this complex, once at the vacuole under amino acid starvation, interacts with Gtr2 only upon refeeding cells with nutrients (Péli-Gulli et al., 2015). These findings motivated us to investigate more about this mechanism of recruitment of the Lst4-Lst7 complex to the vacuole and, indeed we discovered that the vacuolar localization of this complex is regulated by TORC1-dependent phosphorylations of Lst4. We demonstrated that Lst4 is a direct target of TORC1 that phosphorylates this protein on several residues within an unstructured region located between two portions of the Lst4 DENN domain (intra-DENN loop). Upon amino acid starvation, the unphosphorylated Lst4 intra-DENN loop brings the Lst4-Lst7 complex to the vacuole. With the readdition of nutrients, the Lst4-Lst7 complex interacts with Gtr2 promoting its GDP-loading status and the activation of TORC1 that can phosphorylate Lst4, promoting the release of the Lst4-Lst7 complex from the vacuole. In addition, we demonstrated that the Lst4 loop is necessary and sufficient for the vacuolar localization of Lst4-Lst7 complex, but its phosphorylated status does not affect the GAP activity of the complex. Although our results elucidate the mechanism for the dynamic Lst4-Lst7 complex localization and the role of this complex in the feedback inhibitory loop to regulate the TORC1 activity homeostasis, other questions are still unsolved. How can the Lst4-Lst7 complex sense the presence of amino acids to interact with Gtr2? How is this complex anchored to the vacuole though the Lst4 loop? Is it because of an interaction with a vacuolar protein or a direct interaction between the loop and the lipids of the vacuolar membrane? To answer the first question it will be necessary to understand if there is another player that (i) inhibits this interaction until the cells are fed with amino acids after nutrient starvation or that (ii) induces the interaction between Gtr2 and its GAP mediating the amino acids availability signal. The first mechanism could be the most probable, supported by the fact that

the Lst4-Lst7 complex can exercise its GAP activity on Gtr2 *in vitro*, then in the absence of other factors, but we can not completely exclude the second hypothesis. This is because the GAP activity *in vitro* could represent the basal activity of the Lst4-Lst7 complex within cells.

To be able to understand if this additional player exists, we could proceed with pulling down Lst4 and/or Lst7 from cells in two different conditions: amino acid starvation and amino acid starvation followed by amino acid readdition to reveal the interactor(s) of these proteins and likely to identify one or more proteins that interact with one or both Lst4 and Lst7 only in the second condition.

The interaction of Lst4-Lst7 with Gtr2 and the consequent activation of TORC1 is also stimulated by specific amino acids such as glutamine and these data raise the possibility that the Lst4-Lst7 complex could directly sense the presence of a particular amino acid for its interaction with Gtr2. In analogy, mammalian Sestrin2 and CASTOR1/2, negative regulators of mTORC1, can directly sense and bind leucine and arginine respectively, thereby releasing GATOR2 and activating mTORC1 (Chantranupong et al., 2014, 2016). In a similar way, Lst4-Lst7 could sense a specific amino acid and undergo a change in conformation that allows its interaction with Gtr2. In the case of Sestin2 and CASTOR1/2, the leucine or arginine binding suppresses their interaction with GATOR2 promoting TORC1 activation, instead in the case of the Lst4-Lst7 complex, the amino acid-binding could activate the interaction of this complex with Gtr2.

To elucidate the second question about how the Lst4-Lst7 complex is anchored to the vacuolar membrane, a protein pull-down approach similar to that one described above could be used to identify the putative partner of the Lst4 loop that tethers the Lst4-Lst7 complex to the vacuolar membrane under amino acid starvation. A pull-down of Lst4 or even just the Lst4 loop could be performed from cells starved for amino acids with or without the readdition of nutrients. In addition, the Lst4 loop could directly interact with the lipids present in the vacuolar membrane. To investigate this possibility, one could use membrane strips covered with different kind of lipids and incubate them with the Lst4 loop (PIP strip assay) to understand if this portion of Lst4 is able to bind lipids. Another technique could be that involving liposomes, spherical vesicles artificially prepared with different kinds of lipids mixes. In mammals, a recent study involved the use of both membrane strips and

liposomes to investigate the TSC2 protein that together with TSC1 and TBC1D7 forms a complex (the TSC complex) that functions as a GAP for the GTPase Rheb, at the lysosomal membrane (Nakashima et al., 2007; Zech et al., 2016). Zech and coworkers have shown that the N-terminus of TSC2 (TSC2-N) does not interact with a specific lipid using the PIP strip assay. Notably, when incubated with neutral or vacuolar liposomes, TSC2-N binds specifically to the vacuolar lipid mix. However, this binding was weak when compared to the positive control protein Vam7. Thus, TSC2-N binding to the lysosomal membrane contributes to the recruitment of the TSC complex to the lysosomal mebrane, but there are additional elements and factors involved (Zech et al., 2016). Similarly, we could verify if the Lst4 loop could interact with vacuolar lipids and if this interaction contributes to the vacuolar localization of the Lst4-Lst7 complex, maybe helped by the interaction with another vacuolar protein.

In our study we also observed that expressing an allele of Lst4 that can not be phosphorylated by TORC1 ($Lst4^{12A}$) causes cells to have a growth defect on a poor nitrogen source medium. This phenotype was enhanced if we combined the expression of this allele with the deletion of Iml1, a negative regulator of TORC1, confirming that this growth defect was due to the TORC1 hyperactivation. It is possible to exploit this property of this allele expressed in an *iml1Δ* mutant to perform a genetic screening to identify mutants that can suppres this growth inhibition. This may allow the discovery of positive regulators of TORC1. This approach is currently employed in our laboratory.

Is IAA a physiological regulator of TORC1?

In plants, the hormone IAA is mainly involved in plant development, but this compound is also produced by other organisms such as yeast (Basse et al., 1996; Gruen, 1959; Teale et al., 2006), regulating filamentation and growth (Prusty et al., 2004).

Different yeasts can produce IAA in different amounts. It was reported that the yeast-produced IAA is secreted in the environment to inhibit growth of competitors. Notably, yeasts that produce high concentrations of IAA acquire a certain resistance to this compound (Liu et al., 2016).

In our study, we confirmed the inhibitory role of IAA on cell growth and we demonstrated a link between this effect on growth and a direct inhibitory effect on TORC1. These findings have raised an important question: is IAA a physiological inhibitor of TORC1 within cells? To answer to this question it will be necessary to verify that the intracellular concentration of IAA corresponds to that one discovered to negatively act on TORC1 *in vitro* in our study. Notably, since we observed that the lowest IAA concentration (10 μM) used *in vitro* in a TORC1 kinase assay is already sufficient to reduce the kinase activity by 50%, it is likely that the concentration to have an effect on TORC1 could be even lower than 10 μM. In this context, it is even more important to measure the intracellular concentration of IAA to verify if the concentration that we used to inhibit TORC1 *in vitro* is in a range that can be considered physiological. In this case, it could be also interesting to measure the IAA produced by yeast in rich or poor conditions medium to verify if yeast can produce more IAA in shortage of nutrients to modulate its TORC1 activity, according with the environment conditions.

In plants, IAA biosynthesis can occur via a tryptophan-dependent pathway, but this compound can also be produced in a Trp-independent manner (Woodward and Bartel, 2005). Once produced, IAA is stored in plant cells as IAA conjugates to avoid excessive accumulation of no active IAA (Cohen and Bandurski, 1982). In these IAA conjugates, auxin is bound to glucose or amino acids such as alanine, aspartate and leucine. The IAA conjugates are often present in the seeds and, among them, IAA-Ala and IAA-Leu are suggested to be hydrolised to release IAA for the development of the plant from the seeds (Woodward and Bartel, 2005). Similarly, in yeast, IAA could be conjugated with amino acids. Thus a possible mechanism for TORC1 regulation via IAA could be that, in the presence of nutrients, IAA is sequestered in these conjugated complexes and can not act on TORC1 to inhibit its activity. On the contrary, in absence of amino acids, IAA is free within cells and can inhibit TORC1, reflecting its inactivation upon amino acids starvation. This could involve especially leucine that is one of the amino acids that can be sense to activate TORC1. To verify this hypothesis one could use an HPLC method to measure the amount of IAA and the possible amount of the IAA-leucine conjugate produced by yeast cells grown in the presence of leucine. Once verified that the IAA-leucine conjugate is present in yeast cells, a possible approach could be to measure the amount of free IAA as well

as the IAA-leucine conjugate produced in cells grown in the presence of leucine followed by the starvation for this amino acid. We could expect that, upon leucine starvation, the amount of the IAA-leucine conjugate will decrease compared to that one measured from cells grown in the presence of leucine. Vice versa, the amount of free IAA will increase in starved cells compared to that one measured from cells grown in the presence of this amino acid.

It was published that the IAA uptake in yeast involved the transcription factor Yap1 and the Avt transporters, that are considered to be the IAA permease Aux1 orthologs in yeast (Kerr and Bennett, 2007; Prusty et al., 2004). It could be interesting to verify the TORC1 activity in mutants for the Avt transporters or for Yap1. We could expect an IAA-resistant phenotype for the Avt mutants and a hypersensitivity to IAA for the Yap1 mutant in terms of growth and TORC1 activity. In the study of Prusty et al., the authors described Yap1 mutant to be hypersensitive to IAA in liquid YPD culture (EC_{50}: 25 μM) (Prusty et al., 2004). We did not find Yap1 in our robot screen using 3 mM IAA, probably because our study was done on plates using SD complete medium. Thus, the sensitivity of the cells to the drug could vary considering the different growth conditions. In addition, they also verified the hypersensitivity of Yap1 to IAA on plates, but they performed a halo assay using a filter disk saturated of IAA and not a specific concentration of this compound, showing that the halo of growth inhibition of Yap1 mutant cells was bigger compared to the one of WT cells. Our screening results revealed that *yap1Δ* is not hypersensitive to 3 mM IAA, but it could be possible to show its hypersensitivity by increasing the IAA concentration.

Notably, we could also exploit the inhibitory role of IAA on cell growth to perform a screening to find suppressor mutants capable of reverting the growth defect phenotype in the presence of high concentrations of IAA. Thus, we could find new regulators of TORC1 or also new important regulators of the IAA response pathway.

Materials and Methods

Materials & Methods

Strains and plasmids

The strains and the plasmids used in this study are listed in the tables in the next section.

Growth conditions

Unless stated otherwise, the strains were grown in selective medium (0.17% yeast nitrogen base, 0.5% ammonium sulfate, 0.2 % dropout mix, and 2% glucose) to maintain the prototrophic state. The cells were diluted to an OD_{600} of 0.2 and grown at 30°C until they reached OD_{600} of 0.8.

Growth Assay

Cells were incubated overnight in synthetic medium in absence of amino acids and diluted in the same medium at an $O.D._{600}$ of 0.02. A multi well plate of 100 wells was filled of cells in presence of the different concentrations of IAA or vehicle (90% ethanol 10% Tween) or rapamycin and the O.D. of each sample was read each 30 min for 3 days using a Bioscreen C machine that kept the temperature at 30°C for the entire growth time.

Robot Screening

The robot screening was done using a robot apparatus (Singer Instruments) and the knock out yeast collection spotted in quadruplicate on synthetic medium plates depleted of amino acids, in presence of the vehicle (90% ethanol 10% Tween) or the drug (3 mM IAA or 4 nM Rapamycin). The plates were analyzed using the Rothstein lab platform (http://www.rothsteinlab.com).

Galactose induction

For galactose induction, the cells were incubated overnight in synthetic medium (0.17% yeast nitrogen base, 0.5% ammonium sulfate, 0.2% of dropout mix, 2% Raffinose, and 0.1% Sucrose) depleted of Uracil (to maintain the plasmid), diluted the day after in YPGal2% medium (1% yeast extract, 2% peptone, and 2% Galactose) at OD_{600} 0.6-1, and let grow for 6h at 30°C.

Protein purification

Escherichia coli Rosetta strain (Novagen) and *Saccharomyces cerevisiae* were used for all protein purifications.

For the purifications from bacteria, cells transformed with plasmids carrying 6His-tagged Lst4 variants and/or 6His-tagged Lst7 or 6His-Atg29 were grown at 37°C in LB medium (1% NaCl, 1% bactotryptone, and 0.5% yeast extract) supplemented with antibiotics to maintain plasmids. 6His-tagged proteins were produced in the *E. coli* after induction with 0.5 mM IPTG overnight at 16°C. Cells were collected by centrifugation and lysed via sonication in the appropriate buffer. 6His purification was performed using Ni-NTA agarose beads (Qiagen) in Buffer A (50 mM NaH_2PO_4 pH 8.0, 300 mM NaCl, 0.1% NP40, 1 mM DTT, 1X Roche complete protease inhibitor-EDTA, and 10 mM imidazole) and elution was achieved in Buffer A + 250 mM imidazole. Glycerol was added to a final concentration of 20% and proteins were stored at -80°C. GST-Gtr1^{Q65L}-6His/GST-Gtr2 were purified according with Panchaud et al., 2013. Briefly, GST-tagged proteins purification was done using Glutathione-Sepharose beads (GE Healthcare) in Buffer B (50 mM Tris-HCl pH 7.5, 200 mM NaCl, 1.5 mM MgCl2, 5% glycerol, 1 mM DTT, 0.1% NP40, and 0.1 mM GDP, 1X Roche complete protease inhibitor-EDTA) and proteins were eluted with 10 mM reduced glutathione.

For the purifications from yeast, WT cells carrying plasmids expressing all the Atg proteins, GST or TAP-tagged, were grown in synthetic medium without Uracil, in presence of Raffinose and Sucrose. After 6 hours induction with 2% Galactose, the cells were collected by centrifugation and lysed with glass acid-beads in lysis Buffer A for the TAP purifications and in Buffer C (50 mM Tris-HCl pH 7.5, 150 mM NaCl, 1 mM EDTA, 0.5% NP40, 1X Roche complete protease inhibitor-EDTA) for the GST purifications. The clear lysate was incubated 2 hours at 4°C together with Glutathione-Sepharose beads (GE Healthcare) for the GST-tagged Atg proteins, or Ni-NTA agarose beads (Qiagen) for the TAP-tagged Atg proteins, and the elution was achieved using 10 mM of reduced gluthatione for the GST purifications and in Buffer A + 250 mM imidazole for the TAP purifications. Glycerol was added to a final concentration of 20% and proteins were stored at -80°C.

GTP Hydrolysis Assay

Purified GTPases (100 nM) were incubated for 30 min at room temperature in loading buffer (20 mM Tris-HCl pH 8.0, 2 mM EDTA, and 1 mM DTT) in the presence of 40 nM [α-^{32}P]-GTP (Hartman Analytic; 3,000 Ci/mmol). To start the reaction 200 nM of 6His-Lst4/6His-Lst7 were added to the mix, together with 10 mM $MgCl_2$. Reactions were stopped after 20 min of incubation at room temperature by the addition of elution buffer (1% SDS, 25 mM EDTA, 5 mM GDP, and 5 mM GTP). Samples were then heat denatured for 2 min at 65°C. [α-^{32}P]-GTP and [α-^{32}P]-GDP were separated by thin-layer chromatography (TLC) on PEI Cellulose F Plates (Merck). The TLC tank was equilibrated with buffer containing 1.0 M acetic acid and 0.8 M LiCl. Results were visualized using a phosphorimager and quantified with ImageQuant software.

TORC1 Activity Assay *in vivo*

To estimate the TORC1 activity *in vivo* the ratio between the phosphorylation on Thr737 of full-length Sch9 compared to the total amount of Sch9 was calculated, using phosphospecific anti-pThr737-Sch9 and anti-Sch9 antibodies (GenScript).

Lst4 phosphorylation *in vivo*

Phosphorylated forms of tagged-Lst4 were detected by electrophoresis on a 6% SDS-PAGE gel containing 20 mM Phos-tag (Wako) followed by immunoblotting with anti-GFP antibodies (Roche) or by classical SDS-PAGE and immunoblotting using anti-Lst4-pSer523 antibody (GenScript) and anti-V5 antibody (Thermo Fisher Scientific). A standard protocol was applied to *in vitro* dephosphorylate immunoprecipitated Lst4-ENVY with λ-phosphatase (New England Biolabs).

TORC1 Activity *in vitro*

For *in vitro* kinase assays, TORC1 was TAP-purified from a Tco89-TEV-TAP-expressing yeast strain grown in YPD and treated for 10 min with cycloheximide. The extraction buffer (50 mM HEPES/NaOH pH 7.5, 5 mM CHAPS, 400 mM NaCl, 1 mM EDTA, 0.5 mM DTT, 400 mM Pefabloc, 1X Roche complete protease inhibitor-EDTA) was used to resuspend cells that were subjected to cryogenic disruption with an MM 400 Mixer Mill (Retsch). The cleared lysate was incubated with

IgG-coupled Dynabeads (Dynabeads M-270 Epoxy; Invitrogen) for 2 hours at 4° C. After washes, the TORC1 complex was eluted using 2% TEV protease. Recombinant His6-tagged Lst4 variants (600 ng/30 μl reaction) were co-purified with His6-tagged Lst7 (or just His6-tagged $Lst4^{loop}$ for the IAA study) and used as *in vitro* substrates in TORC1 kinase reactions performed according to Urban et al. (2007). Briefly, reactions were performed in kinase buffer (50 mM HEPES/NaOH pH 7.5, 5 mM CHAPS, 400 mM NaCl, 0.5 mM DTT, phosphatase inhibitors), started by adding the ATP Mix (4.2 mM $MgCl_2$, 300 mM ATP, and 3.3 mCi [γ-^{32}P]-ATP [Hartmann Analytic, SRP-501]) and stopped by adding SDS-PAGE sample buffer. Proteins were separated by SDS-PAGE, stained with SYPRO Ruby (Sigma), and analyzed using a phosphorimager (Typhoon FLA 9500; GE Healthcare).

For the kinase assays followed by Mass Spectometry analysis, Atg proteins purified from yeast (GST or TAP tagged) were used as substrates and the reactions were started by adding ATP Mix (4.2 mM $MgCl_2$, and γ-[$^{18}O_4$]-ATP), in presence or absence of 6 μM of Wortmannin (LC Laboratories).

Mass Spectrometry analysis

Mass spectrometric measurements were performed on a Q Exactive Plus mass spectrometer coupled to an EasyLC 1000 (Thermo Fisher Scientific). Prior analysis phosphopeptides were enriched by TiO_2. The mass spectrometry raw data files were analyzed using MaxQuant software (Cox and Mann, 2008), version 1.4.1.2, using a Uniprot *S. cerevisiae* database from March 2016 containing common contaminants such as keratins and enzymes used for in-gel digestion.

Supplementary Tables

Table 1. Strains Used in Chapter I

Strain	Genotype	Source	Figure
KT1961	*MATa*; *his3, leu2, ura3-52, trp1*	(Pedruzzi et al., 2003)	
KP09	[KT1961] *MATa; lst4Δ::KanMX*	(Péli-Gulli et al., 2015)	2D; 2F-H; 4A, C; S1A, B
KP10	[KT1961] *MATa; lst7Δ::KanMX*	(Péli-Gulli et al., 2015)	1C; 3B
MP372-2D	[KT1961] *MATa*; *LST7-GFP::HIS3MX, lst4Δ::KanMX*	(Péli-Gulli et al., 2015)	3C
MP412-1C	[KT1961] *MATa*; *lst4Δ::KanMX, lst7Δ::KanMX*	This study	2F
MP4469	[KT1961] *MATa*; *lst4Δ::KanMX, URA3::LST4p-LST4-ENVY*	This study	1B; 2A, E; 3A; 4A-C
MP4509	[KT1961] *MATa*; *lst4Δ::KanMX, URA3::LST4p-lst4^{12A}-ENVY*	This study	3A; 4A-C
MP4510	[KT1961] *MATa*; *lst4Δ::KanMX, URA3::LST4p-lst4^{5D}-ENVY*	This study	3A; 4A-C
MP4569	[KT1961] *MATa; URA3::CYC1p-lst4^{loop}-GFP*	This study	1B; 1D, E
MP4570	[KT1961] *MATa; lst4Δ::KanMX, URA3::CYC1p-lst4^{loop}-GFP*	This study	1D
MP4571	[KT1961] *MATa; lst7Δ::KanMX, URA3::CYC1p-lst4^{loop}-GFP*	This study	1D
MP4572	[KT1961] *MATa; lst4Δ::KanMX, lst7Δ::KanMX, URA3::CYC1p-lst4^{loop}-GFP*	This study	1D
MP4573	[KT1961] *MATa; gtr1Δ::natMX, gtr2Δ::natMX, URA3::CYC1p-lst4^{loop}-GFP*	This study	1F
MP4638	[KT1961] *MATa; lst4Δ::KanMX, sch9Δ::natMX, pRS414-SCH9^{T492G}, pRS416-LST4p-LST4-V5-HIS6*	This study	2H
MP4680	[KT1961] *MATa; lst4Δ::KanMX, lst7Δ::KanMX, URA3::LST4p-LST4-ENVY*	This study	3B
MP4684	[KT1961] *MATa; lst4Δ::KanMX, lst7Δ::KanMX, URA3::LST4p-lst4^{12A}-ENVY*	This study	3B
MP4684	[KT1961] *MATa; lst4Δ::KanMX, lst7Δ::KanMX, URA3::LST4p-lst4^{12A}-ENVY*	This study	3B
MP4688	[KT1961] *MATa; lst4Δ::KanMX, lst7Δ::KanMX, URA3::LST4p-lst4^{5D}-ENVY*	This study	3B

MP268-2B	[KT1961] *MATa; gtr1Δ::NatMX, gtr2Δ::NatMX*	(Péli-Gulli et al., 2015)	3E
MP4704	[MP268-2B] *MATa; lst4Δ::KanMX, URA3::LST4p-LST4-ENVY*	This study	3E
MP4708	[MP268-2B] *MATa; lst4Δ::KanMX, URA3::LST4p-lst4^{12A}-ENVY*	This study	3E
MP4708	[MP268-2B] *MATa; lst4Δ::KanMX, URA3::LST4p-lst4^{12A}-ENVY*	This study	3E
MP4709	[MP268-2B] *MATa; lst4Δ::KanMX, URA3::LST4p-lst4^{5D}-ENVY*	This study	3E
MP4847	[KT1961] *MATα; iml1Δ::KanMX, lst4Δ::KanMX, URA3::LST4p-LST4-ENVY*	This study	4D, E
MP4849	[KT1961] *MATα; iml1Δ::KanMX, lst4Δ::KanMX, URA3::LST4p-lst4^{12A}-ENVY*	This study	4D, E
MP4642	[KT1961] *MATa; lst4Δ::KanMX, sch9Δ::KanMX, pRS416-LST4p-LST4- V5-HIS$_6$*	This study	S2
MP4693	[KT1961] *MATa; lst4Δ::KanMX, lst7Δ::KanMX, URA3::LST4p-lst4^{Δloop}-ENVY*	This study	1D
MP4697	[KT1961] *MATa; URA3::LST4p-lst4^{Δloop}-ENVY*	This study	1B; 1D, E
MP4698	[KT1961] *MATa; lst4Δ::KanMX, URA3::LST4p-LST4-ENVY*	This study	4D, E
MP4699	[KT1961] *MATa; lst4Δ::KanMX, URA3::LST4p-lst4^{Δloop}-ENVY*	This study	1D
MP4700	[KT1961] *MATa; lst4Δ::KanMX, URA3::LST4p-lst4^{12A}-ENVY*	This study	4D, E
MP4510	[KT1961] *MATa; lst4Δ::KanMX, URA3::LST4p-lst4^{5D}-ENVY*	This study	4D, E
MP4703	[KT1961] *MATa; lst7Δ::KanMX, URA3::LST4p-lst4^{Δloop}-ENVY*	This study	1D
TB50a	*MATa*; *trp1 his3 ura3 leu2 rme1*	(Beck and Hall, 1999)	
RL170-2C	[TB50a] *MATa*; *TCO89-TAP::TRP1*	(Shimada et al., 2013)	2B

Table 2. Plasmids Used in Chapter I

Plasmid	Genotype	Source	Figure
pRS413	CEN, ARS, *HIS3*	(Brachmann et al., 1998)	1B-F; 2A; 2D, E; 2H; 3A, B, E; 4A; 4D; S2
pRS414	CEN, ARS, *TRP1*	(Brachmann et al., 1998)	1B; 1D-F; 2A; 2D-H; 3A; 3D; 4A-D, S1A, B; S2
pRS415	CEN, ARS, *LEU2*	(Brachmann et al., 1998)	1B-F; 2A; 2D-H; 3A, B; 3D; 4A-D; S1A, B
pRS416	CEN, ARS, *URA3*	(Brachmann et al., 1998)	1C; 2D; 2F-H; 3B; 4A; 4C; S1A, B
pMP3008	[pRS413] *LST4p-LST4-V5-HIS6*	This study	2D; 2F, G; S1A, B
pMP3055	[pRS413] *LST4p-lst4^{S523A}-V5-HIS6*	This study	2D
pMP2576	[pRS414] *LST7p-LST7-HA3*	This study	1C; 3B
pAH145	[pRS414] *sch9^{T492G}*	(Huber et al., 2009)	2H
pPL155	[pRS415] *HA3-TOR1^{A1957V}*	(Reinke et al., 2006)	1F
p1392	[pRS415] *MAF1-HA3*	(Huber et al., 2009)	2H; S2
pMP2780	[pRS416] *LST4p-LST4-V5-HIS6*	This study	1C; 2H; 3C; S2
pMP3143	[pRS416] *CYC1p-lst4^{loop}-V5-HIS6*	This study	1C
pMP3147	[pRS416] *LST4p-lst4$^{\Delta loop}$-V5-HIS6*	This study	1C
pMP3149	[pRS416] *LST4p-lst4^{5D}-V5-HIS6*	This study	3C
pMP3165	[pRS416] *LST4p-lst4^{12A}-V5-HIS6*	This study	3C
pRS306	integrative, *URA3*	(Sikorski and Hieter, 1989)	
pMP3042	[pRS306] *LST4p-LST4-ENVY*	This study	1B; 2A, E; 3A; 4A-C
pMP3062	[pRS306] *LST4p-lst4^{12A}-ENVY*	This study	3A; 4A-C
pMP3064	[pRS306] *LST4p-lst4^{5D}-ENVY*	This study	3A; 4A-C
pMP3077	[pRS306] *CYC1p-lst4^{loop}-GFP*	This study	1B; 1D-F
pSIVu	integrative, *URA3*	(Sikorski and Hieter, 1989)	
pMP3166	[pSIVu] *LST4p-LST4-ENVY*	This study	2A; 2E; 3A, B; 4A-D
pMP3167	[pSIVu] *LST4p-lst4$^{\Delta loop}$-ENVY*	This study	1B; 1D, E
pMP3168	[pSIVu] *LST4p-lst4^{12A}-ENVY*	This study	3A, B; 4A-D
pMP3169	[pSIVu] *LST4p-lst4^{5D}-ENVY*	This study	3A, B; 4A-D
pRS423	2μ, *HIS3*	(Christianson et al., 1992)	
pRH2953	[pRS423] *VAC8p-vhhGFP4-PHO8N*	R. Hatakeyama	4B, C

pAS2570	[pET28b^{+}]	*HIS$_6$-LST4*	(Péli-Gulli et al., 2015)	2B; 3D
pAS2571	[pET15b^{+}]	*HIS$_6$-LST7*	(Péli-Gulli et al., 2015)	2B; 3D
pMP3057	[pET28b^{+}]	*HIS$_6$-lst4^{12A}*	This study	2B; 3D
pMP3058	[pET28b^{+}]	*HIS$_6$-lst4^{5D}*	This study	2B; 3D
pNP2038	[pET-24d]	*GST-TEV-GTR2*	(Panchaud et al., 2013b)	3D
pJU1046	[pGEX-6P]	*GST-TEV-gtr1^{Q65L}-HIS$_6$*	R. Loewith	3D
p3285	pYEGFP-GAC111-*RPL25*		D. Kressler	3E
pMP2789	[pRS415]	*GTR1p-GTR1-HA$_3$*	This study	3E
pMP2337	[pRS416]	*GTR1p-GTR1-HA$_3$*	(Péli-Gulli et al., 2015)	3E
pMP2782	[pRS414]	*GTR2p-gtr2^{Q66L}-V5-HIS$_6$*	(Péli-Gulli et al., 2015)	3E

Table 3. Strains Used in Chapter II

Strain	Genotype	Source	Figure
YL515	[BY4741/2]*MATa*; *his3Δ1, leu2Δ0, ura3Δ0*	(Binda et al., 2009)	
Y258	[BY4740]*MATa*; *pep4-3, his4-580, leu2-3,112, ura3-52*	(Gelperin et al., 2005)	
SR5193	[Y258] + [pEG(KG)] *GALp-GST-ATG4*	(Zhu, 2001)	2.2; 2.3; 2.5
SR5196	[Y258] + [pEG(KG)] *GALp-GST-ATG7*	(Zhu, 2001)	2.2; 2.3; 2.5
SR5197	[Y258] + [pEG(KG)] *GALp-GST-ATG8*	(Zhu, 2001)	2.2; 2.3; 2.5
SR5198	[Y258] + [pEG(KG)] *GALp-GST-ATG9*	(Zhu, 2001)	2.2; 2.3; 2.5
SR5199	[Y258] + [pEG(KG)] *GALp-GST-ATG10*	(Zhu, 2001)	2.2; 2.3; 2.5
SR5201	[YL515] + [YEplac195] *GALp-GST-ATG12*	This study	2.2; 2.3; 2.5
SR5202	[Y258] + [pEG(KG)] *GALp-GST-ATG13*	(Zhu, 2001)	2.2; 2.3; 2.5
SR5203	[Y258] + [pEG(KG)] *GALp-GST-ATG14*	(Zhu, 2001)	2.2; 2.3; 2.5
SR5204	[Y258] + [pEG(KG)] *GALp-GST-ATG15*	(Zhu, 2001)	2.2; 2.3; 2.5
SR5205	[YL515] + [YEplac195] *GALp-GST-ATG16*	This study	2.2; 2.3; 2.5
SR5206	[YL515] + [YEplac195] *GALp-GST-ATG17*	This study	2.2; 2.3; 2.5
SR5212	[Y258] + [pEG(KG)] *GALp-GST-ATG23*	(Zhu, 2001)	2.2; 2.3; 2.5
SR5213	[Y258] + [pEG(KG)] *GALp-GST-ATG24*	(Zhu, 2001)	2.2; 2.3; 2.5
SR5216	[Y258] + [pEG(KG)] *GALp-GST-ATG29*	(Zhu, 2001)	2.2; 2.3; 2.5
SR5218	[Y258] + [pEG(KG)] *GALp-GST-ATG32*	(Zhu, 2001)	2.2; 2.3; 2.5
SR5224	[YL515] + [YEplac195] *GALp-GST-ATG40*	This study	2.2; 2.3; 2.5
SR5225	[Y258] + [pEG(KG)] *GALp-GST-ATG41*	(Zhu, 2001)	2.2; 2.3; 2.5
SR5190	[Y258] + [BG1085] *GALp-ATG2-TAP*	(Gelperin et al., 2005)	2.2; 2.3; 2.5
SR5192	[YL515] + [BG1085] *GALp-ATG3-TAP*	This study	2.2; 2.3; 2.5
SR5194	[YL515] + [BG1085] *GALp-ATG5-TAP*	This study	2.2; 2.3; 2.5

SR5195	[YL515] + [BG1085] *GALp-ATG6-TAP*	This study	2.2; 2.3; 2.5
SR5200	[YL515] + [BG1085] *GALp-ATG11-TAP*	This study	2.2; 2.3; 2.5
SR5207	[YL515] + [BG1085] *GALp-ATG18-TAP*	This study	2.2; 2.3; 2.5
SR5208	[Y258] + [BG1085] *GALp-ATG19-TAP*	(Gelperin et al., 2005)	2.2; 2.3; 2.5
SR5209	[Y258] + [BG1085] *GALp-ATG20-TAP*	(Gelperin et al., 2005)	2.2; 2.3; 2.5
SR5210	[YL515] + [BG1085] *GALp-ATG21-TAP*	This study	2.2; 2.3; 2.5
SR5211	[Y258] + [BG1085] *GALp-ATG22-TAP*	(Gelperin et al., 2005)	2.2; 2.3; 2.5
SR5214	[YL515] + [BG1085] *GALp-ATG26-TAP*	This study	2.2; 2.3; 2.5
SR5215	[YL515] + [BG1085] *GALp-ATG27-TAP*	This study	2.2; 2.3; 2.5
SR5217	[Y258] + [BG1085] *GALp-ATG31-TAP*	(Gelperin et al., 2005)	2.2; 2.3; 2.5
SR5219	[Y258] + [BG1085] *GALp-ATG33-TAP*	(Gelperin et al., 2005)	2.2; 2.3; 2.5
SR5220	[YL515] + [BG1085] *GALp-ATG34-TAP*	This study	2.2; 2.3; 2.5
SR5221	[Y258] + [BG1085] *GALp-ATG36-TAP*	(Gelperin et al., 2005)	2.2; 2.3; 2.5
SR5222	[Y258] + [BG1085] *GALp-ATG38-TAP*	(Gelperin et al., 2005)	2.2; 2.3; 2.5
SR5223	[YL515] + [BG1085] *GALp-ATG39-TAP*	This study	2.2; 2.3; 2.5
RL170-2C	[TB50a] *MATa*; *TCO89-TAP::TRP1*	(Shimada et al., 2013)	2.4

Table 4. Plasmids Used in Chapter II

Plasmid	Genotype	Source	Figure
pEG(KG)	2μ, *URA3, leu2-d, GALp, CYCp-GST*	(Zhu, 2001)	
pSR3309	2μ, *URA3, GALp-GST-ATG16*	This study	2.2; 2.3; 2.5
pSR3361	2μ, *URA3, GALp-GST-ATG12*	This study	2.2; 2.3; 2.5
pSR3362	2μ, *URA3, GALp-GST-ATG17*	This study	2.2; 2.3; 2.5
pSR3481	2μ, *URA3, GALp-GST-ATG41*	This study	2.2; 2.3; 2.5
BG1085	2μ, *URA3, GALp-TAP (6HIS-HA-Protease 3C-Prot. A)*	(Gelperin et al., 2005)	

Table 5. Strains Used in Chapter III

Strain	Genotype	Source	Figure
YL515	[BY4741/2]*MATα; his3Δ1, leu2Δ0, ura3Δ0*	(Binda et al., 2009)	3.2; 3.3
SR1-4B	[BY4741/2] *MATα; fpr1Δ::KanMX*	This study	3.2
MB34	[BY4741/2] *MATα; tco89Δ::HIS3*	(Binda et al., 2009)	3.2
MB27	[BY4741/2] *MATα; gtr1Δ::HIS3*	(Binda et al., 2009)	3.2
NP04-C4	[BY4741/2] *MATα; iml1Δ::KanMX*	(Panchaud et al., 2013b)	3.2
SR3301	[TB50] *MATa leu2-3,112 ura3-52 trp1 his3 rme1 GAL HMLa*	R. Loewith	3.3; 3.4; 3.5
TB105-3B	[TB50] *MATa; gln3Δ::KanMX, gat1Δ::HIS3*	(Urban et al., 2007)	3.4; 3.5
KP09	[KT1961] *MATa; lst4Δ::KanMX*	(Péli-Gulli et al., 2015)	3.6; 3.7
RL170-2C	[TB50a] *MATa*; *TCO89-TAP::TRP1*	(Shimada et al., 2013)	3.8; 3.9

Table 6. Plasmids Used in Chapter III

Plasmid	Genotype	Source	Figure
pRS413	CEN, ARS, *HIS3*	(Brachmann et al., 1998)	3.3; 3.4; 3.6
pRS415	CEN, ARS, *LEU2*	(Brachmann et al., 1998)	3.2; 3.3; 3.4; 3.6
pRS416	CEN, ARS, *URA3*	(Brachmann et al., 1998)	3.2; 3.3; 3.4
P1462	[pRS413] *SCH9p-sch9*^{T570A}*-5HA*	(Urban et al., 2007)	3.2
pRS414	CEN, ARS, *TRP1*	(Brachmann et al., 1998)	3.3; 3.4; 3.6
pHAC33	CEN, ARS, *URA3*	T. Beck	
p1290	[pHAC33] *SCH9p-sch9*^{2D3E}	(Urban et al., 2007)	3.4
pMP2780	[pRS416] *LST4p-LST4-V5-HIS*$_6$	(Péli-Gulli et al., 2015)	3.6
pSR3247	[pET28b$^+$] *HIS*$_6$*-LST4*^{loop}	This study	3.8

References

Abel, S., and Theologis, A. (2010). Odyssey of auxin. Cold Spring Harb. Perspect. Biol. *2*.

Alarcon, C.M., Heitman, J., and Cardenas, M.E. (1999). Protein kinase activity and identification of a toxic effector domain of the target of rapamycin TOR proteins in yeast. Mol. Biol. Cell *10*, 2531–2546.

Andrade, M.A., and Bork, P. (1995). HEAT repeats in the Huntington's disease protein. Nat. Genet. *11*, 115–116.

Antonucci, L., Fagman, J.B., Kim, J.Y., Todoric, J., Gukovsky, I., Mackey, M., Ellisman, M.H., and Karin, M. (2015). Basal autophagy maintains pancreatic acinar cell homeostasis and protein synthesis and prevents ER stress. Proc. Natl. Acad. Sci. *112*, E6166–E6174.

Avruch, J., Long, X., Ortiz-Vega, S., Rapley, J., Papageorgiou, A., and Dai, N. (2009). Amino acid regulation of TOR complex 1. Am. J. Physiol. Endocrinol. Metab. *1*, 592–602.

Ballou, L.M., and Lin, R.Z. (2008). Rapamycin and mTOR kinase inhibitors. J. Chem. Biol. *1*, 27–36.

Bar-Peled, L., and Sabatini, D.M. (2014). Regulation of mTORC1 by amino acids. Trends Cell Biol. *24*, 400–406.

Bar-Peled, L., Schweitzer, L.D., Zoncu, R., and Sabatini, D.M. (2012). Ragulator is a GEF for the rag GTPases that signal amino acid levels to mTORC1. Cell *150*, 1196–1208.

Bar-Peled, L., Chantranupong, L., Cherniack, A.D., Chen, W.W., Ottina, K.A., Grabiner, B.C., Spear, E.D., Carter, S.L., Meyerson, M., and Sabatini, D.M. (2013). A Tumor Suppressor Complex with GAP Activity for the Rag GTPases That Signal Amino Acid Sufficiency to mTORC1. Science (80-.). *340*, 1100–1106.

Basse, C.W., Lottspeich, F., Steglich, W., and Kahmann, R. (1996). Two potential indole-3-acetaldehyde dehydrogenases in the phytopathogenic fungus Ustilago maydis. Eur J Biochem *242*, 648–656.

Beck, T., and Hall, M.N. (1999). The TOR signalling pathway controls nuclear localization of nutrient-regulated transcription factors. Nature *402*, 689–692.

Bertram, P.G., Choi, J.H., Carvalho, J., Ai, W., Zeng, C., Chan, T.F., and Zheng, X.F.S. (2000). Tripartite regulation of Gln3p by TOR, Ure2p, and phosphatases. J. Biol. Chem. *275*, 35727–35733.

Beugnet, A., TEE, A.R., TAYLOR, P.M., and PROUD, C.G. (2003). Regulation of targets of mTOR (mammalian target of rapamycin) signalling by intracellular amino acid availability. Biochem. J. *372*, 555–566.

Binda, M., Péli-Gulli, M.P., Bonfils, G., Panchaud, N., Urban, J., Sturgill, T.W., Loewith, R., and De Virgilio, C. (2009). The Vam6 GEF Controls TORC1 by Activating the EGO Complex. Mol. Cell *35*, 563–573.

Bonfils, G., Jaquenoud, M., Bontron, S., Ostrowicz, C., Ungermann, C., and De Virgilio, C. (2012). Leucyl-tRNA Synthetase Controls TORC1 via the EGO Complex. Mol. Cell *46*, 105–110.

Bontron, S., Jaquenoud, M., Vaga, S., Talarek, N., Bodenmiller, B., Aebersold, R., and De Virgilio, C. (2013). Yeast Endosulfines Control Entry into Quiescence and Chronological Life Span by Inhibiting Protein Phosphatase 2A. Cell Rep. *3*, 16–22.

Bos, J., Rehmann, H., and Wittinghofer, A. (2007). GEFs and GAPs : Critical Elements in the Control of Small G Proteins. Cell 865–877.

Bosotti, R., Isacchi, A., and Sonnhammer, E.L.L. (2000). FAT: A novel domain in PIK-related kinases. Trends Biochem. Sci. *25*, 225–227.

Bourne, H.R., Sanders, D.A., and McCormick, F. (1990). The GTPase superfamily: a conserved switch for diverse cell functions. Nature *348*, 125–132.

Brachmann, C.B., Davies, A., Cost, G.J., Caputo, E., Li, J., Hieter, P., and Boeke, J.D. (1998). Designer deletion strains derived from Saccharomyces cerevisiae S288C: A useful set of strains and plasmids for PCR-mediated gene disruption and other applications. Yeast *14*, 115–132.

Broach, J.R. (2012). Nutritional control of growth and development in yeast. Genetics *192*, 73–105.

Brown, E.J., Albers, M.W., Shin, T.B., Ichikawa, K., Keith, C.T., Lane, W.S., and Schreiber, S.L. (1994). A mammalian protein targeted by G1-arresting rapamycin-receptor complex. Nature *369*, 756–758.

Brunn, G.J., Williams, J., Sabers, C., Wiederrecht, G., Lawrence, J.C., and Abraham, R.T. (1996). Direct inhibition of the signaling functions of the mammalian target of rapamycin by the phosphoinositide 3-kinase inhibitors, wortmannin and LY294002. EMBO J. *15*, 5256–5267.

Burman, C., and Ktistakis, N.T. (2010). Regulation of autophagy by phosphatidylinositol 3-phosphate. FEBS Lett. *584*, 1302–1312.

Caplan, S., Hartnell, L.M., Aguilar, R.C., Naslavsky, N., and Bonifacino, J.S. (2001). Human Vam6p promotes lysosome clustering and fusion in vivo. J. Cell Biol. *154*, 109–121.

Cardenas, M.E., Cutler, N.S., Lorenz, M.C., Di Como, C.J., and Heitman, J. (1999). The TOR signaling cascade regulates gene expression in response to nutrients. Genes Dev. *13*, 3271–3279.

Castro, A.F., Rebhun, J.F., Clark, G.J., and Quilliam, L.A. (2003). Rheb binds tuberous sclerosis complex 2 (TSC2) and promotes S6 kinase activation in a rapamycin- and

farnesylation-dependent manner. J. Biol. Chem. *278*, 32493–32496.

Chantranupong, L., Wolfson, R.L., Orozco, J.M., Saxton, R.A., Scaria, S.M., Bar-Peled, L., Spooner, E., Isasa, M., Gygi, S.P., and Sabatini, D.M. (2014). The sestrins interact with gator2 to negatively regulate the amino-acid-sensing pathway upstream of mTORC1. Cell Rep. *9*, 1–8.

Chantranupong, L., Wolfson, R.L., and Sabatini, D.M. (2015). Nutrient-sensing mechanisms across evolution. Cell *161*, 67–83.

Chantranupong, L., Scaria, S.M., Saxton, R.A., Gygi, M.P., Shen, K., Wyant, G.A., Wang, T., Harper, J.W., Gygi, S.P., and Sabatini, D.M. (2016). The CASTOR Proteins Are Arginine Sensors for the mTORC1 Pathway. Cell *165*, 153–164.

Chiu, M.I., Katz, H., and Berlin, V. (1994). RAPT1, a mammalian homolog of yeast Tor, interacts with the FKBP12/rapamycin complex. Proc. Natl. Acad. Sci. U. S. A. *91*, 12574–12578.

Christianson, T.W., Sikorski, R.S., Dante, M., Shero, J.H., and Hieter, P. (1992). Multifunctional yeast high-copy-number shuttle vectors. Gene *110*, 119–122.

Cohen, J.D., and Bandurski, R.S. (1982). Chemistry and physiology of the bound auxins. Annu. Rev. Plant Physiol. *33*, 403–430.

Di Como, C.J., and Arndt, K.T. (1996). Nutrients, via the Tor proteins, stimulate the association of Tap42 with type 2A phosphatases. Genes Dev. *10*, 1904–1916.

Cooper, T.G. (1982). Nitrogen Metabolism in Saccharomyces cerevisiae.

Cortez, D. (2003). Caffeine inhibits checkpoint responses without inhibiting the ataxia-telangiectasia-mutated (ATM) and ATM- and Rad3-related (ATR) protein kinases. J. Biol. Chem. *278*, 37139–37145.

Cox, J., and Mann, M. (2008). MaxQuant enables high peptide identification rates, individualized p.p.b.-range mass accuracies and proteome-wide protein quantification. Nat. Biotechnol. *26*, 1367–1372.

Dames, S.A., Mulet, J.M., Rathgeb-Szabo, K., Hall, M.N., and Grzesiek, S. (2005). The solution structure of the FATC domain of the protein kinase target of rapamycin suggests a role for redox-dependent structural and cellular stability. J. Biol. Chem. *280*, 20558–20564.

Dechant, R., Saad, S., Ibáñez, A.J., and Peter, M. (2014). Cytosolic pH regulates cell growth through distinct gtpases, Arf1 and Gtr1, to promote ras/PKA and TORC1 activity. Mol. Cell *55*, 409–421.

Demetriades, C., Doumpas, N., and Teleman, A.A. (2014). Regulation of TORC1 in response to amino acid starvation via lysosomal recruitment of TSC2. Cell *156*, 786–799.

Dokudovskaya, S., Waharte, F., Schlessinger, A., Pieper, U., Devos, D.P., Cristea, I.M., Williams, R., Salamero, J., Chait, B.T., Sali, A., et al. (2011). A conserved coatomer-related complex containing Sec13 and Seh1 dynamically associates with the vacuole in Saccharomyces cerevisiae. Mol. Cell. Proteomics *10*, M110.006478.

Dubouloz, F., Deloche, O., Wanke, V., Cameroni, E., and De Virgilio, C. (2005). The TOR and EGO protein complexes orchestrate microautophagy in yeast. Mol. Cell *19*, 15–26.

Durán, R. V., Oppliger, W., Robitaille, A.M., Heiserich, L., Skendaj, R., Gottlieb, E., and Hall, M.N. (2012). Glutaminolysis Activates Rag-mTORC1 Signaling. Mol. Cell *47*, 349–358.

Düvel, K., Santhanam, A., Garrett, S., Schneper, L., and Broach, J.R. (2003). Multiple roles of Tap42 in mediating rapamycin-induced transcriptional changes in yeast. Mol. Cell *11*, 1467–1478.

Echols, N., Harrison, P., Balasubramanian, S., Luscombe, N.M., Bertone, P., Zhang, Z., and Gerstein, M.B. (2002). Comprehensive analysis of amino acid and nucleotide composition in eukaryotic genomes, comparing genes and pseudogenes. Nucleic Acids Res. *30*, 2515–2523.

Eltschinger, S., and Loewith, R. (2016). TOR Complexes and the Maintenance of Cellular Homeostasis. Trends Cell Biol. *26*, 148–159.

Enders, T.A., and Strader, L.C. (2015). Auxin activity: Past, present, and future. Am. J. Bot. *102*, 180–196.

Epple, U.D., Suriapranata, I., Eskelinen, E.L., and Thumm, M. (2001). Aut5/Cvt17p, a putative lipase essential for disintegration of autophagic bodies inside the vacuole. J. Bacteriol. *183*, 5942–5955.

Forgac, M. (2007). Vacuolar ATPases: rotary proton pumps in physiology and pathophysiology. Nat. Rev. Mol. Cell Biol. *8*, 917–929.

Fujioka, Y., Suzuki, S.W., Yamamoto, H., Kondo-Kakuta, C., Kimura, Y., Hirano, H., Akada, R., Inagaki, F., Ohsumi, Y., and Noda, N.N. (2014). Structural basis of starvation-induced assembly of the autophagy initiation complex. Nat. Struct. Mol. Biol. *21*, 513–521.

Galweiler, L., Guan, C., Mu ller, A., Wisman, E., Mendgen, K., Yephremov, A., and Palme, K. (1998). Regulation of Polar Auxin Transport by AtPIN1 in Arabidopsis Vascular Tissue. Science (80-.). *282*, 2226–2230.

Gagiano, M., Van Dyk, D., Bauer, F.F., Lambrechts, M.G., and Pretorius, I.S. (1999). Msn1p/Mss10p, Mss11p and Muc1p/Flo11p are part of a signal transduction pathway downstream of Mep2p regulating invasive growth and pseudohyphal differentiation in Saccharomyces cerevisiae. Mol. Microbiol. *31*, 103–116.

Gai, Z., Wang, Q., Yang, C., Wang, L., Deng, W., and Wu, G. (2016). Structural mechanism for the arginine sensing and regulation of CASTOR1 in the mTORC1

signaling pathway. Cell Discov. *2*, 16051.

Gao, M., and Kaiser, C.A. (2006). A conserved GTPase-containing complex is required for intracellular sorting of the general amino-acid permease in yeast. Nat. Cell Biol. *8*, 657–667.

Garami, A., Zwartkruis, F.J.T., Nobukuni, T., Joaquin, M., Roccio, M., Stocker, H., Kozma, S.C., Hafen, E., Bos, J.L., and Thomas, G. (2003). Insulin activation of Rheb, a mediator of mTOR/S6K/4E-BP signaling, is inhibited by TSC1 and 2. Mol. Cell *11*, 1457–1466.

Gaubitz, C., Oliveira, T.M., Prouteau, M., Leitner, A., Karuppasamy, M., Konstantinidou, G., Rispal, D., Eltschinger, S., Robinson, G.C., Thore, S., et al. (2015). Molecular Basis of the Rapamycin Insensitivity of Target Of Rapamycin Complex 2. Mol. Cell *58*, 977–988.

Gelperin, D.M., White, M.A., Wilkinson, M.L., Kon, Y., Kung, L.A., Wise, K.J., Lopez-Hoyo, N., Jiang, L., Piccirillo, S., Yu, H., et al. (2005). Biochemical and genetic analysis of the yeast proteome with a movable ORF collection. Genes Dev. *19*, 2816–2826.

Gilman, A.G. (1987). G Proteins: Transducers of Receptor-Generated Signals. Annu. Rev. Biochem. *56*, 615–649.

Godard, P., Urrestarazu, A., Vissers, S., Kontos, K., Bontempi, G., van Helden, J., and Andre, B. (2007). Effect of 21 Different Nitrogen Sources on Global Gene Expression in the Yeast Saccharomyces cerevisiae. Mol. Cell. Biol. *27*, 3065–3086.

Gong, R., Li, L., Liu, Y., Wang, P., Yang, H., Wang, L., Cheng, J., Guan, K.L., and Xu, Y. (2011). Crystal structure of the Gtr1p-Gtr2p complex reveals new insights into the amino acid-induced TORC1 activation. Genes Dev. *25*, 1668–1673.

Gonzalez, A., Shimobayashi, M., Eisenberg, T., Merle, D.A., Pendl, T., Hall, M.N., and Moustafa, T. (2015). TORC1 promotes phosphorylation of ribosomal protein S6 via

the AGC Kinase Ypk3 in Saccharomyces cerevisiae. PLoS One *10*.

González, A., and Hall, M.N. (2017). Nutrient sensing and TOR signaling in yeast and mammals. EMBO J. *36*, 397–408.

Groves, M.R., and Barford, D. (1999). Topological characteristics of helical repeat proteins. Curr. Opin. Struct. Biol. *9*, 383–389.

Gruen, H.N. (1959). Auxins and fungi. Annu. Rev. Plant Physiol. *10*, 405–411.

Gwinn, D.M., Shackelford, D.B., Egan, D.F., Mihaylova, M.M., Mery, A., Vasquez, D.S., Turk, B.E., and Shaw, R.J. (2008). AMPK Phosphorylation of Raptor Mediates a Metabolic Checkpoint. Mol. Cell *30*, 214–226.

Halliday, K.J., Martinez-Garcia, J.F., and Josse, E.M. (2009). Integration of light and auxin signaling. Cold Spring Harb. Perspect. Biol. *1*.

Han, J.M., Jeong, S.J., Park, M.C., Kim, G., Kwon, N.H., Kim, H.K., Ha, S.H., Ryu, S.H., and Kim, S. (2012). Leucyl-tRNA synthetase is an intracellular leucine sensor for the mTORC1-signaling pathway. Cell *149*, 410–424.

Hara, K., Yonezawa, K., Weng, Q.P., Kozlowski, M.T., Belham, C., and Avruch, J. (1998). Amino acid sufficiency and mTOR regulate p70 S6 kinase and eIF-4E BP1 through a common effector mechanism. J. Biol. Chem. *273*, 14484–14494.

Heitman, J., Movva, N., and Hall, M. (1991). Targets for cell cycle arrest by the immunosuppressant rapamycin in yeast. Science (80-.). *253*, 905–909.

Hosokawa, N., Hara, T., Kaizuka, T., Kishi, C., Takamura, A., Miura, Y., Iemura, S., Natsume, T., Takehana, K., Yamada, N., et al. (2009). Nutrient-dependent mTORC1 Association with the ULK1 – Atg13 – FIP200 Complex Required for Autophagy. Mol. Biol. Cell *20*, 1981–1991.

Huang, W.P., Scott, S. V., Kim, J., and Klionsky, D.J. (2000). The itinerary of a vesicle component, Aut7p/Cvt5p, terminates in the yeast vacuole via the autophagy/Cvt pathways. J. Biol. Chem. *275*, 5845–5851.

Huber, A., Bodenmiller, B., Uotila, A., Stahl, M., Wanka, S., Gerrits, B., Aebersold, R., and Loewith, R. (2009). Characterization of the rapamycin-sensitive phosphoproteome reveals that Sch9 is a central coordinator of protein synthesis. Genes Dev. *23*, 1929–1943.

Hughes Hallett, J.E., Luo, X., and Capaldi, A.P. (2015). Snf1/AMPK promotes the formation of Kog1/raptor-bodies to increase the activation threshold of TORC1 in budding yeast. Elife *4*, 1–19.

Inoki, K., Zhu, T., and Guan, K.-L. (2003a). TSC2 Mediates Cellular Energy Response to Control Cell Growth and Survival. Cell *115*, 577–590.

Inoki, K., Li, Y., Xu, T., and Guan, K.L. (2003b). Rheb GTpase is a direct target of TSC2 GAP activity and regulates mTOR signaling. Genes Dev. *17*, 1829–1834.

Jeong, J.H., Lee, K.H., Kim, Y.M., Kim, D.H., Oh, B.H., and Kim, Y.G. (2012). Crystal structure of the Gtr1pGTP-Gtr2pGDP protein complex reveals large structural rearrangements triggered by GTP-to-GDP conversion. J. Biol. Chem. *287*, 29648–29653.

Jiang, R., and Carlson, M. (1996). Glucose regulates protein interactions within the yeast SNF1 protein kinase complex. Genes Dev. *10*, 3105–3115.

Jiang, Y., and Broach, J.R. (1999). Tor proteins and protein phosphatase 2A reciprocally regulate Tap42 in controlling cell growth in yeast. EMBO J. *18*, 2782–2792.

Jorgensen, P., Rupeš, I., Sharom, J.R., Schneper, L., Broach, J.R., and Tyers, M. (2004). A dynamic transcriptional network communicates growth potential to ribosome

synthesis and critical cell size. Genes Dev. *18*, 2491–2505.

Jung, C.H., Jun, C.B., Ro, S.-H., Kim, Y.-M., Otto, N.M., Cao, J., Kundu, M., and Kim, D.-H. (2009). ULK-Atg13-FIP200 Complexes Mediate mTOR Signaling to the Autophagy Machinery. Mol. Biol. Cell *20*, 1992–2003.

Kamada, Y. (2010). Prime-numbered Atg proteins act at the primary step in autophagy: Unphosphorylatable Atg13 can induce autophagy without TOR inactivation. Autophagy *6*, 415–416.

Kamada, Y., Funakoshi, T., Shintani, T., Nagano, K., Ohsumi, M., and Ohsumi, Y. (2000). Tor-mediated induction of autophagy via an Apg1 protein kinase complex. J. Cell Biol. *150*, 1507–1513.

Kamada, Y., Yoshino, K. -i., Kondo, C., Kawamata, T., Oshiro, N., Yonezawa, K., and Ohsumi, Y. (2010). Tor Directly Controls the Atg1 Kinase Complex To Regulate Autophagy. Mol. Cell. Biol. *30*, 1049–1058.

Kaufmann, W.K., Heffernan, T.P., Beaulieu, L.M., Doherty, S., Frank, A.R., Zhou, Y., Bryant, M.F., Zhou, T., Luche, D.D., Nikolaishvili-Feinberg, N., et al. (2003). Caffeine and human DNA metabolism: The magic and the mystery. Mutat. Res. - Fundam. Mol. Mech. Mutagen. *532*, 85–102.

Kerr, I.D., and Bennett, M.J. (2007). New insight into the biochemical mechanisms regulating auxin transport in plants. Biochem. J. *401*, 613–622.

Khalfan, W.A., and Klionsky, D.J. (2002). Molecular machinery required for autophagy and the cytoplasm to vacuole targeting (Cvt) pathway in S. cerevisiae. Curr. Opin. Cell Biol. *14*, 468–475.

Kim, J.E., and Chen, J. (2000). Cytoplasmic-nuclear shuttling of FKBP12-rapamycin-associated protein is involved in rapamycin-sensitive signaling and translation initiation. Proc. Natl. Acad. Sci. U. S. A. *97*, 14340–14345.

Kim, E., Goraksha-Hicks, P., Li, L., Neufeld, T.P., and Guan, K.-L. (2008). Regulation of TORC1 by Rag GTPases in nutrient response. Nat. Cell Biol. *10*, 935–945.

Kim, J.S., Ro, S.-H., Kim, M., Park, H.-W., Semple, I.A., Park, H., Cho, U.-S., Wang, W., Guan, K.-L., Karin, M., et al. (2015). Sestrin2 inhibits mTORC1 through modulation of GATOR complexes. Sci. Rep. *5*, 9502.

Kira, S., Tabata, K., Shirahama-Noda, K., Nozoe, A., Yoshimori, T., and Noda, T. (2014). Reciprocal conversion of Gtr1 and Gtr2 nucleotidebinding states by Npr2-Npr3 inactivates TORC1 and induces autophagy. Autophagy *10*, 1565–1578.

Kira, S., Kumano, Y., Ukai, H., Takeda, E., Matsuura, A., and Noda, T. (2016). Dynamic relocation of the TORC1-Gtr1/2-Ego1/2/3 complex is regulated by Gtr1 and Gtr2. Mol. Biol. Cell *27*, 382–396.

Kirisako, T., Baba, M., Ishihara, N., Miyazawa, K., Ohsumi, M., Yoshimori, T., Noda, T., and Ohsumi, Y. (1999). Formation process of autophagosome is traced with Apg8/Aut7p in yeast. J. Cell Biol. *147*, 435–446.

Kirisako, T., Ichimura, Y., Okada, H., Kabeya, Y., Mizushima, N., Yoshimori, T., Ohsumi, M., Takao, T., Noda, T., and Ohsumi, Y. (2000). The reversible modification regulates the membrane-binding state of Apg8/Aut7 essential for autophagy and the cytoplasm to vacuole targeting pathway. J. Cell Biol. *151*, 263–275.

Klionsky, D.J. (2007). Autophagy: from phenomenology to molecular understanding in less than a decade. Nat. Rev. Mol. Cell Biol. *8*, 931–937.

Klionsky, D.J., Cregg, J.M., Dunn, W.A., Emr, S.D., Sakai, Y., Sandoval, I. V., Sibirny, A., Subramani, S., Thumm, M., Veenhuis, M., et al. (2003). A unified nomenclature for yeast autophagy-related genes. Dev. Cell *5*, 539–545.

Kobayashi, T., Suzuki, K., and Ohsumi, Y. (2012). Autophagosome formation can be achieved in the absence of Atg18 by expressing engineered PAS-targeted Atg2. FEBS

Lett. *586*, 2473–2478.

Korasick, D.A., Enders, T.A., and Strader, L.C. (2013). Auxin biosynthesis and storage forms. J. Exp. Bot. *64*, 2541–2555.

Laplante, M., and Sabatini, D.M. (2012). MTOR signaling in growth control and disease. Cell *149*, 274–293.

Lempiäinen, H., Uotila, A., Urban, J., Dohnal, I., Ammerer, G., Loewith, R., and Shore, D. (2009). Sfp1 Interaction with TORC1 and Mrs6 Reveals Feedback Regulation on TOR Signaling. Mol. Cell *33*, 704–716.

Levin, D.E. (2005). Cell wall integrity signaling in Saccharomyces cerevisiae. Microbiol. Mol. Biol. Rev. *69*, 262–291.

Li, J., Yan, G., Liu, S., Jiang, T., Zhong, M., Yuan, W., Chen, S., Zheng, Y., Jiang, Y., and Jiang, Y. (2017). Target of rapamycin complex 1 and Tap42-Associated Phosphatases Are Required for Sensing Changes in Nitrogen Conditions in the Yeast *Saccharomyces cerevisiae*. Mol. Microbiol.

Liu, X., and Zheng, X.F.S. (2007). Endoplasmic reticulum and Golgi localization sequences for mammalian target of rapamycin. Mol. Biol. Cell *18*, 1073–1082.

Liu, Q., Wang, J., Kang, S.A., Thoreen, C.C., Hur, W., Ahmed, T., Sabatini, D.M., and Gray, N.S. (2011). Discovery of 9-(6-aminopyridin-3-yl)-1-(3-(trifluoromethyl)phenyl)benzo[h][1,6]naphthyridin-2(1H)-one (Torin2) as a potent, selective, and orally available mammalian target of rapamycin (mTOR) inhibitor for treatment of cancer. J. Med. Chem. *54*, 1473–1480.

Liu, Y.Y., Chen, H.W., and Chou, J.Y. (2016). Variation in indole-3-acetic acid production by wild Saccharomyces cerevisiae and S. paradoxus strains from diverse ecological sources and its effect on growth. PLoS One *11*, 1–13.

Ljungdahl, P.O., and Daignan-Fornier, B. (2012). Regulation of amino acid, nucleotide, and phosphate metabolism in Saccharomyces cerevisiae. Genetics *190*, 885–929.

Loewith, R., and Hall, M.N. (2011). Target of rapamycin (TOR) in nutrient signaling and growth control. Genetics *189*, 1177–1201.

Loewith, R., Jacinto, E., Wullschleger, S., Lorberg, A., Crespo, J.L., Bonenfant, D., Oppliger, W., Jenoe, P., and Hall, M.N. (2002). Two TOR complexes, only one of which is rapamycin sensitive, have distinct roles in cell growth control. Mol. Cell *10*, 457–468.

Lu, J.Y., Lin, Y.Y., Sheu, J.C., Wu, J.T., Lee, F.J., Chen, Y., Lin, M.I., Chiang, F.T., Tai, T.Y., Berger, S.L., et al. (2011). Acetylation of yeast AMPK controls intrinsic aging independently of caloric restriction. Cell *146*, 969–979.

Luschnig, C., Gaxiola, R.A., Grisafi, P., and Fink, G.R. (1998). EIR1, a root-specific protein involved in auxin transport, is required for gravitropism in Arabidopsis thaliana. Genes Dev. *12*, 2175–2187.

Mao, K., Chew, L.H., Inoue-Aono, Y., Cheong, H., Nair, U., Popelka, H., Yip, C.K., and Klionsky, D.J. (2013). Atg29 phosphorylation regulates coordination of the Atg17-Atg31-Atg29 complex with the Atg11 scaffold during autophagy initiation. Proc. Natl. Acad. Sci. U. S. A. *110*, E2875-84.

Martín, H., Rodríguez-Pachón, J.M., Ruiz, C., Nombela, C., and Molina, M. (2000). Regulatory mechanisms for modulation of signaling through the cell integrity Slt2-mediated pathway in Saccharomyces cerevisiae. J. Biol. Chem. *275*, 1511–1519.

Martina, J.A., Diab, H.I., Lishu, L., Jeong-A, L., Patange, S., Raben, N., and Puertollano, R. (2014). The Nutrient-Responsive Transcription Factor TFE3 Promotes Autophagy, Lysosomal Biogenesis, and Clearance of Cellular Debris. Sci. Signal. *7*, ra9-ra9.

Matsuura, A., Tsukada, M., Wada, Y., and Ohsumi, Y. (1997). Apg1p, a novel protein kinase required for the autophagic process in Saccharomyces cerevisiae. Gene *192*, 245–250.

Mavrakis, M., Lippincott-Schwartz, J., Stratakis, C.A., and Bossis, I. (2007). MTOR kinase and the regulatory subunit of protein kinase A (PRKAR1A) Spatially and functionally interact during autophagosome maturation. Autophagy *3*, 151–153.

McCartney, R.R.R., and Schmidt, M.C.C. (2001). Regulation of Snf1 kinase. J. Biol. Chem. *276*, 36460.

McCormick, M.A., Tsai, S. -y., and Kennedy, B.K. (2011). TOR and ageing: a complex pathway for a complex process. Philos. Trans. R. Soc. B Biol. Sci. *366*, 17–27.

McSteen, P. (2010). Auxin and monocot development. Cold Spring Harb. Perspect. Biol. *2*.

Mellman, I., Fuchs, R., and Helenius, A. (1986). Acidification of the endocytic and exocytic pathways. Annu. Rev. Biochem. *55*, 663–700.

Messler, S., Kropp, S., Episkopou, V., Felici, A., Würthner, J., Lemke, R., Jerabek-Willemsen, M., Willecke, R., Scheu, S., Pfeffer, K., et al. (2011). The TGF-β signaling modulators TRAP1/TGFBRAP1 and VPS39/Vam6/TLP are essential for early embryonic development. Immunobiology *216*, 343–350.

Mizushima, N. (2007). Autophagy: Process and function. Genes Dev. *21*, 2861–2873.

Mizushima, N., and Levine, B. (2010). Autophagy in mammalian development and differentiation. Nat. Cell Biol. *12*, 823–830.

Möller, B., and Weijers, D. (2009). Auxin control of embryo patterning. Cold Spring Harb. Perspect. Biol. *1*.

Nadolski, M.J., and Linder, M.E. (2009). Molecular recognition of the palmitoylation

substrate Vac8 by its palmitoyltransferase Pfa3. J. Biol. Chem. *284*, 17720–17730.

Nair, U., Yen, W.L., Mari, M., Cao, Y., Xie, Z., Baba, M., Reggiori, F., and Klionsky, D.J. (2012). A role for Atg8-PE deconjugation in autophagosome biogenesis. Autophagy *8*, 780–793.

Nakashima, A., Yoshino, K. ichi, Miyamoto, T., Eguchi, S., Oshiro, N., Kikkawa, U., and Yonezawa, K. (2007). Identification of TBC7 having TBC domain as a novel binding protein to TSC1-TSC2 complex. Biochem. Biophys. Res. Commun. *361*, 218–223.

Nakashima, N., Noguchi, E., and Nishimoto, T. (1999). Saccharomyces cerevisiae putative G protein, Gtr1p, which forms complexes with itself and a novel protein designated as Gtr2p, negatively regulates the Ran/Gsp1p G protein cycle through Gtr2p. Genetics *152*, 853–867.

Nakatogawa, H., Suzuki, K., Kamada, Y., and Ohsumi, Y. (2009). Dynamics and diversity in autophagy mechanisms: lessons from yeast. Nat. Rev. Mol. Cell Biol. *10*, 458–467.

Navarro, L., Dunoyer, P., Jay, F., Arnold, B., Dharmasiri, N., Estelle, M., Voinnet, O., and Jones, J.D.G. (2006). A Plant miRNA Contributes to Antibacterial Resistance by Repressing Auxin Signaling. Science (80-.). *312*, 436–439.

Neklesa, T.K., and Davis, R.W. (2009). A genome-wide screen for regulators of TORC1 in response to amino acid starvation reveals a conserved Npr2/3 complex. PLoS Genet. *5*.

Nicastro, R., Sardu, A., Panchaud, N., and De Virgilio, C. (2017). The architecture of the Rag GTPase signaling network. Biomolecules *7*, 1–21.

Noda, T. (2017). Regulation of autophagy through TORC1 and mTORC1. Biomolecules *7*, 1–10.

Obara, K., Sekito, T., Niimi, K., and Ohsumi, Y. (2008). The Atg18-Atg2 complex is

recruited to autophagic membranes via phosphatidylinositol 3-phosphate and exerts an essential function. J. Biol. Chem. *283*, 23972–23980.

Ohsumi, Y. (2001). Molecular dissection of autophagy: two ubiquitin-like systems. Nat Rev Mol Cell Biol *2*, 211–216.

Orlova, M., Ozcetin, H., Barrett, L., and Kuchin, S. (2010). Roles of the Snf1-activating kinases during nitrogen limitation and pseudohyphal differentiation in Saccharomyces cerevisiae. Eukaryot. Cell *9*, 208–214.

Ostrowicz, C.W., Meiringer, C.T.A., and Ungermann, C. (2008). Yeast vacuole fusion: A model system for eukaryotic endomembrane dynamics. Autophagy *4*, 5–19.

Panchaud, N., Péli-Gulli, M.P., and De Virgilio, C. (2013a). SEACing the GAP that nEGOCiates TORC1 activation: Evolutionary conservation of Rag GTPase regulation. Cell Cycle *12*, 2948–2952.

Panchaud, N., Péli-Gulli, M.-P., and De Virgilio, C. (2013b). Amino acid deprivation inhibits TORC1 through a GTPase-activating protein complex for the Rag family GTPase Gtr1. Sci. Signal. *6*, ra42.

Papinski, D., Schuschnig, M., Reiter, W., Wilhelm, L., Barnes, C.A., Maiolica, A., Hansmann, I., Pfaffenwimmer, T., Kijanska, M., Stoffel, I., et al. (2014). Early Steps in Autophagy Depend on Direct Phosphorylation of Atg9 by the Atg1 Kinase. Mol. Cell *53*, 471–483.

Parmigiani, A., Nourbakhsh, A., Ding, B., Wang, W., Kim, Y.C., Akopiants, K., Guan, K.L., Karin, M., and Budanov, A. V. (2014). Sestrins Inhibit mTORC1 Kinase Activation through the GATOR Complex. Cell Rep. *9*, 1281–1291.

Pedruzzi, I., Dubouloz, F., Cameroni, E., Wanke, V., Roosen, J., Winderickx, J., and De Virgilio, C. (2003). TOR and PKA Signaling Pathways Converge on the Protein Kinase Rim15 to Control Entry into G0. Mol. Cell *12*, 1607–1613.

Péli-Gulli, M.P., Sardu, A., Panchaud, N., Raucci, S., and De Virgilio, C. (2015). Amino Acids Stimulate TORC1 through Lst4-Lst7, a GTPase-Activating Protein Complex for the Rag Family GTPase Gtr2. Cell Rep. *13*, 1–7.

Peng, M., Yin, N., and Li, M.O. (2014). Sestrins function as guanine nucleotide dissociation inhibitors for rag GTPases to control mTORC1 signaling. Cell *159*, 122–133.

Peterson, T.R., Sengupta, S.S., Harris, T.E., Carmack, A.E., Kang, S.A., Balderas, E., Guertin, D.A., Madden, K.L., Carpenter, A.E., Finck, B.N., et al. (2011). MTOR complex 1 regulates lipin 1 localization to control the srebp pathway. Cell *146*, 408–420.

Petit, C.S., Roczniak-Ferguson, A., and Ferguson, S.M. (2013). Recruitment of folliculin to lysosomes supports the amino acid-dependent activation of rag gtpases. J. Cell Biol. *202*, 1107–1122.

Petrasek, J., and Friml, J. (2009). Auxin transport routes in plant development. Development *136*, 2675–2688.

Powis, K., and De Virgilio, C. (2016). Conserved regulators of Rag GTPases orchestrate amino acid-dependent TORC1 signaling. Cell Discov. *2*, 15049.

Powis, K., Zhang, T., Panchaud, N., Wang, R., Virgilio, C. De, and Ding, J. (2015). Crystal structure of the Ego1-Ego2-Ego3 complex and its role in promoting Rag GTPase-dependent TORC1 signaling. Cell Res. *25*, 1043–1059.

Prouteau, M., Desfosses, A., Sieben, C., Bourgoint, C., Mozaffari, N.L., Demurtas, D., Mitra, A.K., Guichard, P., Manley, S., and Loewith, R. (2017). TORC1 organized in inhibited domains (TOROIDs) regulate TORC1 activity. Nature *550*, 265–269.

Prusty, R., Grisafi, P., and Fink, G.R. (2004). The plant hormone indoleacetic acid induces invasive growth in Saccharomyces cerevisiae. Proc. Natl. Acad. Sci. U. S. A. *101*, 4153–4157.

Rampey, R.A. (2004). A Family of Auxin-Conjugate Hydrolases That Contributes to Free Indole-3-Acetic Acid Levels during Arabidopsis Germination. PLANT Physiol. *135*, 978–988.

Rao, R.P., Hunter, A., Kashpur, O., and Normanly, J. (2010). Aberrant synthesis of indole-3-acetic acid in Saccharomyces cerevisiae triggers morphogenic transition, a virulence trait of pathogenic fungi. Genetics *185*, 211–220.

Rebsamen, M., Pochini, L., Stasyk, T., de Araújo, M.E.G., Galluccio, M., Kandasamy, R.K., Snijder, B., Fauster, A., Rudashevskaya, E.L., Bruckner, M., et al. (2015). SLC38A9 is a component of the lysosomal amino acid sensing machinery that controls mTORC1. Nature *519*, 477–481.

Reggiori, F., Shintani, T., Nair, U., and Klionsky, D.J. (2005). Atg9 cycles between mitochondria and the pre-autophagosomal structure in yeasts. Autophagy *1*, 101–109.

Reinke, A., Anderson, S., McCaffery, J.M., Yates, J., Aronova, S., Chu, S., Fairclough, S., Iverson, C., Wedaman, K.P., and Powers, T. (2004). TOR Complex 1 Includes a Novel Component, Tco89p (YPL180w), and Cooperates with Ssd1p to Maintain Cellular Integrity in Saccharomyces cerevisiae. J. Biol. Chem. *279*, 14752–14762.

Reinke, A., Chen, J.C.Y., Aronova, S., and Powers, T. (2006). Caffeine targets TOR complex I and provides evidence for a regulatory link between the FRB and kinase domains of Tor1p. J. Biol. Chem. *281*, 31616–31626.

Roberg, K.J., Bickel, S., Rowley, N., and Kaiser, C.A. (1997). Control of amino acid permease sorting in the late secretory pathway of Saccharomyces cerevisiae by SEC13, LST4, LST7 and LST8. Genetics *147*, 1569–1584.

Roczniak-Ferguson, A., Petit, C.S., Froehlich, F., Qian, S., Ky, J., Angarola, B., Walther, T.C., and Ferguson, S.M. (2012). The Transcription Factor TFEB Links mTORC1 Signaling to Transcriptional Control of Lysosome Homeostasis. Sci. Signal. *5*, ra42-

ra42.

Rohde, J.R., and Cardenas, M.E. (2004). Nutrient signaling through TOR kinases controls gene expression and cellular differentiation in fungi. Curr. Top. Microbiol. Immunol. *279*, 53–72.

Roth, A.F., Wan, J., Bailey, A.O., Sun, B., Kuchar, J.A., Green, W.N., Phinney, B.S., Yates, J.R., and Davis, N.G. (2006). Global Analysis of Protein Palmitoylation in Yeast. Cell *125*, 1003–1013.

Rubinsztein, D.C., Mariño, G., and Kroemer, G. (2011). Autophagy and aging. Cell *146*, 682–695.

Sabatini, D.M., Erdjument-Bromage, H., Lui, M., Tempst, P., and Snyder, S.H. (1994). RAFT1: A mammalian protein that binds to FKBP12 in a rapamycin-dependent fashion and is homologous to yeast TORs. Cell *78*, 35–43.

Sabers, C.J., Martin, M.M., Brunn, G.J., Williams, J.M., Dumont, F.J., Wiederrecht, G., and Abraham, R.T. (1995). Isolation of a protein target of the FKBP12-rapamycin complex in mammalian cells. J. Biol. Chem. *270*, 815–822.

Sancak, Y., Peterson, T.R., Shaul, Y.D., Lindquist, R.A., Thoreen, C.C., Bar-Peled, L., and Sabatini, D.M. (2008). The Rag GTPases Bind Raptor and Mediate Amino Acid Signaling to mTORC1. Science (80-.). *320*, 1496–1501.

Sancak, Y., Bar-Peled, L., Zoncu, R., Markhard, A.L., Nada, S., and Sabatini, D.M. (2010). Ragulator-rag complex targets mTORC1 to the lysosomal surface and is necessary for its activation by amino acids. Cell *141*, 290–303.

Sato, T., Nakashima, A., Guo, L., and Tamanoi, F. (2009). Specific activation of mTORC1 by Rheb G-protein in vitro involves enhanced recruitment of its substrate protein. J. Biol. Chem. *284*, 12783–12791.

Saucedo, L.J., Gao, X., Chiarelli, D. a, Li, L., Pan, D., and Edgar, B. a (2003). Rheb promotes cell growth as a component of the insulin/TOR signalling network. Nat. Cell Biol. *5*, 566–571.

Saxton, R.A., and Sabatini, D.M. (2017). mTOR Signaling in Growth, Metabolism, and Disease. Cell *168*, 960–976.

Saxton, R.A., Knockenhauer, K.E., Wolfson, R.L., Chantranupong, L., Pacold, M.E., Wang, T., Schwartz, T.U., and Sabatini, D.M. (2016a). Structural basis for leucine sensing by the Sestrin2-mTORC1 pathway. Science (80-.). *351*, 53–58.

Saxton, R.A., Chantranupong, L., Knockenhauer, K.E., Schwartz, T.U., and Sabatini, D.M. (2016b). Mechanism of arginine sensing by CASTOR1 upstream of mTORC1. Nature *536*, 229–233.

Scarpella, E., Barkoulas, M., and Tsiantis, M. (2010). Control of leaf and vein development by auxin. Cold Spring Harb. Perspect. Biol. *2*.

Schmelzle, T., and Hall, M.N. (2000). TOR, a central controller of cell growth. Cell *103*, 253–262.

Sehgal, S.N., Baker, H., and Vézina, C. (1975). Rapamycin (AY-22,989), a new antifungal antibiotic. II. Fermentation, isolation and characterization. J. Antibiot. (Tokyo). *28*, 727–732.

Sekiguchi, T., Hirose, E., Nakashima, N., Ii, M., and Nishimoto, T. (2001). Novel G Proteins, Rag C and Rag D, Interact with GTP-binding Proteins, Rag A and Rag B. J. Biol. Chem. *276*, 7246–7257.

Sekiguchi, T., Kamada, Y., Furuno, N., Funakoshi, M., and Kobayashi, H. (2014). Amino acid residues required for Gtr1p-Gtr2p complex formation and its interactions with the Ego1p-Ego3p complex and TORC1 components in yeast. Genes to Cells *19*, 449–463.

Sekito, T., Fujiki, Y., Ohsumi, Y., and Kakinuma, Y. (2008). Novel families of vacuolar amino acid transporters. IUBMB Life *60*, 519–525.

Shamji, A.F., Kuruvilla, F.G., and Schreiber, S.L. (2000). Partitioning the transcriptional program induced by rapamycin among the effectors of the Tor proteins. Curr. Biol. *10*, 1574–1581.

Shimada, K., Filipuzzi, I., Stahl, M., Helliwell, S.B., Studer, C., Hoepfner, D., Seeber, A., Loewith, R., Movva, N.R., and Gasser, S.M. (2013). TORC2 Signaling Pathway Guarantees Genome Stability in the Face of DNA Strand Breaks. Mol. Cell *51*, 829–839.

Shirra, M.K., McCartney, R.R., Zhang, C., Shokat, K.M., Schmidt, M.C., and Arndt, K.M. (2008). A chemical genomics study identifies Snf1 as a repressor of GCN4 translation. J. Biol. Chem. *283*, 35889–35898.

Sikorski, R.S., and Hieter, P. (1989). A system of shuttle vectors and yeast host strains designed for efficient manipulation of DNA in Saccharomyces cerevisiae. Genetics *122*, 19–27.

Smets, B., Ghillebert, R., De Snijder, P., Binda, M., Swinnen, E., De Virgilio, C., and Winderickx, J. (2010). Life in the midst of scarcity: Adaptations to nutrient availability in Saccharomyces cerevisiae. Curr. Genet. *56*, 1–32.

Spaepen, S., and Vanderleyden, J. (2011). Auxin and plant-microbe interactions. Cold Spring Harb. Perspect. Biol. *3*, 1–13.

Stephan, J.S., Yeh, Y.-Y., Ramachandran, V., Deminoff, S.J., and Herman, P.K. (2009). The Tor and PKA signaling pathways independently target the Atg1/Atg13 protein kinase complex to control autophagy. Proc. Natl. Acad. Sci. U. S. A. *106*, 17049–17054.

Stracka, D., Jozefczuk, S., Rudroff, F., Sauer, U., and Hall, M.N. (2014). Nitrogen source

activates TOR (Target of Rapamycin) complex 1 via glutamine and independently of Gtr/Rag proteins. J. Biol. Chem. *289*, 25010–25020.

Strader, L.C., Culler, A.H., Cohen, J.D., and Bartel, B. (2010). Conversion of Endogenous Indole-3-Butyric Acid to Indole-3-Acetic Acid Drives Cell Expansion in Arabidopsis Seedlings. PLANT Physiol. *153*, 1577–1586.

Sturgill, T.W., Cohen, A., Diefenbacher, M., Trautwein, M., Martin, D.E., and Hall, M.N. (2008). TOR1 and TOR2 have distinct locations in live cells. Eukaryot. Cell *7*, 1819–1830.

Sundberg, E., and Østergaard, L. (2009). Distinct and dynamic auxin activities during reproductive development. Cold Spring Harb. Perspect. Biol. *1*.

Sutter, B.M., Wu, X., Laxman, S., and Tu, B.P. (2013). XMethionine inhibits autophagy and promotes growth by inducing the SAM-responsive methylation of PP2A. Cell *154*.

Suzuki, K., Kubota, Y., Sekito, T., and Ohsumi, Y. (2007). Hierarchy of Atg proteins in pre-autophagosomal structure organization. Genes to Cells *12*, 209–218.

Takahara, T., and Maeda, T. (2012). Transient Sequestration of TORC1 into Stress Granules during Heat Stress. Mol. Cell *47*, 242–252.

Takeshige, K., Baba, M., Tsuboi, S., Noda, T., and Ohsumi, Y. (1992). Autophagy in yeast demonstrated with proteinase-deficient mutants and conditions for its induction. J. Cell Biol. *119*, 301–311.

Tan, X., and Zheng, N. (2009). Hormone signaling through protein destruction: a lesson from plants. Am. J. Physiol. Endocrinol. Metab. *296*, E223–E227.

Tate, J.J., Georis, I., Dubois, E., and Cooper, T.G. (2010). Distinct phosphatase requirements and GATA factor responses to nitrogen catabolite repression and

rapamycin treatment in Saccharomyces cerevisiae. J. Biol. Chem. *285*, 17880–17895.

Teale, W.D., Paponov, I.A., and Palme, K. (2006). Auxin in action: signalling, transport and the control of plant growth and development. Nat Rev Mol Cell Biol *7*, 847–859.

Terman, A., Gustafsson, B., and Brunk, U.T. (2007). Autophagy, organelles and ageing. J. Pathol. *211*, 134–143.

Teter, S.A., Eggerton, K.P., Scott, S. V., Kim, J., Fischer, A.M., and Klionsky, D.J. (2001). Degradation of lipid vesicles in the yeast vacuole requires function of Cvt17, a putative lipase. J. Biol. Chem. *276*, 2083–2087.

Thoreen, C.C., Kang, S.A., Chang, J.W., Liu, Q., Zhang, J., Gao, Y., Reichling, L.J., Sim, T., Sabatini, D.M., and Gray, N.S. (2009). An ATP-competitive mammalian target of rapamycin inhibitor reveals rapamycin-resistant functions of mTORC1. J. Biol. Chem. *284*, 8023–8032.

Torres, J., Di Como, C.J., Herrero, E., and De La Torre-Ruiz, M.A. (2002). Regulation of the cell integrity pathway by rapamycin-sensitive TOR function in budding yeast. J. Biol. Chem. *277*, 43495–43504.

Trahey, M., and McCormick, F. (1987). A cytoplasmic protein stimulates normal N-ras p21 GTPase, but does not affect oncogenic mutants. Science *238*, 542–545.

Tsun, Z.Y., Bar-Peled, L., Chantranupong, L., Zoncu, R., Wang, T., Kim, C., Spooner, E., and Sabatini, D.M. (2013). The folliculin tumor suppressor is a GAP for the RagC/D GTPases that signal amino acid levels to mTORC1. Mol. Cell *52*, 495–505.

Tukalo, M., Yaremchuk, A., Fukunaga, R., Yokoyama, S., and Cusack, S. (2005). The crystal structure of leucyl-tRNA synthetase complexed with tRNALeu in the post-transfer-editing conformation. Nat. Struct. Mol. Biol. *12*, 923–930.

Urano, J., Tabancay, A.P., Yang, W., and Tamanoi, F. (2000). The Saccharomyces cerevisiae Rheb G-protein is involved in regulating canavanine resistance and

arginine uptake. J. Biol. Chem. *275*, 11198–11206.

Urban, J., Soulard, A., Huber, A., Lippman, S., Mukhopadhyay, D., Deloche, O., Wanke, V., Anrather, D., Ammerer, G., Riezman, H., et al. (2007). Sch9 Is a Major Target of TORC1 in Saccharomyces cerevisiae. Mol. Cell *26*, 663–674.

Váchová, L., Čáp, M., and Palková, Z. (2012). Yeast colonies: A model for studies of aging, environmental adaptation, and longevity. Oxid. Med. Cell. Longev.

Valbuena, N., Guan, K.-L., and Moreno, S. (2012). The Vam6 and Gtr1-Gtr2 pathway activates TORC1 in response to amino acids in fission yeast. J. Cell Sci. *125*, 1920–1928.

Vanneste, S., and Friml, J. (2009). Auxin: A Trigger for Change in Plant Development. Cell *136*, 1005–1016.

Verrier, P.J., Bird, D., Burla, B., Dassa, E., Forestier, C., Geisler, M., Klein, M., Kolukisaoglu, Ü., Lee, Y., Martinoia, E., et al. (2008). Plant ABC proteins - a unified nomenclature and updated inventory. Trends Plant Sci. *13*, 151–159.

Vetter, I.R. (2001). The Guanine Nucleotide-Binding Switch in Three Dimensions. Science (80-.). *294*, 1299–1304.

Vézina, C., KUDELSKI, A., and SEHGAL, S.N. (1975). Rapamycin (AY-22,989), a new antifungal antibiotic. I. Taxonomy of the producing streptomycete and isolation of the active principle. J. Antibiot. (Tokyo). *28*, 721–726.

Wan, W., You, Z., Xu, Y., Zhou, L., Guan, Z., Peng, C., Wong, C.C.L., Su, H., Zhou, T., Xia, H., et al. (2017). mTORC1 Phosphorylates Acetyltransferase p300 to Regulate Autophagy and Lipogenesis. Mol. Cell *0*, 1–13.

Wang, S., Tsun, Z.-Y., Wolfson, R.L., Shen, K., Wyant, G.A., Plovanich, M.E., Yuan, E.D., Jones, T.D., Chantranupong, L., Comb, W., et al. (2015). Lysosomal amino acid

transporter SLC38A9 signals arginine sufficiency to mTORC1. Science (80-.). *347*, 188–194.

Wang, X., Campbell, L.E., Miller, C.M., and Proud, C.G. (1998). Amino acid availability regulates p70 S6 kinase and multiple translation factors. Biochem. J. *334 (Pt 1*, 261–267.

Wanke, V., Cameroni, E., Uotila, A., Piccolis, M., Urban, J., Loewith, R., and De Virgilio, C. (2008). Caffeine extends yeast lifespan by targeting TORC1. Mol. Microbiol. *69*, 277–285.

Weisman, R. (2016). Target of Rapamycin (TOR) Regulates Growth in Response to Nutritional Signals. Microbiol. Spectr. *4*, 1–13.

Wolfson, R.L., Chantranupong, L., Saxton, R.A., Shen, K., Scaria, S.M., Cantor, J.R., and Sabatini, D.M. (2016). Sestrin2 is a leucine sensor for the mTORC1 pathway. Science (80-.). *351*, 43–48.

Woodward, A.W., and Bartel, B. (2005). Auxin: Regulation, action, and interaction. Ann. Bot. *95*, 707–735.

Workman, J.J., Chen, H., and Laribee, R.N. (2014). Environmental signaling through the mechanistic target of rapamycin complex 1: mTORC1 goes nuclear. Cell Cycle *13*, 714–725.

Xia, J., Wang, R., Zhang, T., and Ding, J. (2016). Structural insight into the arginine-binding specificity of CASTOR1 in amino acid-dependent mTORC1 signaling. Cell Discov. *2*, 16035.

Yamada, T., Palm, C.J., Brooks, B., and Kosuge, T. (1985). Nucleotide sequences of the *Pseudomonas savastanoi* indoleacetic acid genes show homology with *Agrobacterium tumefaciens* T-DNA. Proc. Natl. Acad. Sci. U. S. A. *82*, 6522–6526.

Yamagata, K., Sanders, L.K., Kaufmann, W.E., Yee, W., Barnes, C.A., Nathans, D., and Worley, P.F. (1994). rheb, a growth factor- and synaptic activity-regulated gene, encodes a novel ras-related protein. J. Biol. Chem. *269*, 16333–16339.

Yamamoto, H., Kakuta, S., Watanabe, T.M., Kitamura, A., Sekito, T., Kondo-Kakuta, C., Ichikawa, R., Kinjo, M., and Ohsumi, Y. (2012). Atg9 vesicles are an important membrane source during early steps of autophagosome formation. J. Cell Biol. *198*, 219–233.

Yamamoto, H., Fujioka, Y., Suzuki, S.W., Noshiro, D., Suzuki, H., Kondo-Kakuta, C., Kimura, Y., Hirano, H., Ando, T., Noda, N.N., et al. (2016). The Intrinsically Disordered Protein Atg13 Mediates Supramolecular Assembly of Autophagy Initiation Complexes. Dev. Cell *38*, 86–99.

Yan, G., Shen, X., and Jiang, Y. (2006). Rapamycin activates Tap42-associated phosphatases by abrogating their association with Tor complex 1. EMBO J. *25*, 3546–3555.

Yang, H., Rudge, D.G., Koos, J.D., Vaidialingam, B., Yang, H.J., and Pavletich, N.P. (2013). mTOR kinase structure, mechanism and regulation. Nature *497*, 217–223.

Yano, H., Nakanishi, S., Kimura, K., Hanai, N., Saitoh, Y., Fukui, Y., Nonomura, Y., and Matsuda, Y. (1993). Inhibition of histamine secretion by wortmannin through the blockade of phosphatidylinositol 3-kinase in RBL-2H3 cells. J. Biol. Chem. *268*, 25846–25856.

Yerlikaya, S., Meusburger, M., Kumari, R., Huber, A., Anrather, D., Costanzo, M., Boone, C., Ammerer, G., Baranov, P. V., and Loewith, R. (2016). TORC1 and TORC2 work together to regulate ribosomal protein S6 phosphorylation in Saccharomyces cerevisiae. Mol. Biol. Cell *27*, 397–409.

Yin, Z., Pascual, C., and Klionsky, D. (2016). Autophagy: machinery and regulation. Microb. Cell *3*, 588–596.

Young, E.T., Dombek, K.M., Tachibana, C., and Ideker, T. (2003). Multiple pathways are co-regulated by the protein kinase Snf1 and the transcription factors Adr1 and Cat8. J. Biol. Chem. *278*, 26146–26158.

Yuan, H.X., Russell, R.C., and Guan, K.L. (2013). Regulation of PIK3C3/VPS34 complexes by MTOR in nutrient stress-induced autophagy. Autophagy *9*, 1983–1995.

Zaman, S., Lippman, S.I., Schneper, L., Slonim, N., and Broach, J.R. (2009). Glucose regulates transcription in yeast through a network of signaling pathways. Mol. Syst. Biol. *5*.

Zazímalová, E., Murphy, A.S., Yang, H., Hoyerova, K., and Hosek, P. (2010). Auxin Transporters — Why So Many ? Cold Spring Harb. Perspect. Biol. *2*, a001552.

Zech, R., Kiontke, S., Mueller, U., Oeckinghaus, A., and Kümmel, D. (2016). Structure of the tuberous sclerosis complex 2 (TSC2) N Terminus provides insight into complex assembly and tuberous sclerosis pathogenesis. J. Biol. Chem. *291*, 20008–20020.

Zhang, T., Péli-Gulli, M.P., Yang, H., De Virgilio, C., and Ding, J. (2012). Ego3 functions as a homodimer to mediate the interaction between Gtr1-Gtr2 and Ego1 in the EGO complex to activate TORC1. Structure *20*, 2151–2160.

Zhang, X., Shu, L., Hosoi, H., Murti, K.G., and Houghton, P.J. (2002). Predominant nuclear localization of mammalian target of rapamycin in normal and malignant cells in culture. J. Biol. Chem. *277*, 28127–28134.

Zhou, M., Meng, Z., Jobson, A.G., Pommier, Y., and Veenstra, T.D. (2007). Detection of in vitro kinase generated protein phosphorylation sites using γ[18O4]-ATP and mass spectrometry. Anal. Chem. *79*, 7603–7610.

Zhu, H. (2001). Global Analysis of Protein Activities Using Proteome Chips. Science (80-.). *293*, 2101–2105.

Zhu, H., Klemic, J.F., Chang, S., Bertone, P., Casamayor, A., Klemic, K.G., Smith, D., Gerstein, M., Reed, M.A., Snyder, M., et al. (2000). Analysis of yeast protein kinases using protein chips. Nat. Genet. *26*, 283–289.

Zoncu, R., Bar-Peled, L., Efeyan, A., Wang, S., Sancak, Y., and Sabatini, D.M. (2011). mTORC1 Senses Lysosomal Amino Acids Through an Inside-Out Mechanism That Requires the Vacuolar H+-ATPase. Science (80-.). *334*, 678–683.

Appendix

Acknowledgements

So, this trip is almost finished...just the time to say "Thanks" to...

Prof. Claudio De Virgilio, because if I never gave up it was also because you never did it with me, giving me your trust until the end. For supporting me and giving me the privilege to do my PhD in your laboratory, having the opportunity to learn a lot both professionally and personally. For your addictive laugh that always manages to get me a smile! I will never forget your teachings and all that I learned here, I promise.

Prof. Robbie Loewith and Prof. Jorn Dengjel, for accepting to review this thesis and being members of my thesis jury board.

Marie, for giving me not only your experience but also your friendship. Even in the most stressful and difficult moments you were there, you made me stronger, sometimes using your "grumpy ways", but always with the best intentions!! Thank you for your support, your advices and for the time you have dedicated to me.

Raffaele, per aver corretto questa tesi con professionalità e competenza. Per tutto ciò che sei riuscito a insegnarmi, nonostante il poco tempo trascorso insieme. Per le risate, la tua amicizia e il supporto morale che sei riuscito a darmi pur non accorgendotene. Guille, per la tua amicizia e per non avermi mai fatto sentire sola, rimpiazzando egregiamente Alessandro!

Riko, for your advices and your fully availability whenever I asked you my questions, both scientific and not! Thanks also for having endured my questionable sense of humor!! Emma, Nicolas, Katie, Yvan, Hélène, Sibilla, Ladislav, Malika and Floriane, for the moments spent together in lab, I learned something from each of you.

Alessandro, Marta e Fernando, perchè senza di voi non sarei arrivata alla fine di questo tortuoso viaggio. Siete stati i miei fantastici compagni di viaggio, più che colleghi amici, la mia famiglia qui in Svizzera.

I miei amici, in particolare Eleonora, Anna e Mariangela, perché siete la fonte della mia forza e determinazione. Perché avete fatto in modo che vi sentissi lontani solo geograficamente.

La mia famiglia, in particolare al mio papà, alla mia mamma, ai miei fratelli e ai miei cognati, siete la mia certezza, la roccia alla quale so che potrò sempre appoggiarmi, grazie per aver creduto in me e non avermi mai fatto sentire la distanza che ci separa.

Fabio, la persona più preziosa che potessi incontrare. Grazie per esserci sempre, per non lasciare che una giornata storta mi abbatta, per prenderti cura di me, per dimostrarmi sempre il tuo amore grande, come quello che provo io per te.

Serena Raucci - *Curriculum Vitae*

PERSONAL INFORMATION Serena Raucci

Rue du Botzet, 3, 1700 Fribourg (Switzerland) (+39) 3463153523

serenaraucci4@gmail.com

WORK EXPERIENCE

Jun 2013–Present **PhD in Biochemistry**

University of Fribourg - Department of Biology - Prof. Claudio De Virgilio, Biochemistry Lab., Fribourg (Switzerland)

- Capacity to develop a project, from the conceptualization to the experimental part.
- Biochemical techniques (protein purification from both bacteria and yeast cells, *in vitro* kinase assay, *in vitro* GAP activity assay).
- Molecular biology techniques (Cloning *in vitro* and by recombination, PCR, Western blot).
- Teaching of biochemistry practical courses to bachelor students.

Sep 2012–Mar 2013 **Trainee**

Pasteur Institut, Department of Development Biology and Stem Cells, Stem cells and Development Unit, Paris (France)

- Characterization and localization of subpopulations of murine satellite cells.
- Evaluation of metabolic and mitochondrial activities and evaluation of entrance in cell cycle in subpopulations of adult satellite mice cells, using cell and molecular biology methods.
- Techniques: Extraction of cells from biological sample using collagenase D/trypsine digestion method, Immunostaining on satellite cells, Immunoistochemistry on muscle sections, Cell culture and FACS, Mitotracker assay, Imaging with confocal microscopy, RNA extraction and quantification, Reverse-Transcriptase Real-Time PCR. Elaboration and statistical analysis of RT-PCR data, imaging analysis.

Jun 2010–Jun 2011 **Trainee**

Researcher Institute of Clinical Physiology, CNR (National Research Council), Pisa (Italy)

- Characterization and evaluation of inflammatory and endothelium dysfunctions biomarkers by alteration in the mRNA expression levels in cardiac, renal and pulmonary tissues of an obesity experimental animal model.
- Set-up and optimization of Real-Time PCR conditions. Selection of reference genes for the normalization of mRNA expression data obtained by Real-Time PCR.
- Techniques: Reverse-Transcriptase Real-Time PCR, Extraction of total DNA/RNA/proteins from biological sample, Purification, quantification and confirmation of RNA integrity by gel electrophoresis techniques and spectrophotometer analysis, Protein purification, Elaboration and statistical analysis of Real-Time PCR data.

Jun 2008–Dec 2008 **Trainee**

Researcher Institute of Clinical Physiology, CNR (National Research Council), Pisa (Italy)

- Characterization and sequencing of genes involved in cardiovascular dysfunctions. Setup and optimization of PCR conditions, gene amplification and gene sequencing.
- Techniques: Reverse-Transcriptase PCR (RT-PCR), gene sequencing with Sanger

method. Extraction of total DNA/RNA/proteins from biological sample using the guanidinium thyocyanate-phenol-chloroform extraction method. Elaboration and statistical analysis of RT-PCR data.

EDUCATION AND TRAINING

Jun 2011–Dec 2011

Licence to practice the profession of biologist and qualification for the registration to the "National Biologist's Register"

Faculty of Mathematics, Physicals and Naturals Sciences, University of Pisa, Pisa (Italy)

- State qualifying examination for the profession of biologist. It consists in four days examinations, including two written proofs, one oral examination and one practical part.

Dec 2008–Jun 2011

Master's Degree in Sciences and Biomolecular Tecnologies. Final mark 110/110 cum laude

Faculty of Mathematics, Physicals and Naturals Sciences, University of Pisa, Pisa (Italy)

- Master's Degree in Sciences and Biomolecular Technologies (Molecular Cellular curriculum).
- Two years studies focused on genetic and molecular biology and related experimental techniques to investigate the molecular aspects of human diseases. The experimental thesis work (entitled "CNP and obesity: study in a rat experimental model" and defended on 14/06/2011) had been performed for 12 months at the CNR. The aim was to evaluate the alteration in the mRNA expression of the Natriuretic Peptides (NPs) system in cardiac, renal and pulmonary tissues of an obesity experimental animal model. In the same study I also selected a set of reference genes for the normalization of mRNA expression data obtained by Real-Time PCR. Part of this work was published in Journal of Molecular Endocrinology (PLoS One. 2013; 8(8): e72959).

Sep 2005–Dec 2008

Bachelor's Degree in Molecular Biological Sciences. Final mark 110/110 cum laude

Faculty of Mathematics, Physicals and Naturals Sciences, University of Pisa, Pisa (Italy)

- Bachelor's degree in Molecular Biological Sciences (Molecular Cellular curriculum).
- The course provided fundamental knowledge of biochemistry, cellular and molecular biology, microbiology and genetics. The experimental thesis (entitled "Sequencing of Apelin gene in the cardiac tissue of Sus Scrofa" and defended on 17/12/2008) was performed during a 7 months internship at the CNR. The aim was to sequence the Apelin gene in Sus Scrofa for future applications to molecular biology studies, This work was published on Pharmacological Research (Pharmacol Res. 2009 Oct;60(4):314-9).

Sep 2000–Jul 2005

Diploma of senior high school specializing in modern language. Score 100/100

Istituto Tecnico Commerciale Statale (I.T.C.) Linguistico "Leonardo Da Vinci", Potenza (Italy)

- After an introductory two-year course, I did a specialization in modern languages (English, French and German).

PERSONAL SKILLS

Mother tongue(s) Italian

Other language(s)

	UNDERSTANDING		SPEAKING		WRITING
	Listening	Reading	Spoken interaction	Spoken production	
English	B2	B2	B2	B2	B2
	Trinity College Certificate				
French	C1	C1	C1	C1	C1
Spanish	C1	C1	C1	C1	B1

Levels: A1 and A2: Basic user - B1 and B2: Independent user - C1 and C2: Proficient user
Common European Framework of Reference for Languages

Communication skills
- Good communication skills gained during my experiences at different universities and living abroad.
- Enthusiast in working in multicultural environment .

Organisational skills
- Good organizational skills gained as teacher of practical courses at the University of Fribourg.

Job-related skills
- Problem solving gained during my PhD and my experiences abroad.
- Ability to work in team, but also independent worker.
- Ability to keep good relationship with colleagues.

Digital skills

SELF-ASSESSMENT				
Informatiion p rocessing	Communication	Content creation	Safety	Problem solving
Independent user	Proficient user	Independent user	Independent user	Independent user

Digital skills - Self-assessment grid

Other skills
- Singing (amateur singer), cooking and reading.

Driving licence B

ADDITIONAL INFORMATION

Conferences
- 28th International Conference on Yeast Genetics and Molecular Biology (ICYGMB). From 27th August 2017 to 1st September 2017, Prague (Czech Republic)

  Authors: Péli-Gulli MP, **Raucci S**, Hu Z, Dengjel J, De Virgilio C.

  Poster title: Feedback inhibition of the Rag GTPase GAP Complex Lst4-Lst7 safeguards TORC1 from hyperactivation by amino acid signals.

- Levures, Modèles et Outils "LMO12". From 13th to 15th April 2016, Bruxelles (Belgium)

- Targeting the kinome III. From 26th to 28th September 2014, Basel (Switzerland)

Publications

- Péli-Gulli MP, **Raucci S**, Hu Z, Dengjel J, De Virgilio C.

  Feedback Inhibition of the Rag GTPase GAP Complex Lst4-Lst7 Safeguards TORC1 from Hyperactivation by Amino Acid Signals.

  Cell Rep. 2017 Jul 11;20(2):281-288. doi: 10.1016/j.celrep.2017.06.058.

- Péli-Gulli MP, Sardu A, Panchaud N, **Raucci S**, De Virgilio C.

  Amino acids stimulate TORC1 through Lst4-Lst7, a GTPase-activating protein complex for the Rag family GTPase Gtr2.

  Cell Rep. 2015 Oct 6;13(1):1-7. doi: 10.1016/j.celrep.2015.08.059

- Cabiati M, **Raucci S**, Liistro T, Prescimone T, Caselli C, Iozzo P, Giannessi D, Del Ry S.

  Impact of obesity on the expression pathway of C-type natriuretic peptides and its specific receptor, NPR-B, in a rat experimental modell.

  PLoS One. 2013; 8(8): e72959. doi: 10.1371/journal.pone.0072959.

- Cabiati M, **Raucci S**, Caselli C, Guzzardi MA, D'Amico A, Prescimone T, Giannessi D, Del Ry S.

  Tissue-specific selection of stable reference genes for real-time PCR normalization in an obese rat model.

  J Mol Endocrinol. 2012 May 8;48(3):251-60. doi: 10.1530/JME-12-0024.

- Del Ry S, Cabiati M, **Raucci S**, Simioniuc A, Caselli C, Prescimone T, Giannessi D.

  Sequencing and cardiac expression of Apelin in Sus Scrofa.

  Pharmacol. Res. 2009 Oct;60(4):314-9. doi: 10.1016/j.phrs.2009.04.008.